Neural Network Adaptation in the Retina: Dopaminergic Signaling Mechanisms

By

Heng Dai

Dissertation

Submitted to the Faculty of the

Graduate School of Vanderbilt University

in partial fulfillment of the requirements

for the degree of

DOCTOR OF PHILOSOPHY

in

Biological Sciences

May, 2018

Nashville, Tennessee

Approved:

Carl H. Johnson, Ph.D., Chair

Douglas G. McMahon, Ph.D., Advisor

Terry L. Page, Ph.D.

David J. Calkins, Ph.D.

For my family:

Mom, Dad,
Grandma Zhanwen, Grandpa Nianci,
Grandma Juzhen, Grandpa Jiangzhong,
Uncle Renzhong,
Uncle Yiping and Aunt Yi
I could not have done it without you
Love you like I always do

ACKNOWLEDGEMENTS

First and foremost, I need to acknowledge my funding sources that allowed me to carry out my dissertation research:

This work was financially supported from 2011 to present by the National Institutes of Health Grants R01 EY015815 and R01 GM117650 awarded to Douglas McMahon; P50 MH096972 and R01 MH105094 awarded to Randy Blakely; P30 EY008126 and T32 EY007135-16 awarded to Vanderbilt Vision Research; F32 EY022850 awarded to Chad Jackson; and F31 MH107132 awarded to Gwynne Davis.

Secondly, I would like to thank the wide variety of people who have been both supportive and influential throughout my time in graduate school, in no particular order:

The McMahon Lab

Post-docs: Chad Jackson, Michael Risner, Manuel A. Giannoni-Guzmán, Justin Siemann, Leigh Jackson, and Holly Resuehr
Graduate students: David Sprinzen, Michael Tackenberg, Jeff Jones, and Noah Green
Research and administrative staff: Lili Xi, Laurel Young, and Patricia McCleskey

Dissertation Committee

Douglas McMahon, Carl Johnson, Terry Page, David Calkins, and Donna Webb

Collaborators

Randy Blakely and Gwynne Davis

Others

Katherine Friedman, Division of Animal Care, and Neurochemistry Core

Third, I would like to reiterate my thanks to Doug McMahon, my dissertation advisor. I would not have survived the ups and downs of my graduate studies without his patience, understanding, and support. He has always encouraged me to follow my curiosity and enthusiasm either in science or career opportunities. He was everything I could have asked for from a mentor and more.

Finally, I want to thank all of my family and friends of whom there are far too many to mention by name. Thank you all for your love, friendship, and support. I wish you all success and happiness in all of the future endeavors you undertake.

Heng Dai

March 22nd, 2018

TABLE OF CONTENTS

LIST OF FIGURES

CHAPTER I
Introduction

1.1 Project Overview

From faint starlight to bright sunlight, our visual system is remarkable in its ability to discern visual information of different quantity and quality over a wide range of light intensities. It creates many of our impressions about the world and our memories of it by recognizing various forms, motions, depths, and colors. The visual system also provides our "built-in clock" in the brain with the information about the time of the day. A bilateral projection from the eyes to suprachiasmatic nuclei (SCN) synchronizes our internal biological rhythms with external environment to achieve adaptive advantages, such as predicting temporal changes in the day and preparing us for daily stressors.

Visual signaling initiates in the retina: a thin (~200-500 μm thick) tissue that lines the back of the eye. Light arrives at the retina after being transmitted and refracted by the optics of the eye (Fig. 1.1). The retina then encodes light into electrical and chemical neural signals in multiple layers of neurons, and eventually sends visual information to the brain for higher order visual or non-image forming processing. In response to a range of 100 million-fold change of illumination conditions during day and night, the retina employs a wide variety of neuromodulations to rapidly and accurately reconfigure its neuronal networks according to the background illumination. Among those neuromodulators, including many neuropeptides and nitric oxide, dopamine is the central modulator and the focus of my study.

We have sought to define how dopamine (DA) modulates retinal functioning at the cellular and network levels. DA was first found to modulate electrical synapses and glutamate receptors in the retina, now recognized as key elements of dopamine function throughout the brain [1]. Elucidation of retinal dopaminergic components will greatly facilitate our understanding of the links between cellular mechanisms, network alterations, and behavior, and shed light on more complex and challenging brain network connectivity and tuning. In this dissertation, I will give insight into and discuss my findings regarding how retinal DA fulfills its role as a chemical messenger for light adaptation and supports multiple dimensions of high spatiotemporal resolution vision. I will first relate many previous findings and background knowledge of retinal circuits and DA to the question posed above in Chapter I.

Next, I will focus on understanding three distinct mechanisms that regulate retinal DA signaling. Chapter II will examine how DA signaling dynamics is regulated by DA transporters (DAT, *SLC6A3*). DAT controls perfusion of DA beyond synaptic zones by promptly reuptaking extracellular DA. By employing a neuropsychiatric disorder-relevant DAT coding substitution, we were able to examine the consequences of disrupted DAT-mediated DA clearance in retinal function. Chapter III will determine the

effects of seasonal light cycles on retinal dopamine and visual function, given that environmental light greatly shapes retinal architecture and dopamine levels. And lastly, Chapter IV will address how dopaminergic modulation of retinal signaling is achieved at the level of ganglion cells via distinct receptor pathways, as a follow-up study of our previous work which shows D1 and D4 receptors contribute to different aspects of light-adapted vision at the physiological level [2].

A mechanistic understanding of the retina is important for decoding the fundamentals underlying normal visual function and thus to lay the foundation of biological or prosthetic means for vision restoration. More critically, the study of the retina is useful for understanding the central nerve system (CNS) in general for many reasons. First, the retina is part of the brain - it develops as an out-pocketing of the diencephalon. Hence, its neuronal and synaptic components and mechanisms are essentially synonymous with those of the rest of the brain (with a few notable exceptions, like visual pigments). Second, the retina possesses extensive physiological diversity, yet a relatively simple structural arrangement compared with other brain regions. It contains only five major types of cells, whose cell body and processes are well-segregated in layers and whose fundamental circuitry is highly defined. Third, the retina is experimentally tractable and approachable. It can be easily isolated intact from the back of the eye and remains viable for several hours (~ 6 hr post-isolation) in artificial, oxygen-rich media. It is also easy to stimulate the retina naturally by patterns of light and the effect of these parameters can be monitored readily by recording ganglion cell discharges or field potentials. By taking the advantages of unique properties of the retina and its connection with the brain, we can greatly advance our understanding of retinal circuits and neural plasticity in CNS.

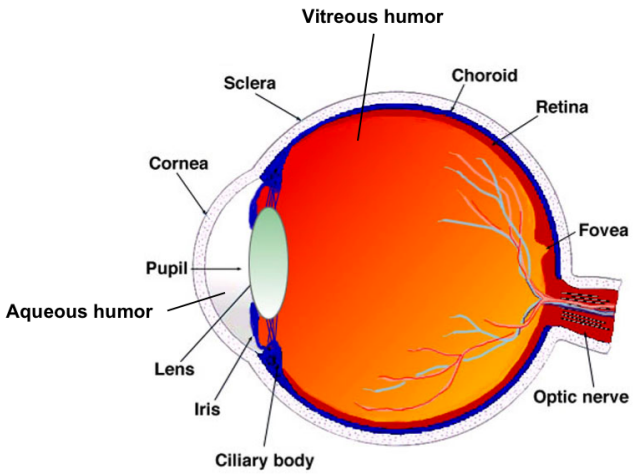

Fig. 1.1 The vertebrate visual system initiates in the eye shown in a schematic drawing.

Light rays are focused onto the retina located at the back of the eye (drawn in dark red line) after passing through chambers of fluid, the aqueous and vitreous humor, and the optical elements of the eye, the cornea and lens. Unlike the cornea whose thickness is not adjustable; the shape of the crystalline lens is controlled by the ciliary body and accommodates for different focus distance. The optic system of the eye allows the visual image to be focused on the retina with minimal, optical distortion. The iris is a beautifully pigmented circular muscle that gives us our eye's color. The central aperture of the iris is the pupil, which controls the amount of light entering the eye. The sclera (the "white of the eye"), continuous with the cornea, forms the outmost layer of the eye maintaining the shape of the eye. The choroid is a vascular layer lying between the retina and sclera, which delivers oxygen and nourishment to the outer layers of the retina. The retina, as the most critical component for vision, converts light into electrical and chemical signals and sends these signals through the optic nerve to the higher centers in the brain for further processing necessary for visual perception (i.e. lateral geniculate nucleus, LGN) or non-image forming processing (i.e. pretectum for pupillary light reflex, suprachiasmatic nucleus for circadian rhythms). In human, a specialized arrangement called fovea serves to improve visual resolution. The overlying cellular layers and blood vessels are displaced so that light can impinge directly on the photoreceptors. Only cones are present in this area. This rod-free area is about 0.3mm in diameter and contains approximately 35,000 cones [3] (modified from Webvision [4]).

1.2 Cellular organization and neuronal wiring of the vertebrate retina

The cell bodies and synaptic connections of the vertebrate retina are organized into distinct laminae, consisting of five major cell classes (Fig. 1.2): photoreceptors, which transduce light into neurochemical signals, are located in the outer nuclear layer (ONL); in the inner nuclear layer (INL), bipolar, amacrine, and horizontal cells relay and modulate the information flow; and lastly ganglion cells form the ganglion cell layer (GCL), and ultimately convey the output of the retina to the brain. In the outer plexiform layer, (OPL), bipolar and horizontal cells synaptically interact with photoreceptors. Bipolar and amacrine cells output to ganglion cells, compose the inner plexiform layer (IPL). Within the IPL, there are cells

depolarized by an increase in illumination and cells hyperpolarized by an increase in illumination. The former are predominantly located in the inner half of the IPL (ON sublamina close to GCL), while the latter are confined to the outer half (OFF sublamina close to INL).

The possessing of visual information is a complex combination of vertical and lateral interactions of neurons. The vertically direct pathway starts with photoreceptors, to bipolar cells and then to ganglion cells. Lateral interactions, on the other hand, are mediated by amacrine and horizontal cells in the IPL and OPL, and also gap junctions between adjacent cells.

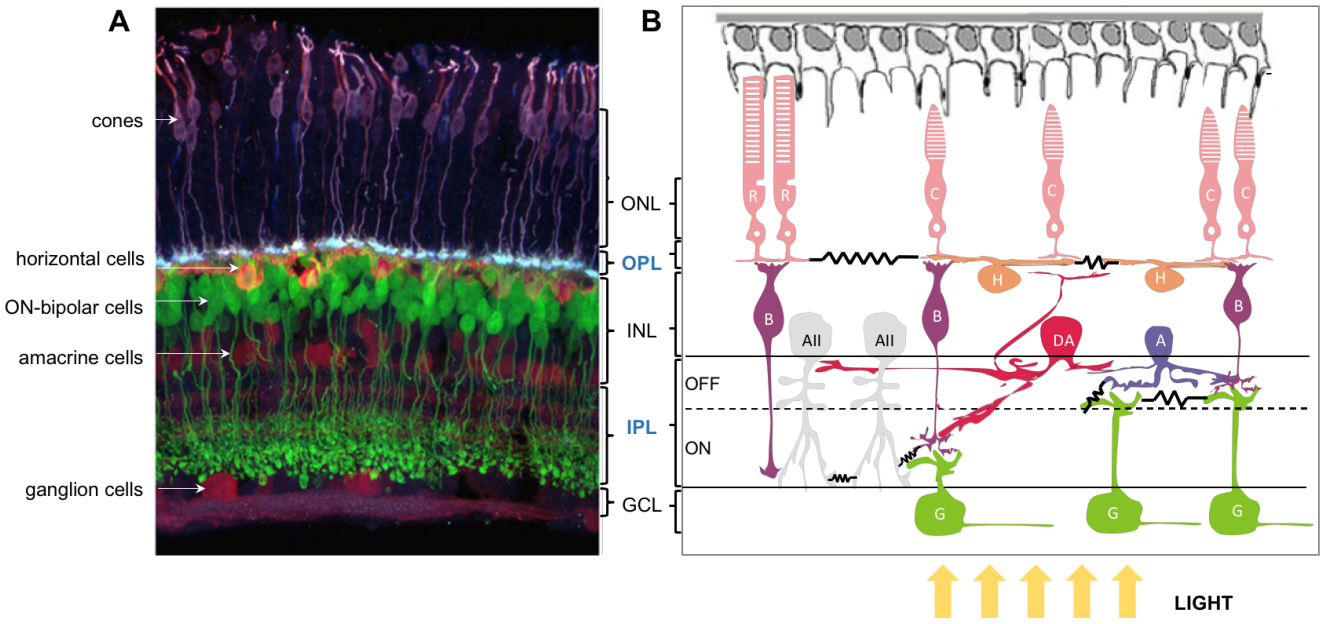

Fig. 1.2 The vertebrate retina shows lamination of cell bodies and synaptic terminals.

(**A**) A cross-section of an immunostained mature mouse retina labels photoreceptors in bluish-purple (immuno-labeled with anti-cone arrestin); horizontal, amacrine and ganglion cells in red (immunostained for calbindin), and bipolar cells in green (expression of *mGlu6* promoter-driven GFP) [5] (modified from Webvision). (**B**) A schematic diagram illustrates the five major cell components positioned in three layers and their projection patterns within two synaptic plexiform layers. Light (yellow arrows) must pass through layers of neurons and their processes before it reaches the photoreceptors. The pigment epithelium (grey cells) is firmly attached to the underlying choroid and in touch with photoreceptors. It supplies nutrients to photoreceptors and eliminates metabolites. In addition to synaptic connections, cells of different types are communicated directly through gap junctions (shown in zigzag lines). R, rod photoreceptor; C, cone photoreceptor; B, bipolar cell; A, amacrine cell; H, horizontal cell; AII, AII amacrine cell; DA, dopaminergic amacrine cell; G, ganglion cell; ONL, outer nuclear layer; OPL, outer plexiform layer; INL, inner nuclear layer; IPL, inner plexiform layer; GCL, ganglion cell layer; OFF, OFF sublamina of the IPL; ON, ON sublamina of the IPL (unpublished diagram by McMahon lab).

1.2.1 Photoreceptors

There are two types of photoreceptors in the vertebrate retina, providing transduction for different aspects of vision: rods are primarily responsible for night vision, whereas cones mediate high-definition daytime and color vision. Both photoreceptors are composed of three major functional regions (Fig. 1.3) with differentiation primarily in the shape and size, as well as the arrangement of the membranous disks in the outer segment. Rods have longer, rod-shaped outer segments and small, spherical terminals, whereas cones often have conical, shorter outer segments, thicker inner segments, and larger terminals. In most retinas there is a single type of rod, expressing rhodopsin as the photopigment, whereas cones have multiple subtypes expressing different visual pigments. For example, in the human retina, there are three types, each with a pigment that is sensitive to a specific range of visible wavelengths of light (S-cones: ~437 nm, M-cones: ~533 nm, L-cones: ~564 nm, respectively [6]. Rods and cones optimize to operate in varying light intensity and spectrum ranges (Fig. 1.4): rods are sensitive to light and therefore function well in the dim light that is present at dusk or at night when most stimuli are too weak to excite the cones. While harboring different photopigments, rods and cones undergo essentially the same three-stage phototransduction cascade to encode light information into graded changes in membrane potential [3]. The change in membrane potential of rod and cones trigger the release of the neurotransmitter glutamate. In the darkness, photoreceptors are in a relatively depolarized state, but are hyperpolarized upon light activation of visual pigments. To capture more light in dim light condition, rods not only contain more photosensitive visual pigments, but also respond slowly to sum all the photons absorbed during a long interval (~100ms interval in human, compared to ~18ms interval in cones). Moreover, rods outnumber cones across vertebrate species with varying rod-to-cone ratios. For example, in C57/BL6 mice, there is a 35-fold difference (approximately 6.4 million of rods and 180 thousand of cones) [7], whereas, in humans, a roughly 20-fold difference (120 million of rods and 6 million of cones) is observed [8]. In many primates, including humans, a small region of the retina only contains cones and is specialized for high-acuity vision (Fig. 1.1). Like other neurons, photoreceptors do not divide, but their outer segments are constantly renewed. Old discs are discarded at the tips of photoreceptors and removed by the phagocytic activity of the pigment epithelial cells (grey cells in Fig. 1.2B).

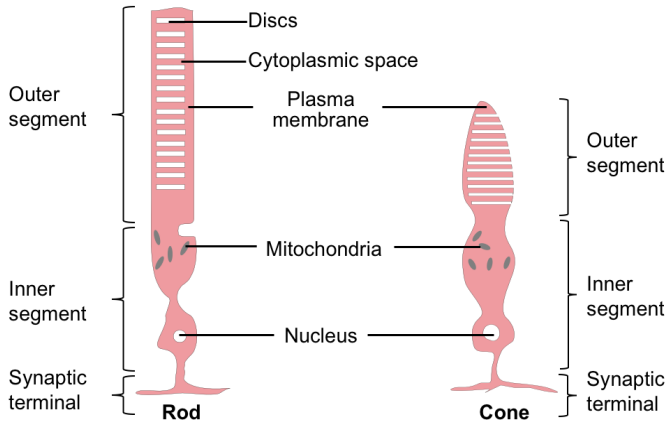

Fig. 1.3 Rod and cone photoreceptors share similar functional regions.

Both rods and cones are composed of three parts: the outer segment is specialized for phototransduction, containing the light-absorbing photopigments; the inner segment functions as the center of biosynthetic machinery, including mitochondria and nucleus; and the synaptic terminal communicates with cells in the INL by releasing neurotransmitters, such as glutamate. Compared to cones, rods typically have longer, rod-shaped outer segments, thinner inner segments, and small spherical terminals. The discs in the outer segment of rods pinch off from the plasma membrane and become individual intracellular organelles, whereas discs of cones are continuous with the plasma membrane. This arrangement of rod discs has functional consequences for the excitation of rods; namely, rods need a messenger molecule cGMP to transfer information from discs to the plasma membrane. Photopigments are located on the membrane of the discs and trigger a cascade of events that eventually change the membrane potential upon the absorption of light. Different types of photopigments in rods and cones enable them to respond to different parts of the light spectrum [8].

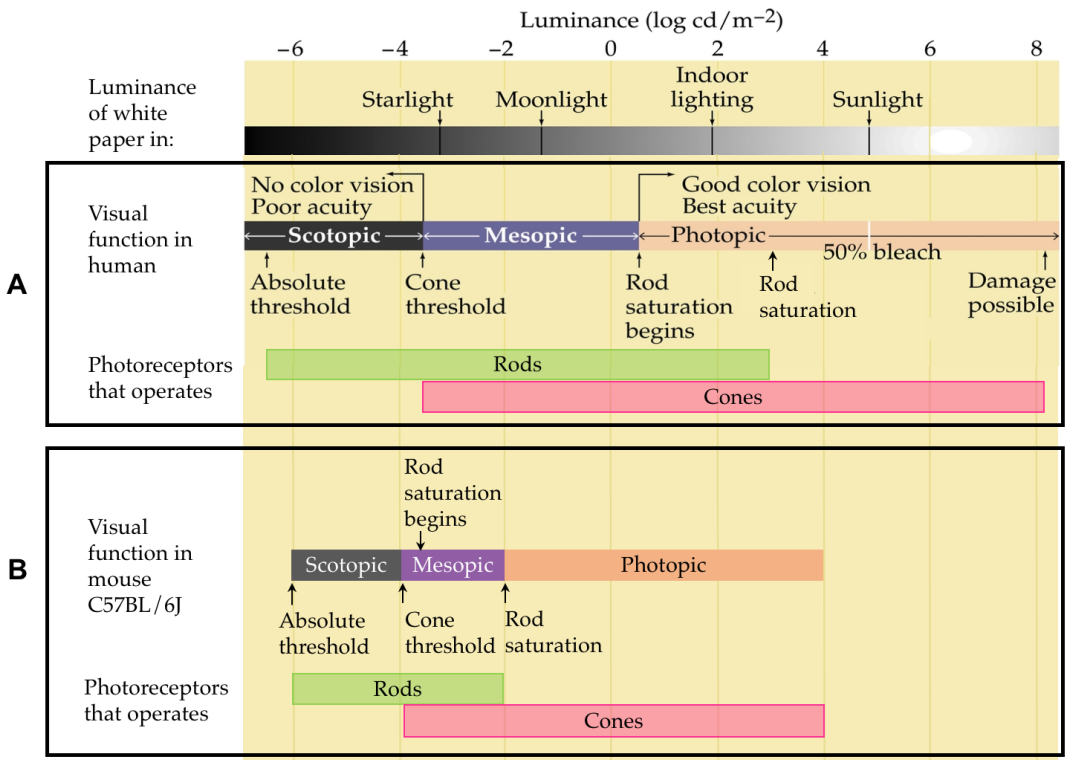

Fig. 1.4 The switching operations between rod and cone photoreceptors enable, in part, the visual system to be responsive to luminance across a dynamic range

(**A**) Human photoreceptors operate selectively under different light conditions. Under dim, scotopic illuminations, only the rod system is active, and thus visual discrimination is poor and color perception is achromatic. With intermediate, mesopic illuminations, there is an increase in both the perceptual quality and gamut of perceivable colors, when the contribution of rods declines and cones gradually become sensitive. Under high illuminations, rods are saturated due to closure of all rod membrane channels, and photopic vision is mediated by cone photoreceptor classes with overlapping spectral sensitivities for trichromatic color perception. Visual functions are defined as patients' visual acuity by presenting them with a visual test chart under certain light conditions [9]. (**B**) The operation ranges of mouse (C57BL/6J strain) photoreceptors are narrower than those of human photoreceptors, based on the measurements of temporal contrast sensitivity over an 8-log unit range of luminance. Since 2.0 log cd/m^2 was the maximum light intensity tested in this study, it is unclear whether the cone photoreceptors would be functional under light conditions of higher intensities [10] (modified from Purves *et al*. Neuroscience [3]).

1.2.2 Bipolar cells

Bipolar cells bridge the communication between photoreceptors and downstream neurons, including ganglion and amacrine cells. With two synapses at opposing poles of the cells, they receive input from the photoreceptors in OPL and output to ganglion and amacrine cells in the IPL (Fig 1.2B). Rods primarily contact and largely converge on one subtype of bipolar cells, rod bipolar cells [11, 12], with the exception of a fast rod pathway to OFF ganglion cell [11]. In mouse retina, each rod diverges to 2 rod bipolar cells, and ~20 rods converge on one rod bipolar cell [11]. The convergence at the bipolar cell level further increases the sensitivity of the rod system to dim light at the expense of low spatial acuity. Cone bipolars, however, have several different forms in mammalian retinas (10-13 subtypes). They segregate into discrete groups based on the location of their branching in the IPL (Fig. 1.2B, OFF vs. ON sublamina), different synapse numbers and distributions, and also diverse inputs from cones or amacrine cells via various neurotransmitters [13]. Some of them contact only a single cone terminal, such as flat midget bipolar (FMB in primates, corresponding to Type 1 cone bipolar in mouse)[14], and others contact several cones, probably as many as 4 to 7 cones [11, 15]. Functionally, these bipolar cell subtypes can be regrouped into two types based on their responses to light stimuli with approximately equal numbers [13]. They separate visual information into "on" and "off" channels and carry out a spatial-type analysis of the visual input, demonstrating a center-surround antagonistic receptor field organization (i.e. the responses of a surround region in their receptive field opposes the center). On-center bipolar cells (ON bipolar) are depolarized by small spot stimuli positioned in the receptive field center, while off-center bipolar (OFF bipolar) cells are hyperpolarized by the same stimuli (Fig. 1.5). Since all photoreceptor synapses release glutamate, how does glutamate have opposite effects on these two classes of cells? As it turns out, the selective responses are achieved by different types of glutamate receptors: OFF bipolar have ionotropic glutamate receptors, whereas ON cells have a sign-inverting synapse mediated by metabotropic glutamate receptors (Fig. 1.7A). Rod bipolars are ON cells, while cone bipolars are either ON or OFF type. In addition to "on" and "off" signals, separate channels for different frequencies and color information are also provided at the level of bipolar cells. The separation, created at the first retinal synapse, is propagated throughout the visual system [13].

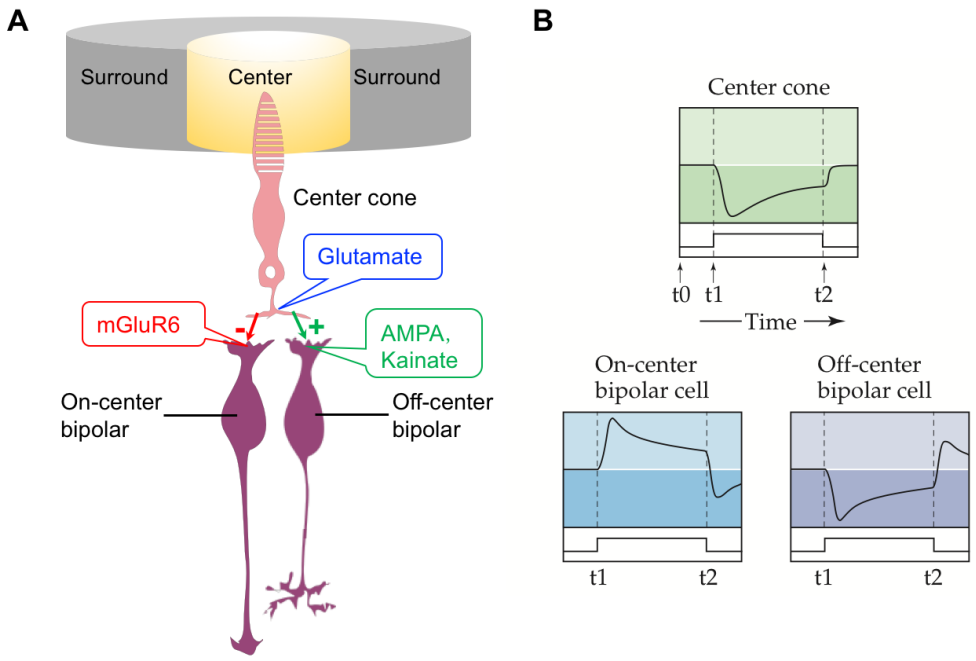

Fig. 1.5 Bipolar cells initiate "on" and "off" responses to create the preliminary contrast and spatial detection.

(**A**) Illustrated in cone photoreceptors, ON- and OFF- bipolar cells establish parallel "on" and "off" pathways by responding oppositely to the same light stimulus passing through a single cone. By expressing distinct types of glutamate receptors, ON- and OFF-bipolar cells respond differently to light increments and decrements. OFF bipolar cells have ionotropic receptors (AMPA and kainate): glutamate opens cation channels, and thus depolarizes OFF-cells. In contrast, ON bipolar cells express G-protein-coupled metabotropic glutamate receptors (mGluR6); these bipolar cells hyperpolarize in response to glutamate. (**B**) When a light spot is presented in the center of the receptor filed of a bipolar cell, photoreceptors hyperpolarize in response to light increments and decrease their release of glutamate (modified from Purves *et al*. Neuroscience [3]). On-center bipolar cells contacted by the photoreceptors are freed from the hyperpolarizing influence of glutamate, and they depolarize. In OFF bipolar cells, the opposite effects occur, and they are hence hyperpolarized. Conversely, a dark spot in the center inhibits (hyperpolarizes) ON-bipolar and excites (depolarizes) OFF-bipolar, respectively. Both types are repolarized by the light stimulation of the peripheral receptive field outside the center. Similar to photoreceptors, bipolar cells translate the light information into graded membrane potentials. A plus indicates a sign-conserving synapse; a minus represents a sign-inverting synapse.

1.2.3 Ganglion cells

Ganglion cells inherit "on" and "off" information from bipolar cells and converge hundreds to thousands of bipolar cells on a single ganglion cell. Up to 32 different morphological and functional subtypes of ganglion cells have been discovered in mouse retina [16], a majority of which contact multiple bipolar cell types, with a combination of major inputs from one or two bipolar cell types and minor inputs from a variety of others [17, 18]. Among the complex connectivity patterns in convergence by different bipolar and ganglion cell types, a few receptive field profiles of ganglion cells have been well studied historically. On-center, off-center or ON-OFF ganglion cells largely reflect the type of bipolar cells that connect to them (Fig. 1.6). Due to the expression of ionotropic glutamate receptors, ganglion cells depolarize in response to glutamate released by bipolar cells (Fig. 1.6A). Because of the 'bistratified' dendritic arborization in both ON and OFF zones of the IPL, ON-OFF ganglion cells excite at the onset and cessation of light stimuli, but are otherwise quiet. Ganglion cells are also capable of computing temporal (i.e. sustained vs. transient), movement and directional aspects of light stimuli processed by the IPL. Ganglion cells are the final output neurons of the vertebrate retina, whose axons form the optic nerve and project to brain visual centers, including the lateral geniculate nucleus (LGN) and the superior colliculus (Fig. 1.1) [19]. Among various types of ganglion cells, intrinsic photosensitive retinal ganglion cells (ipRGCs) are an atypical type, comprising 4-5% of total ganglion cell population[20]. Unlike conventional RGCs that solely rely on rod and cone photoreceptors for inputs, ipRGCs receive information from their own photopigment melanopsin in addition to rods and cones, and thus act like a third type of photoreceptors. The intrinsic light response of ipRGCs differs dramatically from those of rods and cones. Most notable is the difference in response kinetics: ipRGCs are much less sensitive to light than the classical photoreceptors, and capable of very long-lasting light responses, therefore faithfully encoding stimulus energy over relatively long periods of time [21]. These features set ipRGCs apart from all other ganglion cells, which cannot stably represent ambient light levels in this fashion. ipRGCs retrogradely output to dopaminergic amacrine cells, and support non-imaging vision functions, including synchronization of circadian rhythms, modulation of melatonin release, and the circuit that drives the pupillary light reflex [22].

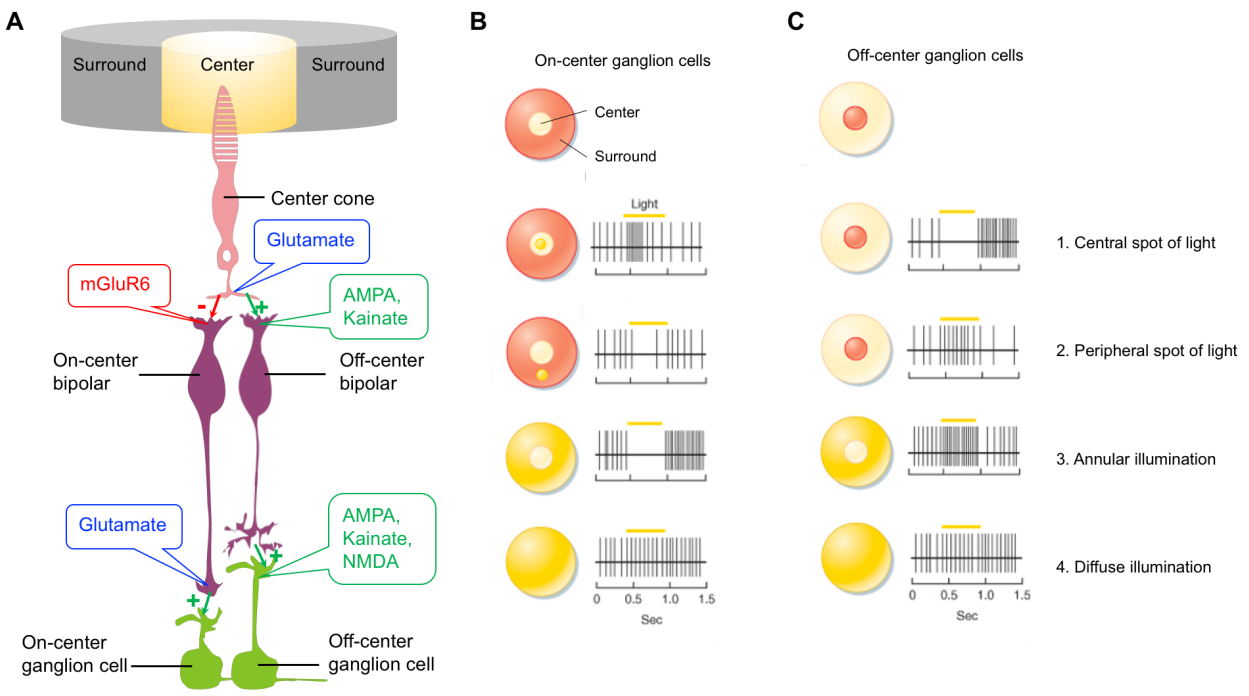

Fig. 1.6 Ganglion cells have circular receptive fields and conserve the "on" and "off" channels from bipolar cells.

(**A**) The responses of the ganglion cells are largely determined by the input from bipolar cells, as each bipolar cell makes an excitatory connection via glutamate with a corresponding type of ganglion cell. The receptive field of a ganglion cell is organized into a center (light yellow) and an antagonistic surround (red), similar to bipolar cells. Ganglion cells only express the ionotropic glutamate receptors, and thus conserve the signals passed by bipolar cells. ON ganglion cells (**B**) increase the number of spikes in response to a spot of light in the center (1) and respond best when the entire central part of the receptive field is stimulated. Illumination of the surround with a spot of light (2) or ring of light (3) suppress the ON cell firing, which resumes more vigorously for a short period after the light is turned off. The OFF ganglion cell (**C**) shows the opposite responses. Both ON and OFF ganglion cells respond to diffuse illumination of the entire receptive field with a relative weak discharge, because the center and surround oppose each other's effects. Unlike photoreceptors and bipolar cells using graded potentials, ganglion cells transmit information as trains of action potentials, and change the firing frequency accordingly (B-C adapted from Basicmedical Key https://basicmedicalkey.com/the-special-senses-2/Figure 8-8.)

1.2.4 Horizontal cells

Retinal interneurons other than bipolar cells, i.e. horizontal and amacrine cells, mediate many lateral interactions and play specific roles in shaping photoreceptor signals transmitted through the retina. Horizontal cells extend processes in the ONL, the first synaptic zone. They modify the information conveyed to the bipolar cells by feeding back onto photoreceptors, or by directly feeding forwarding to bipolar cells. Although appearing in several morphological types, they are usually classified into at least two types in the majority of mammalian retinas: axonless A-type and B-type with axons. A-type contacts solely cones, while B-type has a cell body and dendrites exclusively for contacting cones, and an axon of several hundred microns length that arborizes to contact only rods (Fig 1.7, for simplicity's sake Fig. 1.1 only shows the somata/dendrites in the drawing)[23-25]. In rat and mouse retinas, only the B-type cell is known to exist [13, 26]. Mouse horizontal cell somata/dendrites receive synaptic inputs from cone photoreceptors, whereas its axon terminals receive synaptic inputs solely from rods.

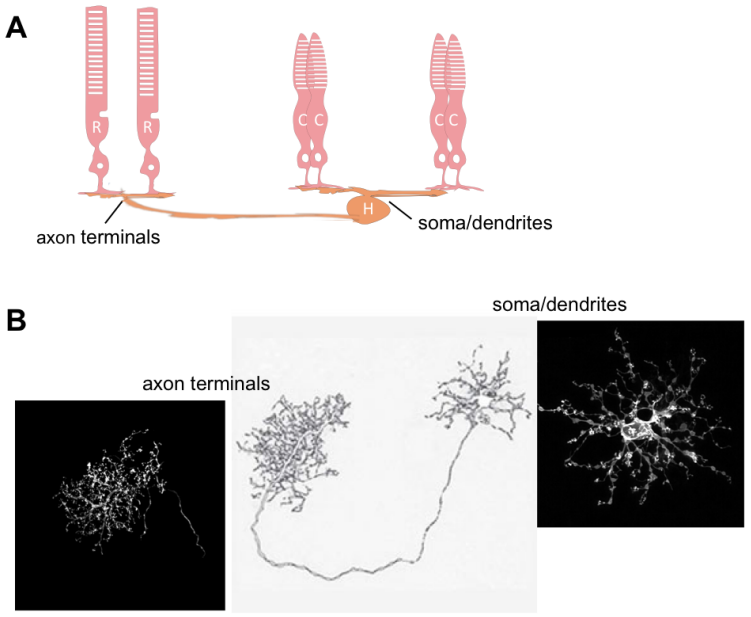

Fig. 1.7 Mouse retinas only contain B-type horizontal cells.

Horizontal cells extend dendritic terminals that connect to the pedicles of cone photoreceptors and an axon terminal system contacting the spherules of rod photoreceptors (**A**, shown in a schematic drawing). (**B**) A staining of a single mouse horizontal cell labeled via AAV virus (grey background, Melanie Samuel lab page, https://www.bcm.edu/research/labs/melanie-samuel) and lipophilic dye (black background). Horizontal cells extend, on average, six primary dendrites from the soma, branching to establish a dendritic field with an average diameter of 79 μm in the OPL. The axon broadens to form the thicker body of the terminal, giving rise to multiple branches, which in turn yield individual branchlets extending into the spherules of rods [24].

Despite the clear isolation of synaptic inputs at cell somata and axon terminals, both the somata and axon terminals of horizontal cells respond to a mixture of rod and cone inputs. Rod signals reach horizontal cell somata via rod-cone connexin 36 (Cx36)-containing gap junctions, whereas the axon terminals receive unidirectional cone inputs from the horizontal cell soma by way of the axon [27]. Horizontal cells support bipolar cell center-surround antagonistic receptive fields through a negative feedback (Fig. 1.8). Mechanistically, this negative feedback involves GABA or ephaptic interaction of horizontal cells and cones that causes the cone Ca^{2+} current to shift and restore glutamate release [28, 29]. Additionally, horizontal cells also contribute to bipolar and ganglion cell surround activation and surround antagonism following both prolonged light and dark adaptation [30]. They adjust the system's response to the overall level of illumination, subtracting a local image from a broad region of illumination and greatly reducing redundancy in the signal transmitted to the inner retina [13]. Horizontal cells employ two independent sets of homotypic gap junctions for coupling, either coupled by dendro-dendritic and axo-axonal gap junctions composed of Cx57 [31], or by Cx50 solely at the axon terminal network [32].

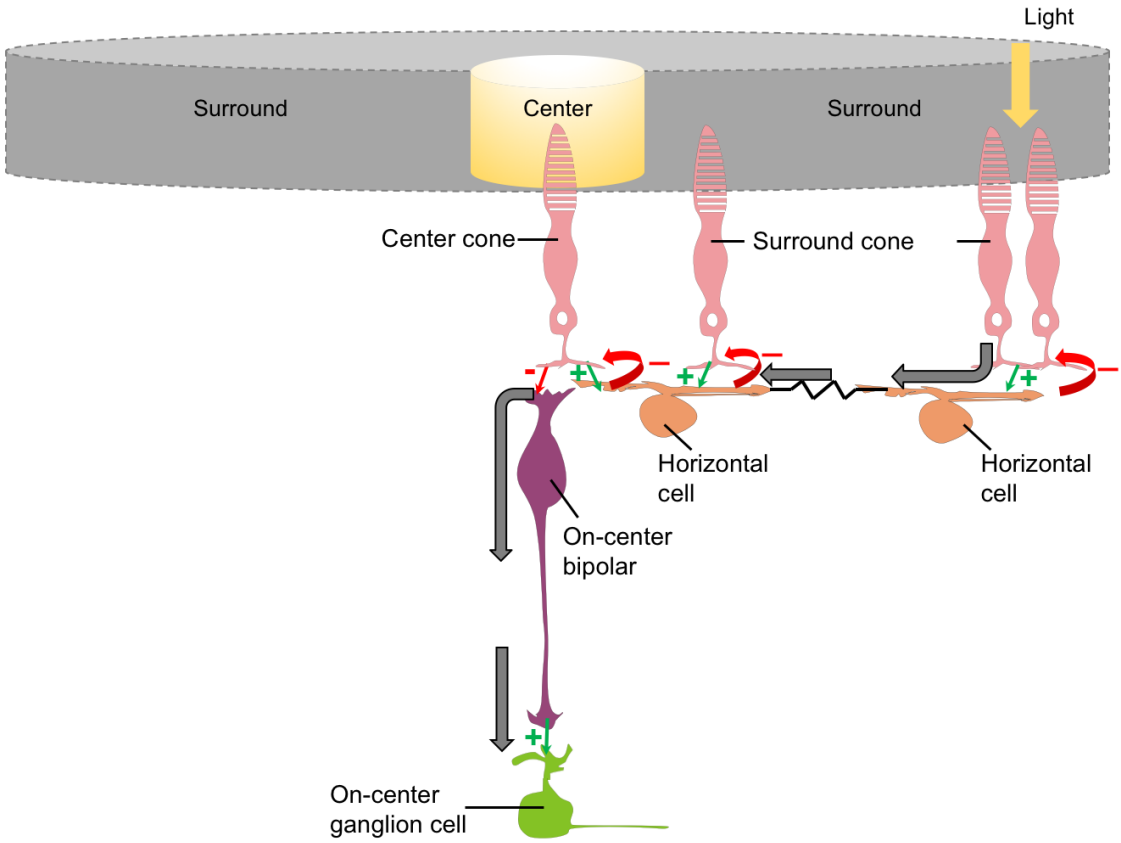

Fig. 1.8 Horizontal cells mediate the center-surround antagonistic organization of bipolar cells.

The mechanism is illustrated here for an on-center bipolar cell. The center light input is mediated by the cone-to-bipolar-to-ganglion cell synapses, while the surround input is predominantly mediated by the feedback pathway from electrical coupled horizontal cell network to cones. The mechanism of negative feedback of horizontal cells involves GABA. Illumination of cones in the bipolar cell's surround hyperpolarize those cones, which in turn hyperpolarize the postsynaptic and neighboring horizontal cells that are homotypically connected by gap junctions. The hyperpolarization of horizontal cells reduces the amount of inhibitory transmitter GABA release onto postsynaptic cones in the receptive field center. As a result, cones in the center depolarize, like they are in the darkness. This, in turn, allows suppression of on-center bipolar cells, the opposite effect of illumination in the receptive field center. Dopamine, as one of the modulators, decreases the coupling between horizontal cells, which is predicted to reduce the size of the antagonistic surround. This antagonism is proposed to have an important role in establishing the receptive field for bipolar cells and ganglion cells, which can be dynamically regulated in response to different light conditions, thus enhancing spatial information and contrast.

1.2.5 Amacrine cells

Amacrine cells, synaptically active in the IPL, are the most diverse group of cells in the retina, comprising ~41% of all cells in the mouse INL [7, 33]. Unlike horizontal cells which have a single broad role, 40 types of amacrine cells with different axon and dendritic architecture and neurotransmitter content carry out specialized tasks to integrate, modulate and interpose spatial and temporal properties of the visual signals passed to the ganglion cells [34, 35]. Some of amacrine cells are displaced into the GCL, making up 60% of the neurons in this layer in the mouse retina. Most amacrine cells receive their main bipolar cell synapses from cone bipolars, and make inhibitory synapses releasing GABA or glycine onto to bipolar cells, ganglion cells, and each other [35]. AII amacrine cells (Fig. 1.2B) are the best-characterized type, due to their indispensable role in rod signal pathway. They are bistratified, narrow-field, glycine-containing amacrine cells that graft the rod circuitry onto the cone pathways to transfer visual information from rod photoreceptors to ganglion cells [36]. In the ON sublamina, the descending arboreal processes output the information obtained from rod bipolar cells onto ON cone bipolar cells via the Cx36-Cx45 heterologous coupling. In contrast, the thick lobular appendages in the OFF sublamina provide output onto OFF-cone bipolar cells [11, 37] and OFF-ganglion cells through conventional inhibitory glycinergic synapses [38]. AII amacrine cells also form a large network with each other through direct Cx36-containing homologous gap junctions [39].

1.2.6 Dopaminergic amacrine neurons

Dopaminergic amacrine neurons (DA neurons) are another subset of amacrine cells whose cell bodies are predominately located at the border of the INL/IPL (Fig. 1.9). The size of the soma is about 12-15 μm in diameter. While there are only ~500 regularly and sparsely distributed DA neurons per mouse retina, each of them exhibits extensive process ramification and dendritic arborization in the outmost part of the OFF sublamina of the IPL (the stratum 1), and also to a lesser extent, descends obliquely to form a loose, tangential plexus in ON sublamina (stratum 3) [40, 41]. The DA cell body gives rise to 2-6 primary dendrites which branch 4-6 times in the stratum 1. The dendritic field of individual DA cells is large, approximately 800 μm measured by the long axis, and thus they overlap with those of neighboring DA neurons, forming a dense network. DA neurons have ascending axon-like fine processes that terminate in the OPL. In mouse retina, 2-3 axon-like processes arise either from the soma or from the primary dendrites, and further bifurcate successively. Similar to dendrites, axon-like processes also overrun each other, with each covering 10-25 μm in length [1]. With this unique architecture, DA neurons are able to reverse the information flow by receiving input in the IPL and then feeding it back to the OPL. GABA and dopamine (DA) are both released by the presynaptic endings of DA neurons [42]. Since it serves as the center of retinal circuit modulation, the studies of DA are especially important and necessary to unveil

mechanisms underlying the plasticity of the retina. We will take a deeper dive into next few sections and chapters to discuss what we have discovered in recent years, covering three main finding at the cellular, physiological, and behavioral levels.

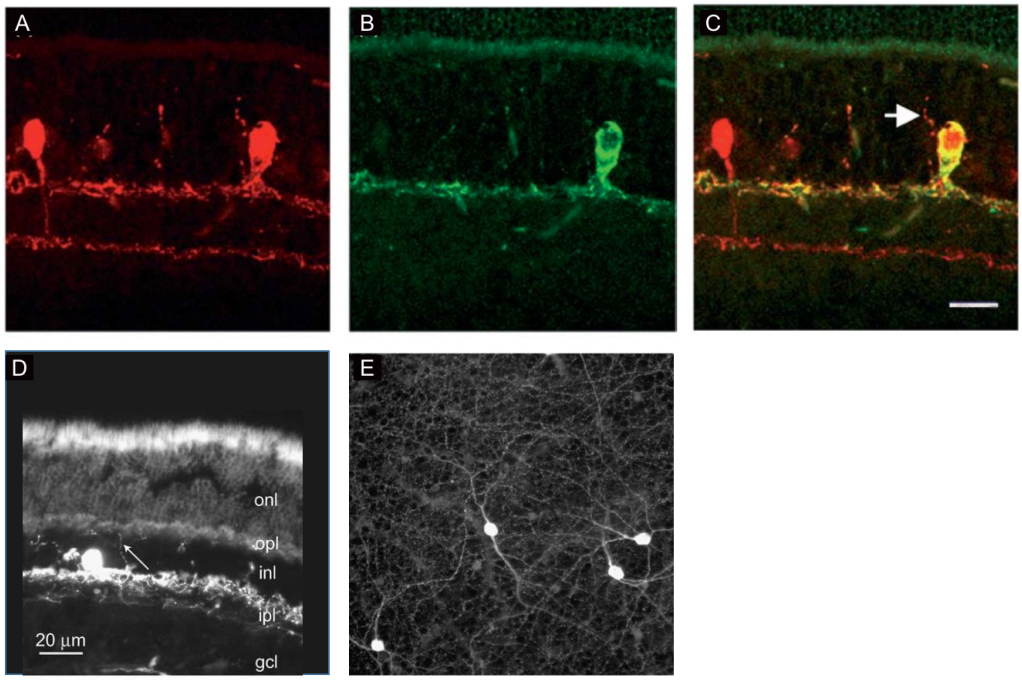

Fig. 1.9 Dopaminergic amacrine cells express tyrosine hydroxylase and branch dendrites in the outermost aspect of the OFF sublamina of the IPL.

(**A-C**) Images were obtained in mouse strain labeled transgenically with red fluorescent protein (RFP) driven by the TH-promoter (tyrosine hydroxylase, the rate-limiting enzyme of catecholamine synthesis) [43]. Two types of amacrine cells express *TH*-driven RFP as immunolabeled by anti-DsRed (**A**, red). Only DA cell are anti-TH immunoreactive (**B**, green). Compared to type 2 catecholaminergic cells, DA neurons have a larger cell body (on average, 13.7 vs. 9.5 µm of type 2 catecholaminergic cell), and branch dendrites primarily in the outer stratum 1 of the IPL, with a few processes, descend to stratum 3 (**B**, faint green line descends obliquely to the inner aspect of the OPL; **C**, the line shows in yellow). (**C**) Overlay of (**A**) and (**B**) shows DA cell in yellow and type 2 cell in red. (**D-E**) anti-tyrosine hydroxylase staining of dopaminergic retinal cells in rat retina [44]. (D) The arrow points to an ascending process which reaches the outer plexiform layer. (**E**) In a retina whole mount, DA neurons form an overlapping, dense plexus of dopaminergic network, forming small rings around the origin of the primary dendrites of AII amacrine cells at the distal IPL.

1.3 Retinal pathways input to dopaminergic amacrine cells

Dopamine (DA) is produced and released at the cell soma [45] as well as multiple sites along the widely-expanding processes, consistent with the global expression of tyrosine hydroxylase (TH), the rate-limiting enzyme in DA synthesis, throughout DA neurons (Fig. 1.10). Despite of the sparse distribution of DA neurons, DA reaches the most distal portions of the retina with extensive processes. Both DA synthesis and release are elevated under photopic conditions ranging from minutes of light exposure to hours [46-48]. In addition, DA synthesis and utilization are synchronized by light/dark (LD) cycles and retinal circadian clock, possibly subject to the feedback of melatonin, with increased levels during the day and decreased levels during the night [49].

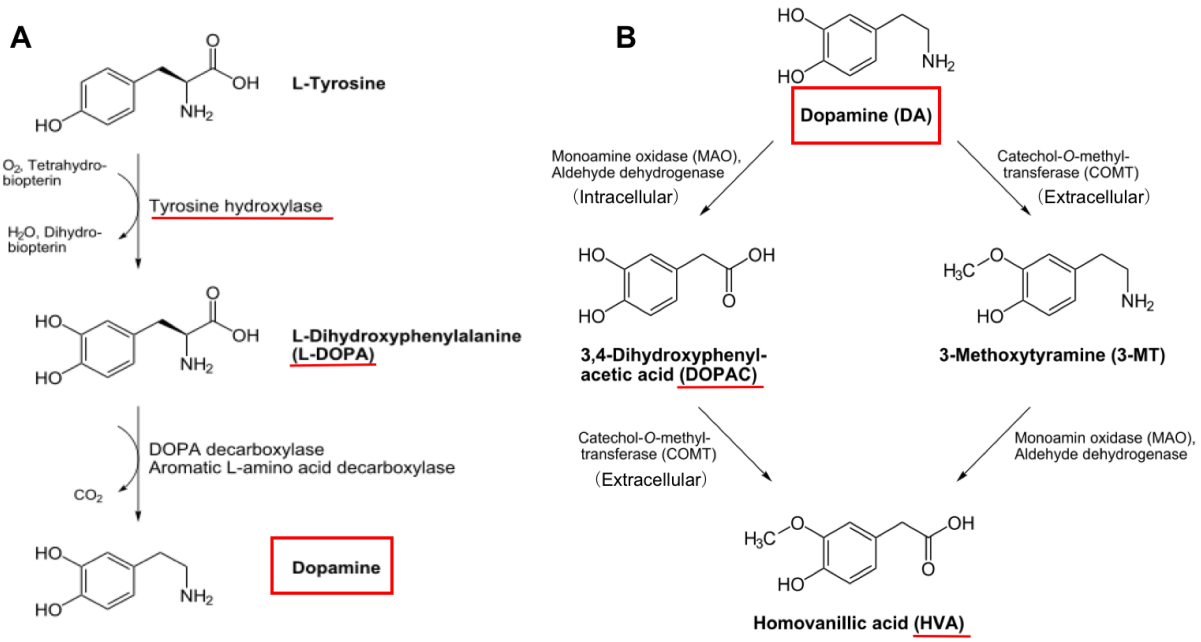

Fig. 1.10 Biosynthesis of DA and metabolism pathways.

(**A**) DA neurons convert the amino acid L-tyrosine to L-dihydroxyphenylalanine (L-DOPA) via hydroxylation of TH. L-DOPA then interacts with DOPA decarboxylase to form the active compound of interest, DA. In mouse line where TH is genetically knocked out in the retina, DA levels are reduced by 90%. Application L-DOPA, bypassing TH's control of synthesis, is commonly used to rescue DA deficiency and restore DA-related retinal visual functions. Once produced, DA is stored in vesicles by the vesicular monoamine transporter (VMAT) proteins and remains there until the cell depolarizes, enabling the vesicles to be released from the cell body and widespread dendritic network. (**B**) The inactivation of dopamine occurs first by the transporter-mediated reuptake of DA on DA neurons themselves. Recaptured DA is metabolized by intraneuronal monoamine oxidase MAO, converting into 3,4-dihydroxyphenylacetic acid (DOPAC), which is subsequently metabolized to homovanillic acid (HVA) via extracellular catechol-O-methyl transferase (COMT)[50]. DA also directly degrade to HVA extracellularly. DOPAC/DA and HVA/DA ratios are often used as an indicator of DA turnover and utilization [44] (modified from http://flipper.diff.org/app/pathways/1597).

DA neurons are considered as a morphologically homogenous class. However, DA release has revealed a surprising heterogeneity in different lighting conditions, including flickering light, steady light, and even prolonged darkness. Two distinct synaptic inputs have been identified to support DA functional heterogeneity. They generate two classes of light responses demonstrating different temporal dynamics in DA neurons (Fig. 1.11): (1) the majority of DA cells (transient DA neurons, t-DA neurons) receive information from rod/cone photoreceptors via ON-bipolar cells, and only exhibit a rapid burst of spikes elicited near the onset of the light stimulus; (2) the rest are sustained DA neurons (s-DA) driven by the ipRGCs, which maintain the light-evoked increase in firing frequency throughout the light duration [40, 51, 52]. In both pathways, DA neurons employ AMPA-type glutamate receptors to respond glutamate released by these two sources. In addition to light responsive pathways, a third circuit is formed by GABAergic and glycinergic amacrine cells to maintain the intrinsic bursting activity of DA neurons in the dark [40].

Because light evokes increases in firing frequency and DA release with no OFF responses [40], one would expect that DA cells receive excitatory synaptic input from ON-cone bipolar cells. However, the extensive anatomical projection of DA cell processes in the OFF sublamina appears to contradict the effect of photopic light on dopamine release. A plausible hypothesis is that DA cells contact ON-bipolar cells in a special manner that breaks the stratification rules of the IPL. Indeed, DA neurons smartly overcome this obstacle by forming contacts with cone ON-bipolar cells in both ON- and OFF-sublamina, and also contacting directly with the intrinsically photosensitive neurons in the GCL (see Section 1.2 intrinsically photosensitive retinal ganglion cells, ipRGCs). The axons of ON cone bipolar cells (type 6 cone bipolar cells in mouse) make *en passant* ribbon synapses with the dendrites of DA neurons as they pass through the OFF layer [52, 53]. Furthermore, as we mentioned in the previous section (Section 1.2 Dopaminergic amacrine cells) that DA neurons also send a few processes to more proximal stratum (stratum 3), where mouse type 5 cone bipolar cells make glutamatergic dyad synapses onto DA cell processes and receive reciprocal GABAergic synapses from DA neurons [40, 41]. It has not been fully understood whether a bipolar axon that ultimately synapses with DA cells in S3 would also connect *en passant* with DA cell dendrites in stratum 1, although current data suggest that mouse stratum 1 and stratum 3 synapses are possibly established by different types of bipolar cells.

The sustained-type light response of retinal DA neuron is melanopsin-dependent. M1 ipRGCs dendrites are in synaptic contact with DA cells in the OFF sublamina of the IPL [54-57]. DA cells, in turn, synaptically influences the activity and/or gene expression in ipRGCs via releasing DA or GABA, or both. DA cells are also implicated in guiding M1 cell dendrites to the OFF layer of the IPL [37]. The canonical flow of visual signals within the retina is completely reversed by this circuit. Light transduction initiates in ganglion cells (the canonical output neurons), is transmitted to the DA interplexiform cells in the INL,

which then make their output in the outer retina, potentially modulating photoreceptors. This novel retrograde light-signaling pathway is especially of interest, because it suggests a circuitry that links light-adaptation mediated by DA with central circadian rhythms dependent on ipRGC function. ipRGCs are specialized for sustained signaling of overall luminance, and therefore their intraretinal feedback is very likely to include circadian synchronization and sustained signaling. DA neurons, as the receiver, could be greatly influenced by ipRGCs in modulating light-adaptation and synchronization of retinal circadian rhythms [5,20]. The establishment of this retinal pathway shows a strong evidence that visual signaling has retrograde feedback circuits originating in ganglion cell, which influence outer retinal components partly through DA neurons.

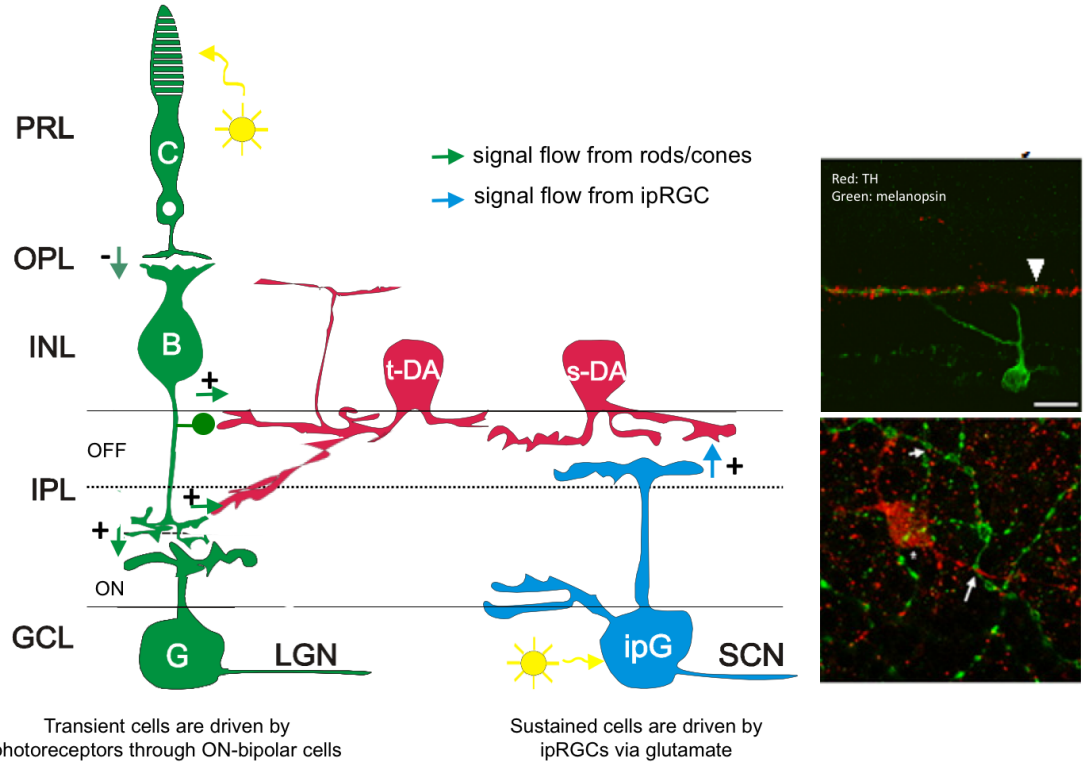

Fig. 1.11 The distinct light input pathways to DA cells give rise to two classes of light responses.

Green arrows show the light signal flow from rods and cones to transient DA cells through ON-bipolar cells and to the lateral geniculate nucleus (LGN) [58]. Blue arrows represent the light signal flow from melanopsin-positive intrinsic photosensitive retinal ganglion cells (ipRGCs) to sustained dopamine cells and to the suprachiasmatic nucleus (SCN). Yellow arrows represent light input. Both types of DA neurons respond to glutamate via AMPA/kainate-type glutamate receptors. The insert [57] shows ipRGCs (green) bifurcate and ramify dendrites extensively in the stratum 1 of the IPL, where they form a discrete plexus with dendrites of DA amacrine cells (red) (upper insert). Large arrow indicates a putative point of contact between the proximal dendrites of DA cells and varicosities of ipRGCs. The small arrow indicates a putative point of contact between the smaller axonal varicosities of DA cells and melanopsin-positive varicosities (lower inset). A plus indicates a sign-conserving synapse; a minus represents a sign-inverting synapse. C, cones; B, on-center cone bipolar cells; t-DA, transient DA cells; s-DA, sustained DA cells; G, conventional ganglion cells; ipG, melanopsin-expressing intrinsically photoreceptive ganglion cells; PRL, photoreceptor layer; OPL, outer plexiform layer; INL, inner nuclear layer; IPL, inner plexiform layer; OFF, the outer, OFF sublamina of the IPL; ON, the inner, ON sublamina of the IPL; GCL, ganglion cell layer; LGN, the thalamic visual nuclei of the brain that are innervated by conventional ganglion cells; SCN, the hypothalamic master biological clock nuclei that are innervated by ipRGCs (modified from Zhang DQ, 2008 [58])

1.4 Dopamine reconfigures retinal circuits for high-resolution, light-adapted vision

In the retina, the central neuromodulatory system lies in the DA neurons. The dopaminergic output from DA neurons restructures retinal function by modulations of chemical and electrical synapses, as well as by modifications of the functional properties of retinal neurons. The overall effect of DA on retinal function has been hypothesized to involve in multiple aspects of light adaptation. DA influences all levels of retinal circuitry and all layers of neurons primarily through volume conduction [59-61]. Four of the five dopamine receptor subtypes are expressed (D1, D2, D4, D5), while D3 receptor transcripts are so far not detectable in the mammalian retina. Dopamine receptors are grouped into two families based on their actions on the cyclic adenosine monophosphate (cAMP) level: D1-like receptors, including D1 and D5 receptors, activate adenylate cyclase (AC) and increase cAMP in the target cells, whereas D2-like receptors, including D2 and D4 receptors, cause a decrease in cAMP by inhibiting AC activity [44]. Many studies, using autoradiography and immunocytochemistry, have sought where in the retina different receptor subtypes are located. We have known that D5 receptors show in the pigment epithelium [62] and ganglion cells [63], while mouse rod and cone photoreceptors mainly express D4 receptors [64]. D1 receptors are commonly present in the INL and GCL, but not in photoreceptors [65, 66]. DA neurons themselves also express D2 receptors, which function to inhibit DA release [67]. D1 receptors display much lower sensitivity (2 to 3 orders of magnitude lower) to DA and thus respond selectively to the high levels of retinal DA achieved during light adaptation. D4 receptors, on the other hand, can be activated in darkness by more modest circadian clock-driven daytime increase in baseline retinal DA [68]. The higher sensitivity of D4 receptor to DA may be important, given that D4 receptors are found on cones in the mouse OPL, which is the retinal cell group distant from the source of DA.

Out of these 4 subtypes, D1 and D4 receptors are particularly interesting due to their prominent and separate roles in retinal dopaminergic signaling [2] (Fig. 1.12). D1 receptor signaling specifically supports increased amplitude of photopic light responses and high acuity in the presence of background-adapting light, whereas D4 receptor signaling contributes to the enhancement of contrast sensitivity and circadian regulation of light response amplitude [2]. Many studies have attempted to resolve the cellular mechanisms underlying the discrete roles of these two receptors. The influence of DA via D1 receptors on electrical synapses is well documented, including decreasing the coupling of horizontal cells [69] and AII amacrine cells [70, 71], as well as increasing those of OFF α-ganglion cells [72]. There is considerable evidence supporting the notion that uncoupling of horizontal cells by DA underpins the contraction of ganglion cell receptive field surround [1, 73, 74], leading to increased spatial resolution (high acuity), although the contribution of dopaminergic modulation of horizontal cells to receptive field organization has been challenged by other inner retina mechanisms [75-77]. The increase in OFF α-ganglion cell coupling triggered by D1 receptors augments the concerted ganglion cell activity under light conditions,

thereby increasing the capacity and efficiency of the visual information flow to the brain [72]. DA also alters functional properties of retinal neurons via D1 receptors, such as horizontal cell calcium channel currents [78], bipolar [79] and ganglion cell [63, 80-83] sodium currents, and melanopsin-containing M1(ipRGC, M1) ganglion cell photocurrent [84]. D4 receptors, in contrast, are highly expressed in mouse cones and in the inner retina [20], having effects on rod-cone coupling [85], cone adaptation [86] and ganglion cell coupling [72, 87]. D4 receptor-based disruption of rod-cone coupling, together with AII amacrine cell coupling regulated by D1 receptors, largely restricts the flow of visual signals from rods to ganglion cells during light-adapted condition [1].

The widespread expression and functional diversity of DA receptors illustrate the actions of DA in initiating slow sustained changes in the physiology of retinal neurons and synapses. DA fundamentally alters retinal circuits and processing of visual signals to support light-adapted vision. The resultant effects ensure that the retina prioritizes visual signals from cone photoreceptors, improves the spatial resolution and contrast sensitivity, and strengthens the capacity and efficiency of information flow across the optic nerve. Moreover, DA is also involved in the circadian regulation of light-adapted responses, which may contribute to prompting the system for daily changes of prevailing illumination conditions and signals.

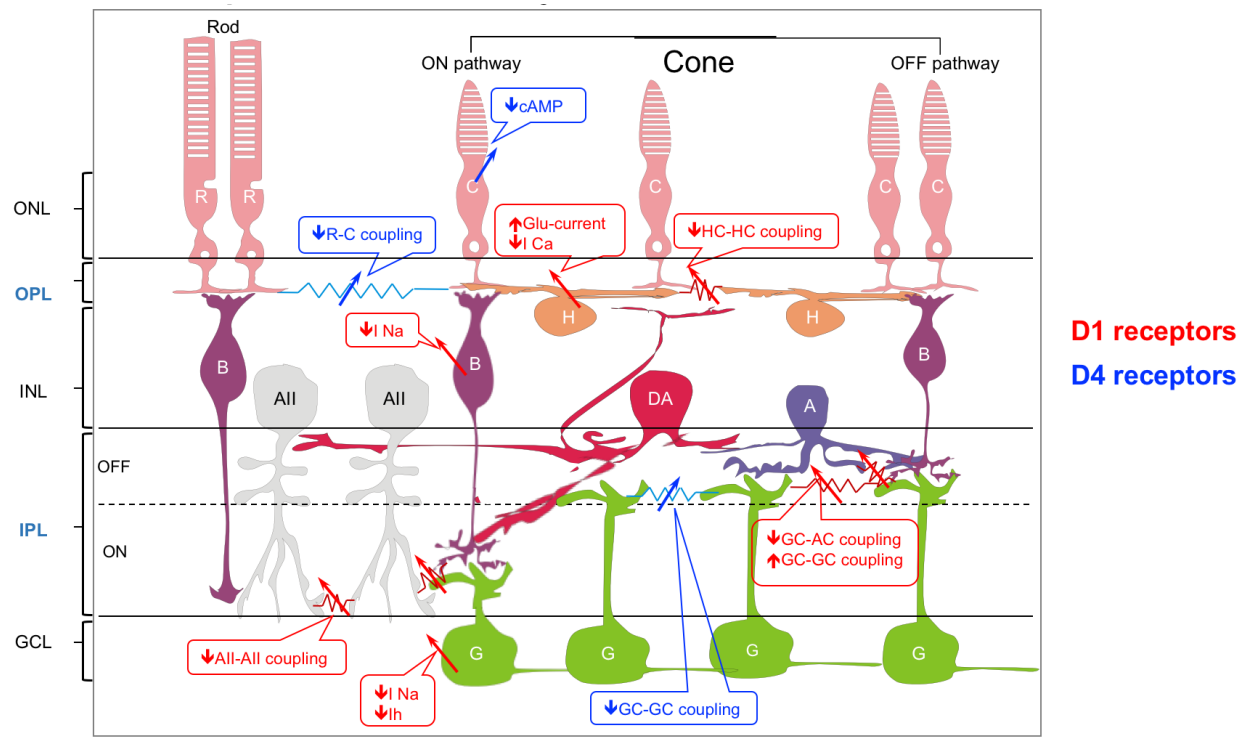

Fig. 1.12 D1 and D4 receptors direct differential actions on major neurons and electrical coupling.

D1 receptors (shown in red) are primarily expressed on the cells in the INL and GCL, whereas D4 receptors (shown in blue) are dominant on cones. The activation of receptor signaling in response to dopamine release by volume transmission not only changes the connectivity of gap junctions, but also alters the properties of retinal neurons.

1.5 Useful tools to assess the role of retinal dopamine in vision

We have employed three main tools, namely genetic, electrophysiological and psychophysical techniques, to accelerate our study in understanding of how DA regulates retinal circuits underlying spatiotemporal resolution vision.

Genetic tools provide us with a platform where we create mouse models that carry retina- or retinal cell-specific modifications of important DA-related genes, thus avoiding widespread effects on the rest of the brain, or retina, by any systemic pharmacological or genetic manipulation of the dopaminergic system. The creation of the retinal DA depletion mouse line (rTHKO) was led by Dr. Chad Jackson, whose study confirmed that the reduction of retinal DA disrupts 4 specific aspects of light-adapted vision, causing low amplitude light responses in the presence of adapting background light, low acuity, low contrast sensitivity, and the loss of circadian regulation of light response amplitude [2]. Retinal DA is necessary for mediating multiple dimensions of vision, under the condition that brain DA levels are preserved in the rTHKO model. This study lays a foundation for our future work in elucidating differential actions of dopamine D1 and D4 receptors on specific retinal function by designing horizontal cell-specific D1 receptor and cone-specific D4 receptor knockout mouse lines. Our progress in developing innovative and appropriate mouse models facilities the field's understanding of retina dopaminergic system, and also overcomes the long-standing limitation of the inability to study the effects of retinal DA on vision in intact animals [2].

The electroretinogram (ERG) is a method to noninvasively assess the physiological integrity of the retina in a live animal. It is a graphical representation of field potential changes across the eye elicited by a light stimulus (Fig.) [88]. In our study, we used the flash ERG, in which the massed electrical activity of retinal response to a discrete flash of light was recorded under either dark (scotopic ERG)- or light-adapted (photopic ERG) background illumination. Different ERG protocols assess the retina's ability to adapt to changes according to prevailing illumination, mimicking night vision (scotopic ERG) or the transition from nighttime to daytime vision (photopic ERG)[89]. Each of several discrete components is attributed to a specific cellular origin and event in the transfer of visual information through the retina. The a-wave is the negative deflection at the beginning of the response (reflecting a corneal negative potential), which reflects the first event in visual transduction: activation of photoreceptors by light. In the mouse, the measurable a-wave is driven by rods, since mouse cones are too few to contribute significantly to the a-wave. However, some species (including humans) with more cone-rich retinas can have a large cone a-wave. Subsequent to the a-wave, the b-wave, shown as a corneal positive deflection, is thought to reflect the activity of second-order neurons, specifically ON-bipolar cells that respond following the photoreception by either rods or cones. Superimposed on the b-wave, high frequency wavelets, termed as oscillatory potentials, represent the activation of amacrine and/or ganglion cells. Other components, such

as c- and d-wave, may also appear depending on the duration of the flash stimulus and recording conditions [90].

Because of the noninvasive nature of the test, ERG has been commonly used as a diagnostic test in the clinical setting for detecting abnormality of human retinal physiology caused by various disease conditions, such as Parkinson's disease and aging [91-93]. The finding of signature ERG waveforms in disease-related mouse models could have great implications for inventing new diagnostic methods for human subjects, who suffer from the same condition. Over the years clinical ERG recording techniques have become progressively more sophisticated. For example, optical coherence tomography (OCT) and pattern ERG techniques enable more precise mapping of dysfunctional areas of the retina [94].

Multi-electrode array (MEA) is an advanced tool for electrophysiological studies of *in vitro* retina at the cellular level. Unlike the conventional cell-attached patch-clamp recording with which researchers record individual neurons in succession [95], MEA allows measurements of many neurons at multiple sites simultaneously by consisting of dozens of electrode contacts. It assesses the spontaneous and light-evoked electrical properties of single retinal ganglion cells, measuring neuron firing patterns under various visual stimuli [96]. MEA recordings are especially powerful and efficient in the retina, because of the layered structure with ganglion cells which lie close to the proximal surface. With MEA, we are able to quantify the effects of specific modifications of the dopaminergic system, which disrupt the processing of the visual input in the neural circuits and culminate at the output ganglion cells [97]. In our experimental setting, we extracted the retina from the eye and placed it ganglion cell-side down onto the electrodes of the MEA chamber containing carboxygenated Ames' solution. We stimulated the tissue from the top of the MEA with 10x objective lens. Different light stimulation protocols measured ganglion cells' response polarity, response duration, size of the receptive field, light adaptation curve, acuity, contrast sensitivity, and direction-selectivity in various mouse lines.

Mouse vision can also be quantified by a behavioral method, optokinetic tracking (OKT), emphasizing the assessment of visual acuity and contrast sensitivity threshold in behaving mice. To examine our visual acuity, we would go to see an eye doctor and read an eye chart to measure how well we can see the letters of different shapes and sizes. A mouse, however, cannot tell the researchers whether it has a trouble recognizing the stimuli we present to them. To solve this difficulty, Dr. Glen Prusky's group developed a virtual-reality OKT system to simply and rapidly quantify the spatial vision of mice [98]. They took advantage of reflexive head movements of the mouse in response to a recognizable stimulus which is a rotating sine-wave gradient projected surrounding the mouse. The mouse reflexively moves its head to track in the same direction and speed as the rotation of the sine-wave gradient if the retina can resolve the stripes. The acuity threshold is measured by increasing spatial frequency of the grating (i.e. decreasing the size of black/white bars of the gradient) until the animal no longer responds.

For the contrast sensitivity, the contrast of the black/white bars starts with 100% (i.e. pure black and white) and reduces to the level that the animal thinks the stimulus is homogeneous grey. OKT tracking helps us to identify and screen for a wide range of visual phenotypes in mouse models. Recently, a novel automated system that robustly detects both head and eye movements in mice has been introduced, and thus providing a device and algorithms of improved objectivity and ease of use [99].

CHAPTER II

Attention-Deficit/Hyperactivity Disorder-Associated Dopamine Transporter Variant Val559 Alters Retinal Function *in vivo*

2.1 Summary

Dopamine (DA) is a critical neuromodulator in the retina. Disruption of retinal DA synthesis and signaling significantly attenuates light-adapted, electroretinogram (ERG) responses, as well as contrast sensitivity and acuity. As these measures can be detected noninvasively, they may provide opportunities to detect disease processes linked to perturbed DA signaling. Recently, we identified a rare, functional DA transporter (DAT, SLC6A3) coding substitution, Ala559Val, in subjects with attention-deficit/hyperactivity disorder (ADHD), demonstrating that DAT Val559 imparts anomalous DA efflux (ADE) with attendant physiological, pharmacological, and behavioral phenotypes. To understand the broader impact of ADE on ADHD, noninvasive measures sensitive to DAT reversal are needed. Here, we explored this question through ERG-based analysis of retinal light responses, as well as HPLC measurements of retinal DA in DAT Val559 mice. Male mice homozygous (HOM) for the DAT Val559 variant demonstrated increased, light-adapted ERG b-wave amplitudes compared to wild-type (WT) and heterozygous (HET) mice, whereas dark-adapted responses were indistinguishable across genotypes. The elevated amplitude of the photopic light responses in HOM mice could be mimicked in WT mice by applying D1 and D4 DA receptor agonists and suppressed in HOM mice by introducing D4 antagonist, supporting elevated retinal DA signaling arising from ADE. Following the challenge with amphetamine, WT exhibited an increase in light-adapted response amplitudes, while HOM did not. Total retinal DA content was similar across genotypes. Interestingly, female DAT Val559 HOM animals revealed no significant difference in photopic ERG responses when compared with WT and HET littermates. These data reveal that noninvasive, in vivo evaluation of retinal responses to light can reveal physiological signatures of ADE, suggesting a possible approach to the segregation of neurobehavioral disorders based on the DAT-dependent control of DA signaling.

* This chapter has been published. Dai H., Jackson C.R., Davis G.L., Blakely R.D., McMahon D.G. J Neurodev Disord. 2017 Dec 28;9(1):38 [100]. Dai H., Jackson C.R., Blakely R.D., and McMahon D.G. designed the research; Dai H. performed the research; Davis G.L. contributed mice, genotyping tools, and advice on animal use; Dai H. and McMahon D.G. analyzed data; and Dai H., Blakely R.D., and McMahon D.G. wrote the paper.

2.2 Introduction

The neurotransmitter dopamine (DA) exerts powerful control over brain circuits that regulate reward, attention, and locomotor activity [101-103]. Accordingly, DA dysfunction is believed to contribute to the etiology of several neuropsychiatric disorders, including attention-deficit/hyperactivity disorder (ADHD) [104, 105], bipolar disorder (BPD) [106], schizophrenia [107, 108], and Parkinson's disease [109-111]. Interestingly, increasing evidence supports findings that patients with these diseases exhibit impaired retinal and visual functions, suggesting that altered DA signaling in the retina may be under the control of the same molecular perturbations that support the etiology of these disorders [2] and that assessment of retinal DA signaling might offer a novel window into the diagnosis and treatment of neuropsychiatric disorders.

In the retina, DA mediates light adaptation and exhibits circadian rhythms of synthesis and release, such that DA signaling is higher during the daytime and during light exposure [49, 112]. DA is secreted by amacrine neurons in the inner nuclear layer of the retina, and it mediates feedback of photic information to the outer retina from the inner retina [40, 86]. DA-secreting amacrine cells influence other retinal neurons through volume conduction [61]. Among the retinal targets of DA, the influence of DA on electrical synapses is well described. Specifically, DA uncouples the gap junctions between horizontal cells [69], AII amacrine cells [70, 113], and rods and cones [85], leading to a reduction of receptive field size and blockade of rod signaling to ganglion cells. As a result, retinal circuits are reconfigured to a light-adapted state with increased light-induced response amplitudes in the presence of background light and enhanced acuity [2]. Retinal DA signaling is reflected in the amplitude of the photopic electroretinogram (ERG) with retinal-specific DA depletion producing decreased ERG amplitudes and rescue of retinal DA levels with L-DOPA restoring ERG amplitudes [2]. In addition, contrast sensitivity, spatial acuity, and circadian rhythms of light-adapted responses are all compromised in absence of retinal DA, further confirming that DA is important for light-adaptive mechanisms [2]. DA exerts its action on target neurons and circuits through D1-like (D1 and D5) and D2-like (D2, D3, and D4) receptors. In the retina, D4 receptor-mediated signaling pathways modulate light-adapted ERG rhythms and contrast sensitivity, whereas D1 receptor signaling contributes to high light-adapted ERG b-wave amplitudes and high spatial resolution [2].

The DA transporter (DAT, SLC6A3) is a key determinant of DA signaling capacity in the brain, limiting the action of the neurotransmitter through high-affinity clearance of extracellular DA, with recycling of DA into the presynaptic cytosol [114]. In the absence of DAT, extracellular DA levels are elevated in the striatum [115] whereas intra-neuronal levels of DA are decreased [114, 116]. The psychostimulant amphetamine (AMPH), structurally similar to DA, competes with extracellular DA at DAT and also induces DAT-mediated, non-vesicular release of cytosolic DA, providing two routes for

elevation of extracellular DA levels. AMPH formulations and other agents that elevate extracellular DA (e.g., methylphenidate, MPH, Ritalin™) are also commonly prescribed for the treatment of ADHD (e.g., Adderall [117, 118]). In addition to its significant expression in the brain [119], DAT is also expressed in the somata and processes of dopaminergic amacrine cells in rat and mouse retina [120, 121]. In DAT-knockout mice, a significant decrease in retinal sensitivity is observed under dark-adapted (scotopic) conditions [122]. DAT has also been suggested to play a role in form-deprivation myopia, as DAT binding in myopic retinas is lower than that in the normal control eyes [123].

Genetic variation in DAT has functional consequences for brain DA signaling and behavior. Recently, we identified a rare human DAT coding substitution (DAT Ala559Val) in two male siblings diagnosed with ADHD [105]. The Val559 variant had been previously identified in a female subject with bipolar disorder (BPD) [124] and following our ADHD report, was identified in two unrelated male subjects with autism spectrum disorder (ASD) [125]. In both heterologous expression studies [34, 35] and in the DAT Val559 knock-in mouse model [126, 127], there was anomalous dopamine efflux (ADE) consistent with changes in DAT function. In the mouse model, we observed an altered pattern of locomotion with decreased vertical activity and increased horizontal locomotion speed (darting) in response to imminent handling, significantly elevated extracellular levels of striatal DA under basal conditions without a change in DA tissue content, and a blunted response to AMPH or MPH paralleled by reduced locomotor activation by these psychostimulants [127]. We have previously proposed [126] that ADHD drugs containing AMPH formulation block the ADE of DAT Val559, which is distinct from blocking reuptake. In the former case, normal excitation coupling to vesicular release is restored, whereas in the latter case, the coupling to release is not modulated, only the amplitude of the response. We propose that it is the "noise" from a leak that is more of a problem, at least for a subset of subjects, and thus, the release of DA cannot be sensed appropriately. Ex vivo brain slice studies revealed tonic presynaptic DA receptor activation that supported a blunting of depolarization-evoked DA release. Altogether, our findings in the DAT Val559 model reveal a state of tonic hyperdopaminergia that leads to changes in locomotor patterns and anomalous responses to psychostimulants.

Although rare, the DAT Val559 variant may represent a genetic form of a functional state common to the broader etiology of idiopathic ADHD. If true, noninvasive tests of DA action that can be employed in ADHD subjects demonstrating ADE may allow for improved ADHD diagnosis and/or treatment. In the current study, we sought to evaluate DA-sensitive measures in the retina that can be detected using ERG. Specifically, we determined whether the DAT Val559 allele alters light-adapted retinal responses under basal conditions and as a consequence of AMPH administration. We observed DAT Val559 animals exhibit retinal responses consistent with the reported role of the variant in elevating tonic dopaminergic

signaling and blunted responses to AMPH. Moreover, we observed differential retinal responses dependent on sex, which is of interest given the sex bias in ADHD diagnoses [128].

2.3 Materials and Methods

2.3.1 Animal usage and care. All animal protocols were approved and in accordance with the guidelines established by the Vanderbilt University Animal Care Division and the National Institutes of Health Guide for the Care and Use of Laboratory Animals. WT, homozygous (HOM), and heterozygous (HET) Val559 DAT littermates with a hybrid background (~ 75% 129S6/SvEvTac and ~ 25% C57BL/6 J) [127] were reared in a 12-h-light and 12-h-dark lighting condition. Only animals aged postnatal day 40 (P40) to P120 were subject to further tests. Unless otherwise noted, mice were tested or humanely killed during the middle of light phase of their light cycles (10:00 A.M.–2:00 P.M, Central Standard Time). The light intensity of the housing room was 100 ± 15 lx, provided by fluorescent bulbs. Mice were provided with water and food *ad libitum*.

2.3.2 Electroretinogram (ERG). The ERG was used to measure global retinal responses to light stimuli using the LKC Technologies UTAS visual electrodiagnostic test system (Gaithersburg, MD). Scotopic and photopic ERG recordings were performed as previously described [2, 129]. All animals were dark-adapted overnight (~ 16–20 h) and tested during 4–8 h after subjective light onset (6:00 A.M., Central Standard Time). Mice were anesthetized with an intraperitoneal injection (IP injection) of ketamine (70 mg/kg) and xylazine (7 mg/kg), and their pupils dilated with 1% tropicamide (AKORN, NDC17478–102-12, Lake Forest, IL) under dim red light (Kodak GBX-2 Safelight, Rochester, NY). Their eyes were kept moist with 1% carboxymethyl-cellulose sodium eye drops (CVS, Extra Strength Lubricant Gel Drops Dry Eye Relief, Woonsocket, RI), and core body temperature was maintained at ~ 37.0 °C using a thermostatically controlled heating pad regulated by a rectal temperature feedback probe (CWE, Model TC-1000 Temperature Controller, Ardmore, PA). Needle electrodes placed in the middle of the forehead and the base of the tail served as reference and ground leads, respectively. A gold contact lens electrode was used for recording ERG responses (LKC Technologies; #N30).

Scotopic ERG responses were differentially amplified and filtered (bandwidth 0.3–500 Hz), with responses digitized at 1024 Hz. The recording epoch was 250 ms, with a 20-ms prestimulation baseline. Stimulus flashes were presented in an LKC BigShot ganzfeld. A total of 15 stimulus intensities, ranging from – 6.50 to 2.00 log cd*s/m^2, were used under dark-adapted conditions. Each flash duration was 20 μs, and stimuli were presented in order of increasing intensity. As flash intensity increased, retinal dark adaptation was maintained by increasing the interstimulus interval from 30 to 180 s.

For photopic ERGs, mice were first given two flashes (–0.1 log cd*s/m^2) under dark-adapted conditions to assess for a normal retinal response. A steady background-adapting field (40 cd/m^2) inside the UTAS BigShot ganzfeld followed to saturate rod photoreceptors, and simultaneously, 0.90 log cd*s/m^2 bright light flashes were presented at 0.75 Hz for a light adaptation session of 16 min. Data were collected and averaged in 2-min bins, totaling 8 bins. All other test parameters were similar to the scotopic ERG.

For the photopic ERG rescue experiment, IP injection of 1 mg/kg D1 receptor agonist (SKF38393, Sigma-Aldrich, Cat# D047, St. Louis, MO) and 1 mg/kg D4 receptor agonist (PD168077, Tocris Bioscience, Cat# 1065, Bristol, United Kingdom) were administered to WT mice 1 h before testing. Mice were injected under dim red light and returned to dark box until testing.

For the photopic ERG suppression experiment, IP injection of 1 mg/kg selective D4 DA receptor antagonist (L-745,870, Tocris Bioscience, Cat# 1002) was administered to HOM mice for 5 days 30 min prior to light onset in the morning. On the fifth day, animals were subject to photopic ERG tests.

The effects of D-AMPH on light-adapted ERG were explored by IP injections of 4 mg/kg AMPH to HOM and WT mice 15 min before the testing.

The scotopic a-wave was measured from the onset of flashes to the trough of the first negative deflection and b-wave was from the trough of the a-wave to the peak of the b-wave amplitude. Regarding photopic recordings, only b-wave amplitude could be reliably measured, which was defined as the difference from the onset of the stimuli to the peak of b-wave.

2.3.3 HPLC determination of DA and its metabolites. Animals from all groups were dark-adapted overnight (~ 16-20 h) and then sacrificed under either dark or light conditions. Retinas were collected, immediately frozen in liquid nitrogen in 1.5-mL tubes, and stored at – 80 °C until processed for HPLC analysis. Under dark conditions, mouse retinas were dissected from the whole eye and separated from the retinal pigment epithelium in the presence of dim red light (Kodak GBX-2 Safelight). Under light conditions, after approximately 15 min lighting exposure, retinas were obtained in the presence of room lighting similar to the background light during the photopic ERG test. HPLC analyses were conducted in the Vanderbilt Brain Institute Neurochemistry Core.

Retinas were homogenized, using a tissue dismembrator, in 100–750 µL of 0.1 M TCA, which contained 10^{-2} M sodium acetate, 10^{-4} M EDTA, 5 ng/mL isoproterenol (as internal standard), and 10.5% methanol (pH 3.8). Samples were spun in a microcentrifuge at 10,000 g for 20 min. The supernatant was removed and stored at – 80 °C [130]. The pellet was saved for protein analysis. The supernatant was thawed and spun for 20 min, and samples of the supernatant were then analyzed for biogenic monoamines. Retinal biogenic amines were determined by HPLC using an Antec Decade II (oxidation 0.65)

electrochemical detector operated at 33 °C. Twenty microliter samples of the supernatant were injected using a Waters 2707 autosampler onto a Phenomenex Kinetex (2.6 μm, 100Å) C18 HPLC column (100 × 4.60 mm). Biogenic amines were eluted with a mobile phase consisting of 89.5% 0.1 M TCA, 10^{-2} M sodium acetate, 10^{-4} M EDTA, and 10.5% methanol (pH 3.8). The solvent was delivered at 0.6 mL/min using a Waters 515 HPLC pump. Using this HPLC solvent, the following biogenic amines elute in the following order: dihydroxyphenylacetic acid (DOPAC), DA and homovanillic acid (HVA) [131, 132]. HPLC control and data acquisition are managed by Empower software. In this report, retinal biogenic amine analyses are represented as ng/mg protein. Total retinal protein concentration was determined using BCA Protein Assay Kit (Thermo Scientific, Cat# 23225, Waltham, MA). Ten-microliter tissue homogenate was distributed into a 96-well plate and 200 μL of mixed BCA reagent (25 mL of protein reagent A is mixed with 500 μL of protein reagent B) was added. Incubate the plate at room temperature for 2 h for the color development. A bovine serum albumin standard curve was generated at the same time, spanning the concentration range of 20–2000 μg/mL. The absorbance of standards and samples were measured at 562 nm. The inter-day variation of biogenic amine analysis using HPLC with electrochemical detection has been determined for the following analytes as: DOPAC, 2.3%; DA, 1.2%; 5- HIAA, 4.3%; HVA, 2.6%; 5-HT, 8.6%; and 3-MT, 10.2%. The intra-day variation for these analytes are DOPAC, 2.7%; DA, 0.8%; 5-HIAA, 1.2%; HVA, 2.6%; 5-HT, 8.8%; and 3-MT, 7.1%.

2.3.4 Statistical analysis. Two-tailed t-test and one- and two-way ANOVAs were used where applicable and reported. *Post hoc* analyses followed ANOVAs to confirm the difference among groups. Significance levels were set at $P < 0.05$ and represented as means ± SEM as indicated in each graph (GraphPad, La Jolla, CA and Sigmaplot, San Jose, CA).

2.4 Results

2.4.1 DAT Val559 homozygous male mice have increased light-adapted retinal responses

To evaluate the impact of the DAT Val559 variant on retinal function in vivo, we measured retinal responses in male DAT Val559 homozygous (HOM), heterozygous (HET), and wild-type (WT) animals under dark-adapted and light-adapted conditions and used the ERG positive b-wave amplitude as the readout. All recordings were made at midday in the 12:12 light-dark cycle that the animals were maintained on, under dark-adapted or light-adapted conditions.

Dark-adapted ERG responses were recorded after overnight dark adaptation. Full-field light flashes of increasing intensity were presented to the animals on a completely dark background. This test measures the summed responses of rod and cone photoreceptors (corneal negative a-wave) and ON-bipolar cell responses (corneal positive b-wave) to flashes of increasing light intensity. Although HOM showed a

small decreasing trend in rod sensitivity, statistically, we observed no significant difference in a- and b-wave amplitudes in DAT Val559 HOM and HET animals compared to WT littermates under dark-adapted conditions (Fig. 2.1A, a-wave; $P = 0.32$; b, b-wave; $P = 0.08$, two-way ANOVA), in agreement with previous results with genetic suppression of retinal DA synthesis [2, 133].

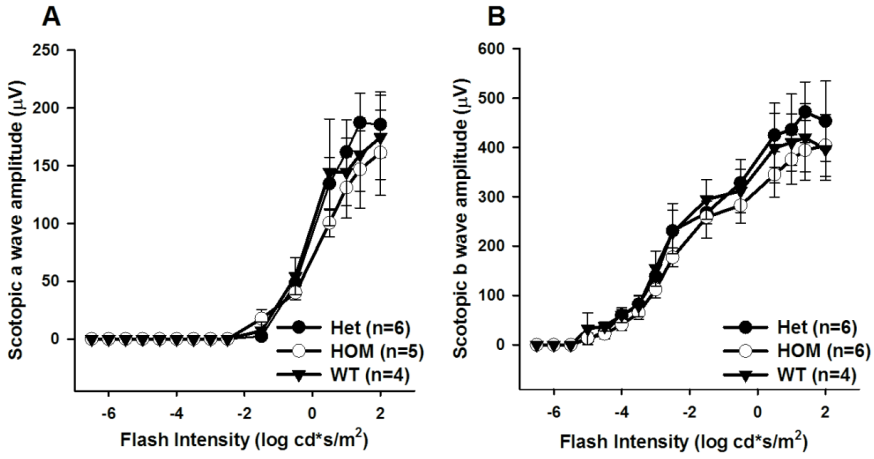

Fig. 2.1 The dark-adapted ERG is not affected by the DAT Val559 mutation in male mice.

Dark-adapted a-wave (**A**) and b-wave (**B**) amplitudes (μV) are plotted as a function of stimulus intensity (log cd*s/m^2) in Val559 homozygous (HOM: open circles), heterozygous (HET: filled circles), and wild-type (WT: filled triangles) animals. There is no significant effect of genotype on either a-wave or b-wave as revealed by two-way ANOVA (a-wave: $F_{(2,180)} = 1.146$, $P = 0.32$; b-wave $F_{(2,195)} = 2.530$, $P = 0.08$; $n = 4$–6 mice). All data are represented as means ± SEM.

Light-adapted ERG responses were assessed using bright light flashes in the presence of rod-saturating, light-adapting background illumination over a period of approximately 16 min. This test assays the transition from dark-adapted to light-adapted vision, indicating the retina's ability to adapt to background illumination. Cone-driven ERG responses increase over time as the retina adapts to the rod-saturating background, and this adaption is dependent on retinal DA [2]. Thus, we expected that mice harboring DAT Val559 would exhibit enhanced retinal ERG responses during light-adaptation. WT, DAT Val559 HOM, and HET groups all exhibited increases in b-wave amplitude with time in light adaptation. However, the DAT Val559 HOM mice displayed significantly elevated photopic b-wave amplitudes at each level of light adaptation as compared with WT and HET littermates, whereas WT and HET were indistinguishable (Fig. 2.2A; HOM vs. WT and HET, $^{***}P < 0.001$, two-way ANOVA). As the increased light-adapted ERG amplitude is mediated by DA acting through D1 and D4 receptors [2], we tested whether the increased b-waves observed in the DAT Val559 HOM mice also used these signaling pathways. The light-induced increase in b-wave amplitude in HOM was mimicked by applying D1 and

D4 DA receptor agonists (SKF38393 and PD168077, 1 mg/kg, respectively) to dark-adapted WT mice (Fig. 2.2B; $*P = 0.044$, two-way ANOVA) and suppressed in HOM mice by the D4 antagonist (L-745,870, 1 mg/kg, 5-day injection) (Fig. 2.2C; $***P < 0.001$, two-way ANOVA), suggesting altered retinal DA signaling due to the constitutive ADE of DAT Val559.

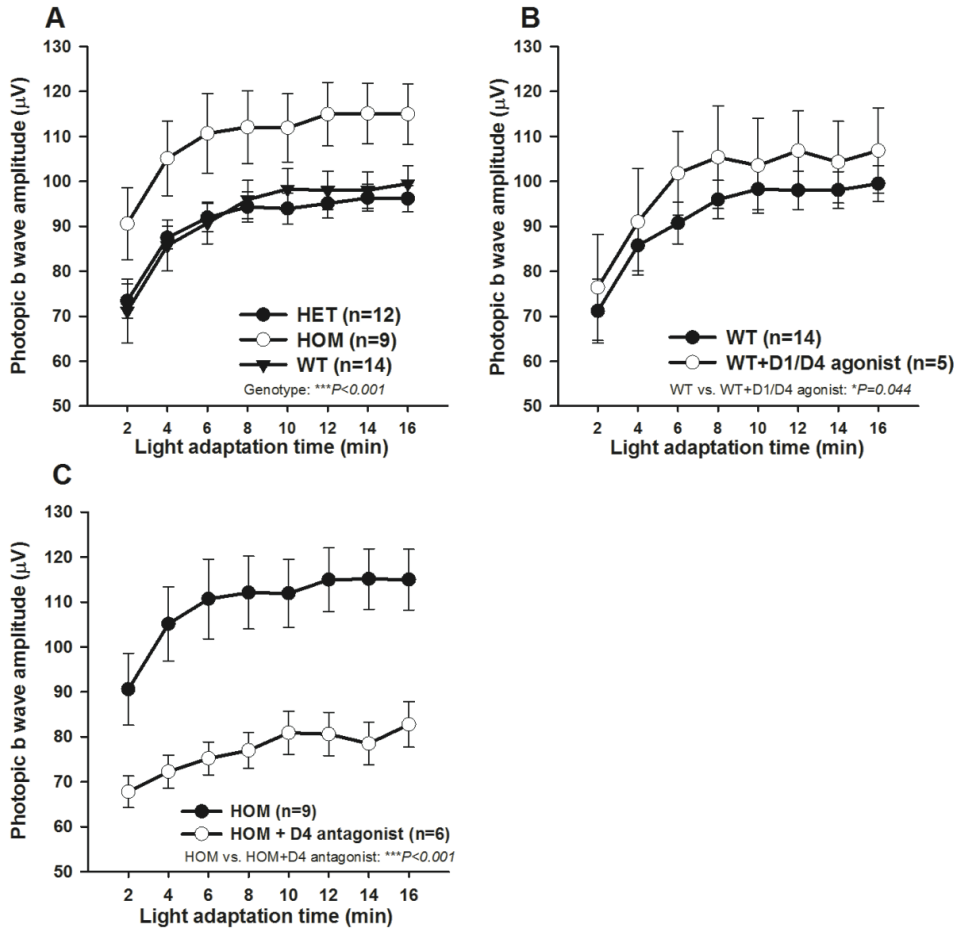

Fig. 2.2 The DAT Val559 homozygous mutation affects light-adapted retinal function via dopaminergic signaling in male mice.

(**A-C**) Light-adapted (photopic) ERG b-wave amplitudes (μV) are plotted as a function of light adaption time (minutes) in all groups. (**A**) Mice carrying a homozygous Val559 mutation of DAT (HOM: open circles) have significantly higher photopic b-wave amplitudes compared to WT (filled triangles) and HET (filled circles; $F_{(2,256)} = 26.98$, $***P < 0.001$, two-way ANOVA, $n = 9–14$ mice). (**B**) Injection of D_1/D_4 receptor agonists (SKF38393 and PD168077, 1 mg/kg, respectively) elevates the photopic ERG in WT animals (open circles) compared with untreated group (filled circles; $F_{(1,136)} = 4.124$, $*P = 0.044$, two-way ANOVA, $n = 5–14$ mice). (**C**) Injection of D_4 receptor-selective antagonist L-745,870 (1 mg/kg) significantly reduces the response amplitude of DAT HOM (open circles; $F_{(1,104)} = 82.06$, $***P < 0.001$, two-way ANOVA, $n = 6–9$ mice). All data are represented as means ± SEM.

2.4.2 Retinal responses to amphetamine are blunted in male DAT Val559 HOM mice

After observing a significant difference in light response amplitude between HOM and WT, we further challenged this mouse line with amphetamine (AMPH). DAT Val559 HOM knock-in mice show blunted AMPH-induced striatal DA elevations and motor activity in vivo [127]. To assess whether these alterations are penetrant at the level of the retina, AMPH was injected systemically followed by light-adapted ERG measurements. AMPH indeed increased the b-wave amplitudes in WT (Fig. 2.3A; $***P < 0.001$, two-way ANOVA), but these effects were blunted in the retinas of HOM mice (Fig. 2.3B; $P = 0.411$, two-way ANOVA). The average increase of ERG amplitudes at each time point following AMPH treatment were quantified by genotypes (Fig. 2.3C; $**P = 0.002$, t-test), in which WT displayed significant overall elevation of b-wave amplitude by AMPH compared to HOM, indicating a possible ceiling effect due to partial depletion of DA reservoir caused by ADE in HOM animals.

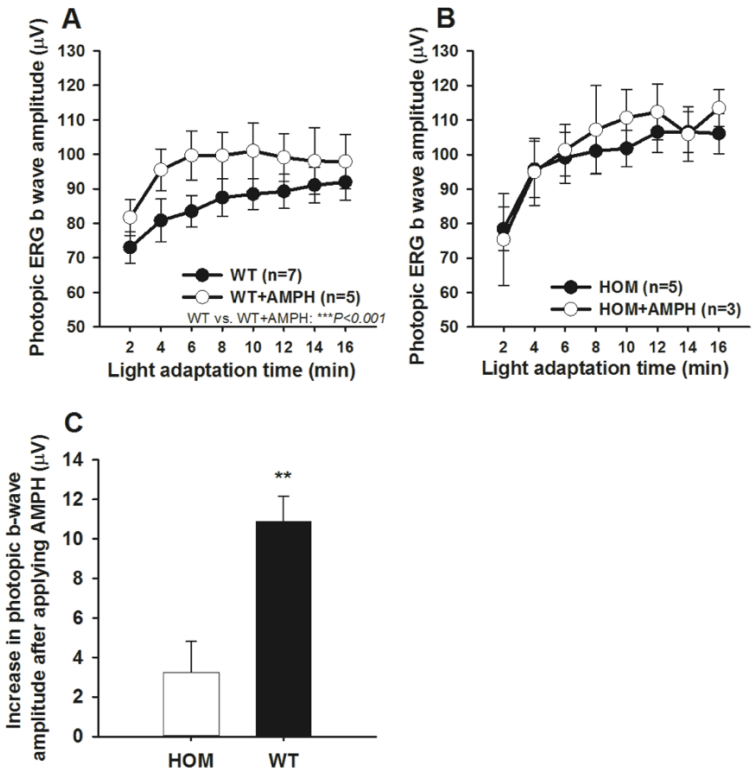

Fig. 2.3 AMPH treatment alters photopic b-wave amplitudes differently in male WT vs. DAT Val559 HOM mice. AMPH-treated (4 mg/kg) WT (**A**) ($F_{(1,80)} = 12.758$, $***P < 0.001$, two-way ANOVA, $n = 5–7$ mice) show increased light-adapted b-wave amplitudes, but homozygous mutants (**B**) are not affected by AMPH ($F_{(1,48)} = 0.688$, $P = 0.411$, two-way ANOVA, $n = 3–5$ mice). (**C**) The increments of ERG amplitude following AMPH injection are quantified by each genotype (HOM: white bar; WT: black bar) ($t = –3.774$, $**P = 0.002$, t-test). All data are represented as means ± SEM.

2.4.3 Overall retinal DA content is not influenced by DAT Val559

The increased photopic ERG amplitudes in DAT Val559 HOM and pharmacological evidence suggested possible changes in retinal DA and its turnover, so we next measured total levels of DA and its metabolites with HPLC. However, the ADE of DAT Val559 mice has been found to result in no significant changes in tissue DA levels in the brain [127]. Similar to brain findings, HOM mice showed no significant genotype-dependent changes in basal retinal DA, DOPAC, and HVA levels (Fig. 2.4A) or after 20 min of light exposure (Fig. 2.4B; DA: $P = 0.737$; DOPAC: $P = 0.929$; HVA: $P = 0.654$, two-way ANOVA). This lack of increase in total DA content is also consistent with findings in the retina of DAT-knockout mice [122]. Retinal levels of DOPAC and HVA increased in both WT and HOM mice in response to light (DOPAC: WT, an increase of 0.461 ng/mg, basal vs. light, $***P < 0.001$; HOM, an increase of 0.409 ng/mg, basal vs. light, $***P < 0.001$, two-way ANOVA, *post hoc* Student-Newman-Keuls method) (HVA: WT, an increase of 0.223 ng/mg, basal vs. light, $***P < 0.001$; HOM, an increase of 0.167 ng/mg, basal vs. light, $**P = 0.002$, two-way ANOVA, *post hoc* Student-Newman-Keuls method).

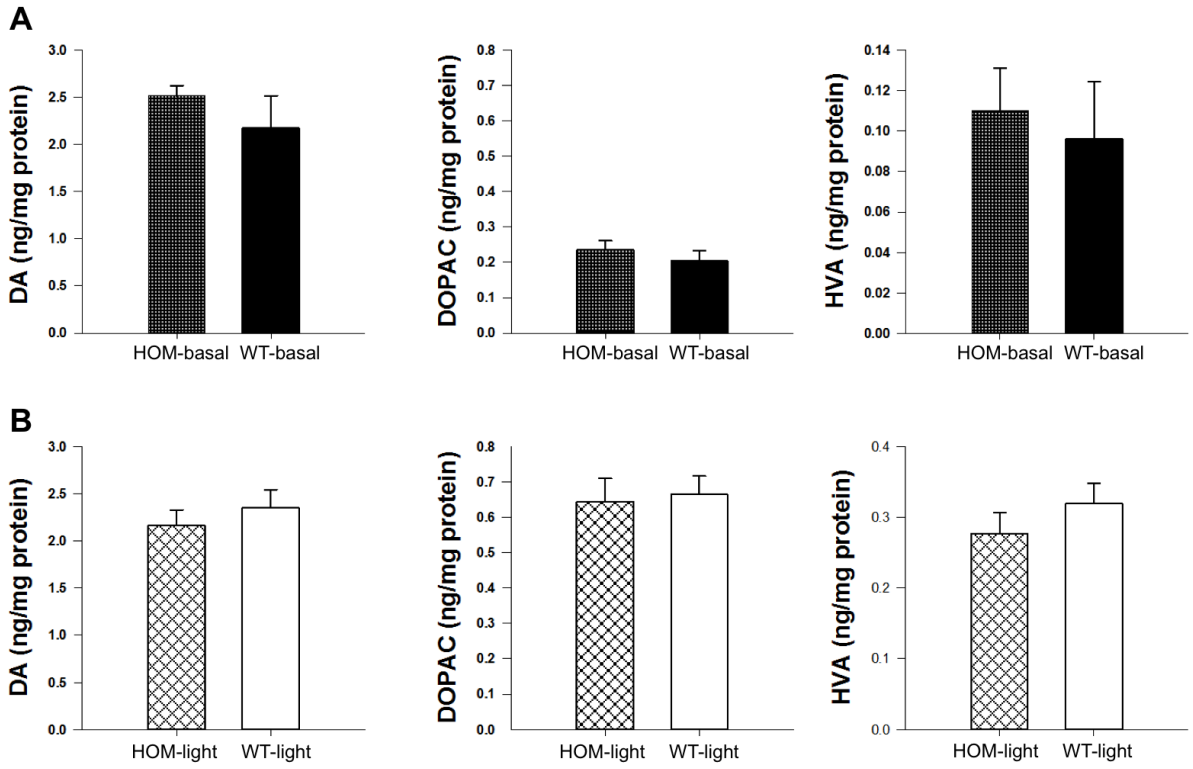

Fig. 2.4 Retinal dopamine content and its metabolite levels do not differ in male DAT Val559 homozygous mutant mice.

Retinal DA, DOPAC, and HVA were measured by HPLC either under complete darkness (**A** HOM: checked black bar, WT: black bar) or light conditions following 15–20 min of light exposure (**B** HOM: checked white bar, WT: white bar). Dopamine levels do not exhibit differences between genotypes or light conditions (HOM vs.

WT, $F_{(1,20)} = 0.116$, $P = 0.737$; basal vs. light, $F_{(1,20)} = 0.143$, $P = 0.710$, two-way ANOVA). HOM and WT also show similar levels of DOPAC and HVA. Exposure to light elevates the DOPAC and HVA levels in both WT and HOM animals (DOPAC: HOM vs. WT, $F_{(1,20)} = 0.008$, $P = 0.929$; basal vs. light, $F_{(1,20)} = 70.281$, $^{***}P < 0.001$, two-way ANOVA; within WT, basal vs. light, $^{***}P < 0.001$; within HOM, basal vs. light, $^{***}P < 0.001$, *post hoc* Student-Newman-Keuls method) (HVA: HOM vs. WT, $F_{(1,20)} = 0.207$, $P = 0.654$; basal vs. light, $F_{(1,20)} = 40.626$, $^{***}P < 0.001$, two-way ANOVA; within WT, basal vs. light, $^{***}P < 0.001$; within HOM, basal vs. light, $^{**}P = 0.002$, *post hoc* Student-Newman-Keuls method). Data are represented as means ± SEM (n = 6–8 mice).

2.4.4 The effect of DAT Val559 on photopic ERG amplitude is sex-dependent

Because the diagnosis of ADHD is more common in males, we initially focused our studies on male mice. Interestingly, upon testing a female cohort, we observed differential retinal light-adapted responses and effects of the DAT Val559 allele. Thus, in contrast to our findings in males, female DAT Val559 HOM animals revealed no significant difference in photopic ERG responses when compared with WT and HET littermates (Fig. 2.5A; $P = 0.422$, two-way ANOVA). The lack of difference was mainly due to increases in photopic b-wave amplitudes of female WT and HET in a comparison with male cohorts, which averaged 23.0% (Fig. 2.5B, C, left column, HET; $^{***}P < 0.001$, two-way ANOVA) and 22.8% (Fig. 2.5B, C, right column, WT; $^{***}P < 0.001$, two-way ANOVA), respectively. The light-adapted responses of DAT in female Val559 HOM animals were similar to the male HOM cohort in amplitude (Fig. 2.5B, C, middle column, HOM; $P = 0.052$, two-way ANOVA).

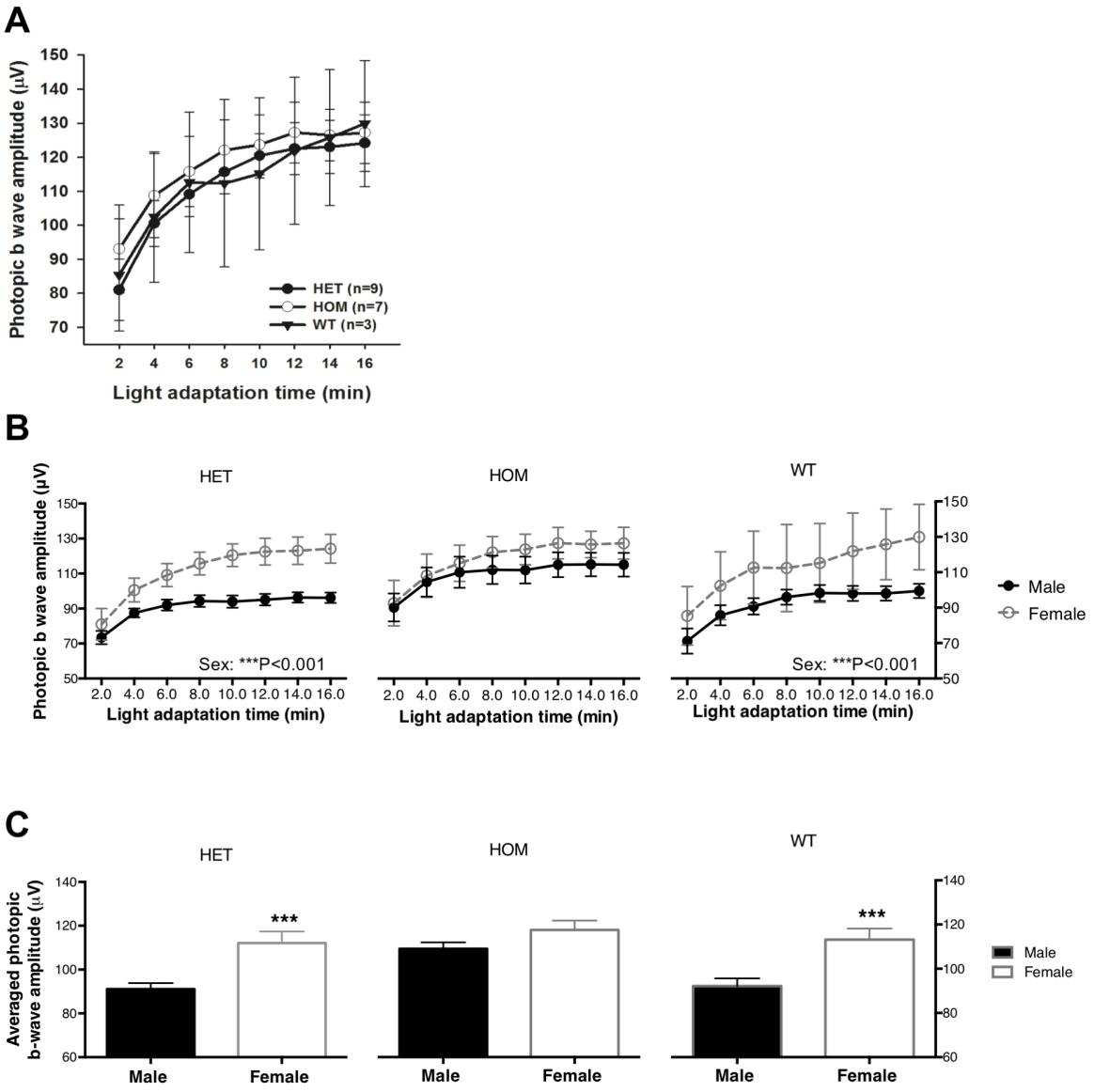

Fig. 2.5 Female mice do not exhibit the effect of DAT Val559 on photopic ERG responses.

(**A**) Photopic ERG b-wave amplitudes (μV) of female mice are plotted as a function of light adaption time (minutes; HOM: open circles; HET: filled circles; and WT: filled triangles). The HOM group does not differ from HET or WT ($F_{(2,128)} = 0.869$, $P = 0.422$, two-way ANOVA, $n = 3$–9 mice). (**B**) Female HET (left column, open circles, $F_{(1,152)} = 64.43$, $^{***}P < 0.001$, two-way ANOVA, $n = 9$–12 mice) and WT (right column, open circles, $F_{(1,120)} = 18.89$, $^{***}P < 0.001$, two-way ANOVA, $n = 3$–14 mice) show elevated photopic amplitudes compared to the male cohort (filled circles), while amplitudes in HOM remain the same independent of sex (middle column, $F_{(1,112)} = 3.860$, $P = 0.0519$, two-way ANOVA, $n = 7$–9 mice). (**C**) Averaged increases are quantified by genotype and sex (from left to right, HET: $^{**}P = 0.0070$, Mann-Whitney test; HOM: $P = 0.052$, Mann-Whitney test; WT: $^{**}P = 0.0038$, t-test). All data are represented as means ± SEM.

2.5 Discussion

To evaluate the possible utility of retinal measures as an aid in the evaluation of DA-linked neurobehavioral disorders and to further our understanding of the role of DA and DAT in the retinal function, we employed a mouse model that expresses the human DAT coding variant Val559. This variant has been demonstrated to disrupt multiple aspects of DA homeostasis and signaling in the brain in vivo, producing elevated basal striatal extracellular DA levels and blunted DA elevation upon local and systemic AMPH application [127]. Here, using noninvasive electrophysiological approaches, we assessed the effects of the variant on retinal DA and retinal function in intact mice and found that Val559 specifically enhanced the light-adapted ERG response amplitude and blunted AMPH enhancement of light response amplitude. We also found that the alteration of ERG amplitudes by the Val559 variant of DAT to be sex-dependent, with genotype effects detectible only in males.

2.5.1 Val559 DAT increases light-adapted retinal responses

Retinal circuits are modulated dynamically according to background illumination, with rod and cone systems for dark-adapted and light-adapted vision, respectively. The reconfiguration of circuits for high-resolution, light-adapted vision is achieved, in part, through intra-retinal retrograde signaling mechanisms mediated by retinal DA. The retina's ability to adapt to a change in background illumination can be observed in the increased light-adapted ERG b-wave response mediated by the light-stimulated release of DA [2]. Retinal DA also contributes to enhanced contrast sensitivity and high spatial resolution [2], through acting on gap junctions and chemical synaptic transmission, voltage-gated ion channels, and cAMP metabolism [44]. In mice in which tyrosine hydroxylase (TH, the rate-limiting enzyme of DA synthesis) is specifically depleted in the retina, retinal DA levels are markedly reduced, resulting in specific loss of the light-adapted ERG b-wave response amplitude [2]; however, brain DA levels remain normal. The deficiency in retinal DA is rescued by L-DOPA treatment and D4 receptor agonist, indicating the indispensable role of retinal DA in regulating photopic ERG responses.

In addition to the synthesis pathway, DA signaling is tightly coordinated through DAT-mediated DA clearance. Our results demonstrate that male mice homozygous for the Val559 DAT allele exhibit increased photopic b-wave amplitudes compared to WT and heterozygous littermates. The suppression of these elevated responses by D4 receptor antagonist in Val559 HOM and the increase in these responses by D1/D4 receptor agonists in WT and HET suggest the possibility that increased extracellular retinal DA and altered retinal DA signaling is associated with this DAT variant. Lavoie et al. conducted research on the DAT-knockout mouse model, in which they observed a decrease in rod sensitivity in scotopic

condition but no changes in other parameters in both scotopic and photopic conditions [122]. The difference between our findings and theirs may be due to the different photopic protocols we applied. Our protocols emphasize the time-dependent light adaptation of the retina from a dark condition whereas they assessed retinal responses to light stimuli of increasing intensities after light adaptation. However, we did not observe a change in the overall content of retinal DA, DA metabolites, and DA turnover with tissue-level measurements in Val559 DAT HOM animals. This result in the retina is consistent with a lack of change in overall DA content in the striatum, cortex, and midbrain previously reported in this mouse model [127]. This finding is also in agreement with DAT-knockout mice, in which no change was found in DA tissue content in the retina [122]. Since our experiments used tissue extracts and measured global DA content, it is possible that DA in the vesicular reservoir, or in the cytosol of synaptic terminals, masked any changes in the extracellular DA in our measurements.

2.5.2 Val559 DAT blunts retinal responses to AMPH

AMPH alters the action of presynaptic DAT to terminate DA signaling, leading to DA efflux and increased synaptic DA. Previously, we found AMPH evokes DA elevation in WT animals causing increased D2R-mediated IPSC amplitude and duration in striatal brain slices and enhances horizontal and vertical activity at the behavior level. However, in Val559 DAT HOM mice, AMPH-induced DA release and hyperactivity are significantly blunted [127]. Our observations in the retina parallel these behavioral and synaptic observations from the brain. Application of AMPH increased the photopic b-wave amplitude in WT, but failed to do so in the Val559 DAT HOM. The b-wave amplitude in Val559 was not affected by AMPH, indicating a possible ceiling effect due to partial depletion of DA reservoir caused by anomalous DA efflux in Val559 HOM. Although the AMPH is given systematically, the readout of photopic ERG amplitudes represents the changes in the local retinal DA, as supported by findings in retinal dopamine-specific knockout mouse line, where brain DA is normal but retinal DA is depleted [2].

2.5.3 Sex dependency

In our study, we observed a different effect of the DAT Val559 variant in male and female mice. DAT Val559 failed to increase the photopic b-wave amplitude in females, an effect mainly ascribable to the higher baseline b-wave amplitude of WT females. This may be due to elevated tonic DA signaling compared to WT males. In humans, adult females have significantly different neuroretinal functions from males, with females exhibiting larger scotopic b-wave amplitude [134], earlier onset of photopic oscillatory potentials [135], and shorter implicit time both locally and globally [136]. In patients with Parkinson's disease, where retinal dopaminergic signaling and multiple dimensions of visual function are compromised, the reduction of amplitude of visually evoked cortical potentials (VEP) and pattern ERG is

significantly different in male and female patients [137]. Estrogen has been suggested to increase DA synthesis, metabolism, and transport [138-141] and protect dopaminergic neurons from neurotoxic damage [142, 143]. ADHD, another psychiatric disorder closely associated with the dopaminergic function, exhibits sex differences, with a higher prevalence in men (i.e., ~ 2.1–5.4%) and lower in women (i.e., ~ 1.1–3.2%) [144, 145]. Taken together, these results suggest that the increased penetrance of DAT Val559 on retinal function in males may be due to lower baseline DA signaling in males vs. females.

2.5.4 ERG as a potential biomarker for ADHD

ADHD has a prevalence rate of 4–12% [117, 146, 147] in school-age children and 4–5% in adults [145, 148, 149], exhibiting symptoms of inattention, hyperactivity, and impulsivity. The current diagnostic methodology relies on behavioral observations and questionnaires without reliance on biomarkers that could help distinguish alternative disorders or subtypes or assist in quantifying treatment response.

Here, we provide evidence that the altered DA signaling induced by a human DAT mutation associated with ADHD can be detected in a mouse model using the non-invasive ERG. Apart from this specific rare DAT Val559 variant, the potential use of ERG and measurements of vision-related responses have broader implications in diagnoses of ADHD caused by changes in extracellular DA particularly mediated by DAT. Previous studies in several other psychiatric disorders, including seasonal affective disorder (SAD) [150, 151] and autism spectrum disorders (ASD), have shown changes in visual measurements [152-154]. Patients with SAD exhibit decreases in both rod sensitivity and cone-driven b-wave amplitude and a lengthening of cone-driven b-wave implicit time during a depression episode. Retinal anomalies represent a state marker of SAD and can be normalized in summertime or by a 4-week bright light therapy treatment [151]. In addition to retinal functions, pupillary light reflex (PLR) measurements are also valuable for diagnosing early autism. A delayed pupil response to light was observed in children with ASD. Using PLR latency alone, ASD group can be discriminated from the individuals with typical development with a high cross-validated success rate (89.6%) [152]. Additionally, Constable et al. suggested ASD patients have altered cone-ON bipolar signaling. They observed reduced b-wave amplitude across the ASD group under light-adapted conditions, along with the ON response of the prolonged flash ERG. Some ASD individuals also showed subnormal dark-adapted ERG b-wave amplitudes [154].

CHAPTER III

Circadian Perinatal Photoperiod Has Enduring Effects on Retinal Dopamine and Visual Function

3.1 Summary

Visual system development depends on neural activity, driven by intrinsic and light-sensitive mechanisms. Here, we examined the effects on retinal function due to exposure to summer- and winter-like circadian light cycles during development and adulthood. Retinal light responses, visual behaviors, dopamine content, retinal morphology, and gene expression were assessed in mice reared in seasonal photoperiods consisting of light/dark cycles of 8:16, 16:8, and 12:12 h, respectively. Mice exposed to short, winter-like, light cycles showed enduring deficits in photopic retinal light responses and visual contrast sensitivity, but only transient changes were observed for scotopic measures. Dopamine levels were significantly lower in short photoperiod mice, and dopaminergic agonist treatment rescued the photopic light response deficits. Tyrosine hydroxylase mRNA expression was reduced in short photoperiod retinas. Therefore, seasonal light cycles experienced during retinal development and maturation have a lasting influence on retinal and visual function, likely through developmental programming of retinal dopamine.

* This chapter has been published. Jackson C.R., Capozzi M., Dai H., McMahon D.G. J Neurosci. 2014 Mar 26;34(13):4627-33 [129]. Dai H. performed ERG and immunohistochemistry experiments. Jackson C.R., Capozzi M., Dai H., and McMahon D.G. analyzed data.

3.2 Introduction

The structure and function of the visual system are influenced by light input during development. Altered visual or photic input results in enduring changes in the structure and function of central visual centers in the visual cortex and the rhythmic nature of the light-modulated suprachiasmatic nuclei located in the hypothalamus [155, 156]. Upstream from these sites, the neural retina transduces environmental light signals to these brain areas; moreover, the retina can also be developmentally programmed by light stimulation. Here, we examined whether circadian light cycles experienced during development can have enduring effects on retinal function in adulthood.

Light-driven neural activity influences the development of retinal circuits, and rearing mice in darkness alters retinal synaptic organization, which leads to permanent alterations in visual function [157, 158]. While rearing animals in constant darkness alters retinal and visual function, we have focused on the potential for enduring effects of altered circadian light cycles–short photoperiods with 8 h of light per day that mimic winter light cycles at mid-latitudes, and long photoperiods with 16 h of light per day that mimic summer photoperiods– presented during the perinatal period of mouse development and maturation. Seasonal circadian light cycles experienced during development can imprint the properties of other neural and endocrine systems in mammals, shaping the function of circadian clock neurons in the central circadian clock [156] and the rate of sexual maturation [159]. Moreover, recent results in mice suggest the potential for circadian light reception by melanopsin-expressing retinal ganglion cells *in utero*, extending the concept of the developmental influence of light on the retina [160], but without an identified mechanism.

Here, we found that mice reared on a short, winter-like, photoperiod display enduring decreases in retinal light responses and contrast sensitivity. These physiological changes are underlain by decreases in retinal dopamine levels, reduced expression of the transcripts for the principal synthetic enzyme for dopamine synthesis, and an activity-dependent transcription factor. Thus, circadian photoperiods experienced during perinatal development and maturation have a long-lasting impact on retinal function.

3.3 Materials and Methods

3.3.1 Animal usage and care. All animal protocols were approved and in accordance with the guidelines established by the Vanderbilt University Animal Care Division, and the National Institutes of Health Guide for the Care and Use of Laboratory Animals. For this investigation, male C57/BL/6 mice were reared in three different lighting conditions: (1) Long photoperiod (L), mice were exposed to 16 h of light and 8 h of dark; (2) Short photoperiod (S), mice were exposed to 8 h of light and 16 h of dark; and (3) Equinox photoperiod, mice were exposed to 12 h of light and 12 h of dark (Fig. 3.1). The Equinox group is considered the control group in this study. Mice were reared in their respective lighting environments

from embryonic day 0 (E0) to postnatal day 40 (P40), and then were either switched to the opposing light cycle or maintained on the original cycle (Fig. 3.1; Long photoperiod to Short photoperiod [L:S], Short photoperiod to Long photoperiod [S:L], Long photoperiod to Long photoperiod [L:L], Short photoperiod to Short photoperiod [S:S]). Once mice were switched to the new lighting environment, they were allowed to acclimate to the new environment for at least 3 weeks before testing. Unless otherwise noted, mice were tested during the middle of the light phase of their respective light cycles (11:00 A.M.–1:00 P.M. on all light cycles; Fig. 3.1, denoted by gray arrow). Studies show that retinal development, maturation, and vision in mice become mature at approximately P30 [98, 157]; therefore, we chose P40 as the photoperiod switch day to (1) allow the retina to mature and (2) distinguish between developmental and transient effects. The mouse housing environments' light intensity was 100 ± 15 lux, provided by fluorescent bulbs. Food and water were provided *ad libitum*.

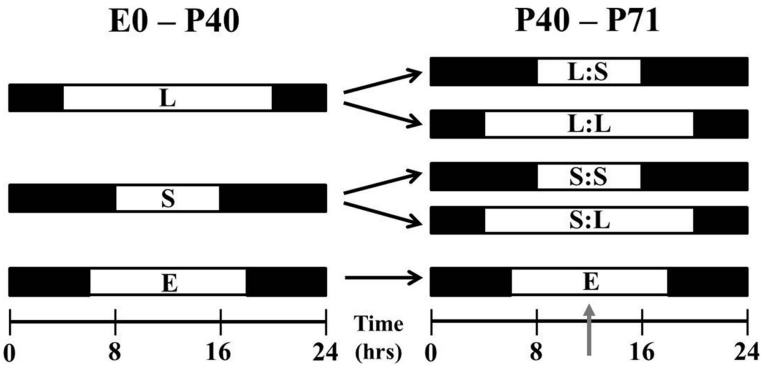

Fig. 3.1 Photoperiod paradigm.

Experimental photoperiod for mice began at E0 with either long (L) or short (S) light exposure. Between P40 and P50, groups either remained in the initial photoperiod or entered the opposing photoperiod for ~3 weeks. Other mice were exposed to an Equinox (E; 12:12 h) light/dark cycle for comparison. Gray arrow signifies midday test time point.

3.3.2 Electroretinogram (ERG). The electroretinogram (ERG) was used to assess global retinal cell function using the LKC Technologies UTAS visual electrodiagnostic test system as previously reported [2]. Here, we investigated the photopic (light-adapted) and scotopic (dark-adapted) ERG recordings in the photoperiod groups, as previously described [90, 133] with minor modifications. Mice were dark adapted overnight (~15 to 18 h), then under dim red light (Kodak GBX-2 Safelight) they were anesthetized with an intraperitoneal injection of ketamine (70 mg/kg) and xylazine (7 mg/kg) and their pupils dilated with 1% tropicamide. For ERG analysis, Long, Short, and Equinox mice were tested at the middle of the light

phase (8, 4, and 6 h after subjective light onset; Fig. 3.1, gray arrows). Eyes were kept moist with 10% methylcellulose eye drops and core body temperature was maintained at ~37.0°C using a thermostatically controlled heating pad regulated by a rectal temperature feedback probe (Model TC-1000 Temperature Controller; CWE). Needle electrodes were placed in the middle of the forehead and base of the tail, which served as reference and ground leads, respectively. A gold contact lens electrode was used for recording ERG responses (LKC Technologies; Order #N30).

Scotopic ERG responses were differentially amplified and filtered (bandwidth: 0.3–500 Hz), with responses digitized at 1024 Hz. The recording epoch was 250 ms, with a 20 ms prestimulation baseline. A total of eight stimulus intensities, ranging from –3.60 to 1.37 log cd*s/m^2, were used under dark-adapted conditions. Flash duration was 20 μs and performed in order of increasing intensity. As flash intensity increased, retinal dark adaptation was maintained by increasing the interstimulus interval from 30 to 180s.

For photopic ERGs, mice were presented with a steady rod photoreceptor-saturating background-adapting field (40 cd/m^2) inside the UTAS BigShot ganzfeld. Simultaneously, 0.90 log cd*s/m^2bright light flashes were presented at 0.75 Hz during a 20.8 min period of light adaptation. Data were collected and averaged in 2.6 min bins, totaling eight bins (6 bins for the photopic circadian experiment). Data collection occurred at similar time periods as the scotopic tests; however, additional photopic ERGs were recorded during the middle of the animals' dark phase. All other test parameters were similar to the scotopic ERG.

For the photopic ERG rescue experiment, intraperitoneal injections of 1 mg/kg SKF38393 (Sigma-Aldrich) and 1 mg/kg PD168077 (Tocris Bioscience) were administered to S:S mice 1 h before testing. Mice were injected under dim red light and returned to dark box until testing. Previous studies show that the 1 mg/kg drug concentration used fully restores a dopamine-depleted retina's function at the electrophysiological, behavioral, and pharmacological levels [2, 161]. The S:S injected mice were compared with uninjected S:S mice.

The a-wave and b-wave amplitudes and implicit times of the respective ERG tests were analyzed off-line. ERG waveforms were filtered (low-pass 60 Hz) to remove the influence of oscillatory potentials. For scotopic ERGs, the amplitude of the a-wave was measured from the prestimulus baseline (corresponding to flash onset) to the trough of the first negative deflection and the b-wave, from the trough of the a-wave to peak of the b-wave amplitude. For photopic ERG, only the b-wave was measurable, and was determined from the onset of the flash to the peak of the wave. The implicit times of each ERG test were measured from flash onset to the peak of each wave.

3.3.3 Visual Psychophysical testing. The visual-behavioral performance was assessed using the optokinetic head-tracking reflex, testing for spatial frequency threshold (acuity) and contrast detection

(sensitivity) using the OptoMotry system (Cerebral Mechanics). Video analysis enabled an observer to track the reflexive head movements of mice in response to rotating sinusoidal-wave gradients projected by four interfacing Dell LCD monitors. Tracking was defined as smooth head movements tracked in the same direction and speed as the rotation of the sinusoidal-wave gradient. Spatial frequency threshold was measured using a staircase method with a random and separate display of spatial frequencies and rotation direction, respectively, of the sinusoidal gradient. This procedure automatically increased the spatial frequency of the sinusoidal-wave gradient until the observer could no longer determine head-tracking movements.

Contrast sensitivity detection was measured similarly to spatial frequency threshold; however, the sinusoidal contrast gradients were systematically reduced from 100% contrast, at each spatial frequency, until no reflexive head movements were observed. The last contrast level where the observer noticed tracking was deemed the animals contrast sensitivity threshold. As described by Prusky et al. (2004) [98], we measured contrast sensitivity threshold at six spatial frequencies (0.031, 0.064, 0.092, 0.103, 0.192, and 0.272 cycles/degree). The contrast sensitivity was calculated using a Michelson contrast from the screen's luminance (maximum − minimum)/(maximum + minimum) as previously described [98, 162].

For each visual test Long, Short, and Equinox mice were tested at the middle of the light phase on their light cycle - 8, 4, or 6 h after light onset, respectively, under typical room lighting.

3.3.4 HPLC determination of biogenic amine concentration. Retinas from all groups were removed from the whole mouse eye and separated from the retinal pigment epithelium. Retinas were collected under either dark or light conditions at the middle of the subjective light phase, approximately 8 h or 4 h after light onset. Under dark conditions, mouse retinas were dissected in the presence of filtered dim-red light (Kodak GBX-2 Safelight). Under light conditions, retinas were dissected in the presence of room lighting, which is similar to the background light presented during the photopic ERG test. Immediately, both retinas from a single mouse, once dissected, were placed in a 1.5 ml tube, frozen on dry ice, and stored at −80°C until processed for HPLC analysis.

Retinas were homogenized, using a tissue dismembrator, in 100–750µl of 0.1 m TCA, which contains 10^{-2} M sodium acetate, 10^{-4} M EDTA, 5 ng/ml isoproterenol (as internal standard), and 10.5% methanol, pH 3.8. Samples were spun in a microcentrifuge at 10,000 *g* for 20 min. The supernatant was removed and stored at −80°C [130]. The pellet was saved for protein analysis. The supernatant was thawed and spun for 20 min and samples of the supernatant were then analyzed for biogenic monoamines.

Retinal biogenic amines were determined by a specific HPLC assay using an Antec Decade II (oxidation: 0.4; 3 mm GC WE, HyREF) electrochemical detector operated at 33°C. Twenty microliter samples of the supernatant were injected using a Waters 2707 autosampler onto a Phenomenex Kinetex

(2.6u, 100A) C18 HPLC column (100 × 4.60 mm). Biogenic amines were eluted with a mobile phase consisting of 89.5% 0.1 M TCA, 10^{-2} M sodium acetate, 10^{-4} M EDTA, and 10.5% methanol, pH 3.8. The solvent was delivered at 0.6 ml/min using a Waters 515 HPLC pump. Using this HPLC solvent the following biogenic amines elute in the following order: dopamine, dihydroxyphenylacetic acid (DOPAC), homovanillic acid (HVA) [131]. HPLC control and data acquisition are managed by Empower software. For this investigation retinal biogenic amine analysis are represented as ng/mg protein.

Total retinal protein concentration was determined using BCA Protein Assay Kit purchase (Pierce Chemical Company). The frozen pellets were allowed to thaw and reconstituted in a volume of 0.5 N HCl that equals that previously used for tissue homogenization; 100 µl of this solution was combined with 2 ml of color reagent and allowed to develop for 2 h. A bovine serum albumin standard curve was run at the same time spanning the concentration range of 20–2000 µg/ml. The absorbance of standards and samples were measured at 562 nm.

3.3.5 Immunohistochemistry. L:L and S:S mice were assessed for changes in tyrosine hydroxylase positive (TH+) cell numbers. During the middle of the animals' light phase, L:L and S:S mice were killed by cervical dislocation and their eyes were removed and hemisected to remove cornea and lens; the eyecups were fixed in 4% formaldehyde for 1 h. The retinas were then removed, washed with 1× PBS, and protected by sucrose gradients (10% for 30 min, 20% for 2 h, and 30% overnight). After freezing on dry ice and thawing twice, retinal whole mounts were washed in 1× PBS, then blocked for 2 h with 5% goat serum, 0.1% Triton X-100 in 1× PBS, and incubated with primary anti-tyrosine hydroxylase antibody (Millipore Bioscience Research Reagents; AB152) at 4°C overnight (1:500 anti-TH, 3% goat serum, and 0.1% Triton X-100 in 1× PBS). After rinsing with 1× PBS, the fluorescent secondary antibody was applied (1:500 Alexa Fluor 488, 1% goat serum, and 0.1% Triton X-100 in 1×PBS), followed by a final series of PBS washes. Whole mounts were covered in Vectashield (Vector Laboratories) and viewed by a confocal microscope. Images were processed via ImageJ (National Institutes of Health, Bethesda, MD) and MetaMorph (Molecular Devices).

3.3.6 Retinal RNA extraction and quantitative RT-PCR. L:L, S:S, and Equinox mouse retinas were removed from the whole eye, then frozen in a 1.5 ml tube on dry ice. Samples were collected at six time points under the following light conditions: (1) L:L light phase–Zeitgeber Time (ZT) 2, 6, 10, and 14 and dark phase–ZT 18 and 22; (2) S:S light phase–ZT 2 and 6 and dark phase–ZT 10, 14, 18, and 22; (3) Equinox light phase–ZT 2, 6, and 10 and dark phase–ZT 14, 18, and 22. Samples were collected during the animal's dark phase under filtered dim-red light (Kodak GBX-2 Safelight) and stored at –80°C until RNA extraction. Total RNA was extracted using a Qiagen RNeasy mini kit (catalog #74104), measured

by a NanoDrop system (Thermo Scientific), and reverse-transcribed (~500 ng) into cDNA using the QuantiTect Reverse Transcription Kit (Qiagen; category #205311). Total cDNA was also measured to use for normalization. Quantitative RT-PCR reactions were performed in 25 µl total volume with 2 µl cDNA, 12.5 µl of SsoAdvanced SYBR Green Supermix (Bio-Rad), 8.5 µl sterile water, and 1 µl of 300 nM intron-spanning gene-specific forward and reverse primers in a Bio-Rad CFX96 Real-Time System. Quantification of transcript levels was performed by comparing the threshold cycle for amplification of the unknown to those of six concentrations of standard cDNAs for each respective transcript, then normalizing the standard-calculated amount to the total concentration of cDNA in each sample. Each sample was assayed in duplicate.

3.3.7 Statistical analysis. Two-tailed t-test and one- and two-way ANOVAs were used where applicable and reported. *Post hoc* Student-Newman-Kuels and Dunn's methods were used to identify sample means that are significantly different from each other after ANOVAs. Significance levels were set at $p < 0.05$ and graphs are represented as means ± SEM or SD where applicable and reported.

3.4 Results

To test the effect of seasonal circadian light cycles on retinal function, C57 mice were raised on modified photoperiods from E0 to P71 (Fig. 3.1), which consisted of Long (16 h light:8 h darkness) and Short (8 h light:16 h darkness) light cycles. In addition, to test for reversibility or persistence of developmental photoperiod effects, at P40–P50 some mice were switched to the opposing photoperiod for at least 3 weeks, followed by testing between P61 and P71. Finally, for comparison, cohorts of mice raised on the standard 12:12 Equinox photoperiod were considered controls in the study.

3.4.1 Developmental photoperiod imprints retinal function

We used the ERG to examine impacts of photoperiod on retinal function. Figure 3.2 shows photopic (Fig. 3.2A) and scotopic (Fig. 3.2B, C) ERG responses following development and maintenance on Long, Short, and Equinox photoperiods (left column), or developmental exposure followed by photoperiod switch (right column). Development in the Short photoperiod led to significant deficits in photopic responses where, on average, the S:S group (8:16 photoperiod from E0 to P61–P71) showed an averaged 26% decrease in photopic b-wave amplitudes as compared with the L:L (16:8 photoperiod from E0 to P61–P71) and Equinox groups (12:12 photoperiod from E0 to P61–P71), while L:L and Equinox were indistinguishable (Fig. 3.2A, left column; S:S vs L:L and Equinox, $***P < 0.001$). Switching from Short to Long photoperiods at P40–P50 until testing at P61–P71 did not restore the amplitudes of the Short photopic b-wave; in fact, a small but significant 15% average amplitude decrease was observed (S:L

group; Fig. 3.2A, right column; S:S vs S:L, *$P < 0.017$), indicating that the developmental effect of Short photoperiods persists even following ~3 weeks of Long photoperiod exposure. In addition, switching the Long group to the short photoperiod decreased the amplitude of the photopic ERG to levels similar to the S:S group (Fig. 3.2A, left column, L:S; ***$P < 0.001$, as compared with L:L).

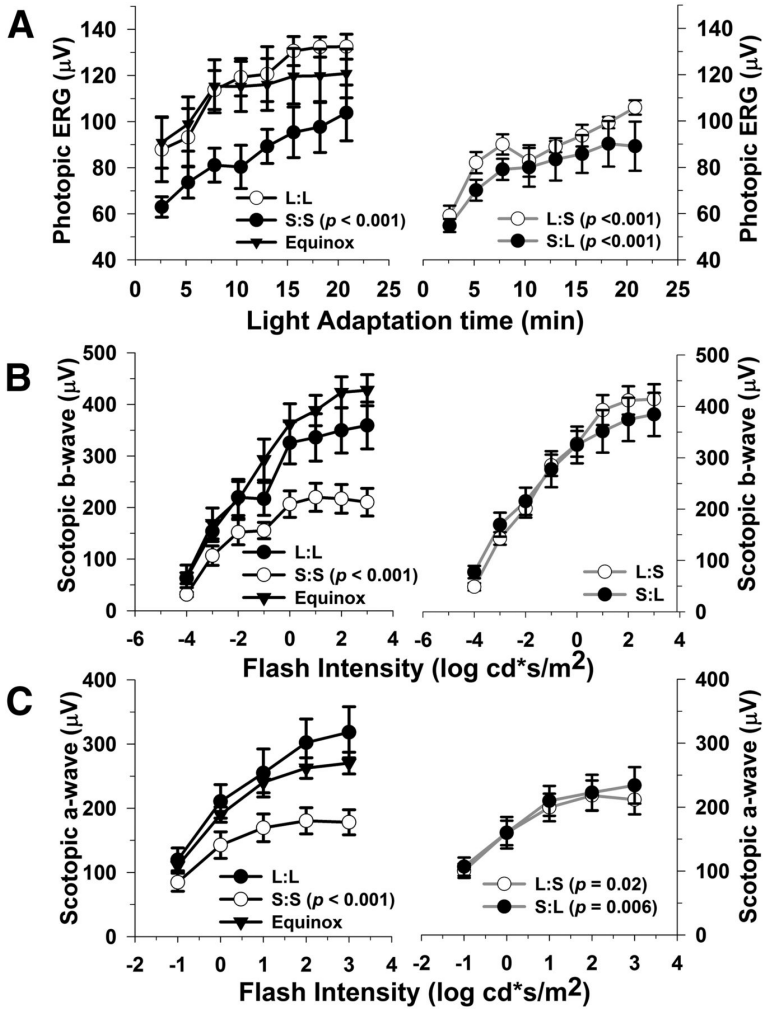

Fig. 3.2 Photoperiod affects light- and dark-adapted retinal function.

(**A**) Light-adapted (photopic) b-wave amplitudes are significantly lower in mice exposed to S:S, L:S, and S:L photoperiods as compared with L:L (***$P < 0.001$, all groups). (**B**), Dark-adapted (scotopic) b-wave amplitudes are significantly reduced in the S:S mice compared with the L:L group (***$P < 0.001$). In contrast, the L:S and S:L groups do not differ from L:L; however, they are significantly higher in amplitude compared with S:S mice (*$P < 0.05$, both comparisons). (**C**), Dark-adapted (scotopic) a-wave amplitudes are lower in the S:S, L:S, and S:L groups in relation to L:L mice (*$P \leq 0.001, 0.022, 0.006$, respectively). Also, the L:S and S:L groups significantly differ in amplitude compared with S:S mice (*$P = 0.018$ and 0.024, respectively). All data points represent means ± SEM; $n = 6–10$.

Because the photopic ERG b-wave response is expressed with a circadian rhythm [2, 133, 163], we tested whether the decrement in photopic ERG amplitude we had observed at midday was also present at midnight. Indeed photopic ERG amplitudes from both L:L and S:S groups displayed day/night differences, with reduced amplitudes at night (Fig. 3.3A, B, left column, L:L *** $P < 0.001$; right column, S:S ***$P < 0.001$, day vs night). Moreover, the photopic response in S:S mice was significantly reduced at both midday and midnight time points compared with L:L (Fig. 3.3A, B; ***$P < 0.001$ for all comparisons). Photopic a-waves could not be reliably measured in our system.

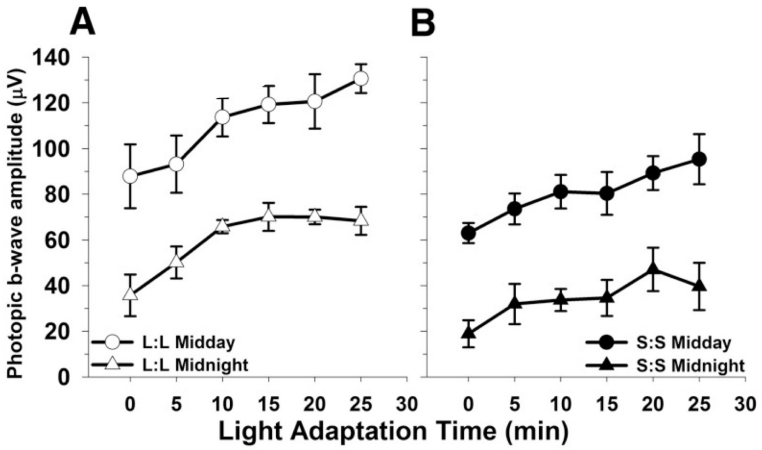

Fig. 3.3 Photoperiod does not affect photopic ERG rhythm phenotype, only the amplitude differs between groups. (**A-B**), L:L and S:S animals display rhythmic responses to the photopic test (***$P < 0.001$, both groups: day vs. night); however, the amplitude in the S:S group is significantly lower as compared with the L:L at the corresponding test time point (L:L vs S:S midday, ***$P < 0.001$; L:L vs S:S midnight, ***$P < 0.001$). All data points represent means ± SEM; n = 6.

The scotopic b-wave was also reduced in S:S reared mice compared with the L:L and Equinox groups (Fig. 3.2B, left column; 36% vs L:L, ***$P < 0.001$). In contrast, the scotopic b-wave response was restored by switching mice from the short to long photoperiod (S:L), which indicates that this activity responds to the longer light cycle. In addition, the amplitudes of the scotopic b-wave were maintained at high levels in the L:S group demonstrating a sustained ERG phenotype (Fig. 3.2B, right column; L:S vs S:S, ***$P < 0.001$; S:L vs S:S, ***$P < 0.001$).

The S:S, L:S, and S:L groups demonstrated an average 36%, 25%, and 21% decrease, respectively, in scotopic a-wave amplitudes in relation to the L:L and Equinox groups (Fig. 3.2C; *$P \leq 0.001$, 0.022, and 0.006, respectively). Moreover, L:S and S:L groups were ~15% higher than the S:S group (Fig. 3.2C; *$P = 0.018$ and 0.024, respectively). L:S and S:L group a-wave amplitudes were partially reduced and restored, respectively, indicating an intermediate phenotype.

Psychophysical-visual tests using optokinetic tracking were performed to assess the impact of seasonal photoperiods on vision. Contrast sensitivity in S:S, L:S, and S:L mice was significantly decreased compared with the L:L photoperiod group (Fig. 3.4, 0.064 cycles/degree; ***$P = 0.001$), and the S:S mice also showed a significant deficit relative to the L:L and L:S groups at 0.103 cycles/degree (Fig. 3.4; **$P < 0.01$). Spatial frequency threshold (acuity) was also measured across all photoperiod groups; however, no differences were found (data not shown).

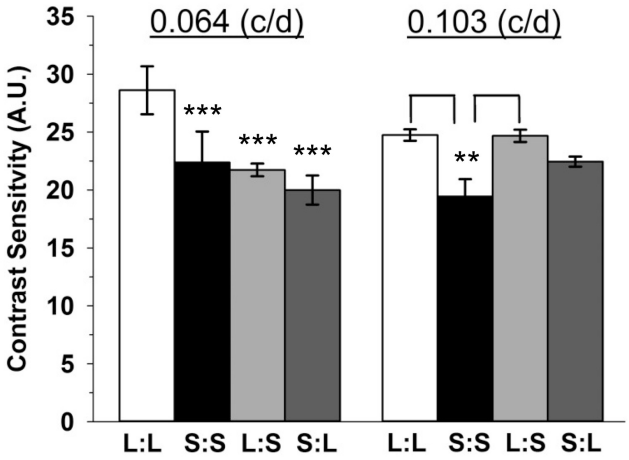

Fig. 3.4 Contrast sensitivity detection is impacted by perinatal photoperiod exposure.

Contrast sensitivity is lower in S:S, L:S, and S:L groups at 0.064 cycles per degree (c/d) compared with L:L mice (***$P < 0.001$). Also, at 0.103 c/d, contrast sensitivity is significantly reduced in S:S mice compared with L:L and L:S exposed mice (**$P = 0.004$). All data represent means ± SEM; n = 4–6 mice. A.U., arbitrary units.

3.4.2 Dopamine content is influenced by photoperiod

The deficits in retinal function in the Short photoperiod mice–reduced photopic b-wave amplitude and contrast sensitivity– are similar to those produced by genetic depletion of dopamine in the mouse retina [2]. Therefore, to determine whether the retinal dopaminergic system is influenced by seasonal photoperiods, we assayed for changes in dopamine, DOPAC, and HVA levels. The S:S, L:S, and S:L groups displayed approximately 20%, 28%, and 50% reductions in retinal dopamine levels, respectively, compared with the L:L group (Fig. 3.5B; *$P < 0.05$). S:S and L:S groups show 18% and 50% lower amounts of retinal DOPAC in relation to L:L (Fig. 3.5C; *$P < 0.05$); in contrast, the S:L group did not differ. It is noted that there is a substantial increase in DOPAC in the S:L group when compared with the S:S and L:S groups (Fig. 3.5C; Δ*$P < 0.05$). HVA levels were 25% lower in the L:S exposed mice (Fig. 3.5D; *$P < 0.05$), while all other groups did not significantly differ compared with L:L. The DOPAC/dopamine (DA) ratio was approximately doubled in the S:L group as compared with the L:S

mice (*$P < 0.05$); all other groups did not differ. Also, HVA/DA ratios among the photoperiod groups did not differ (data not shown).

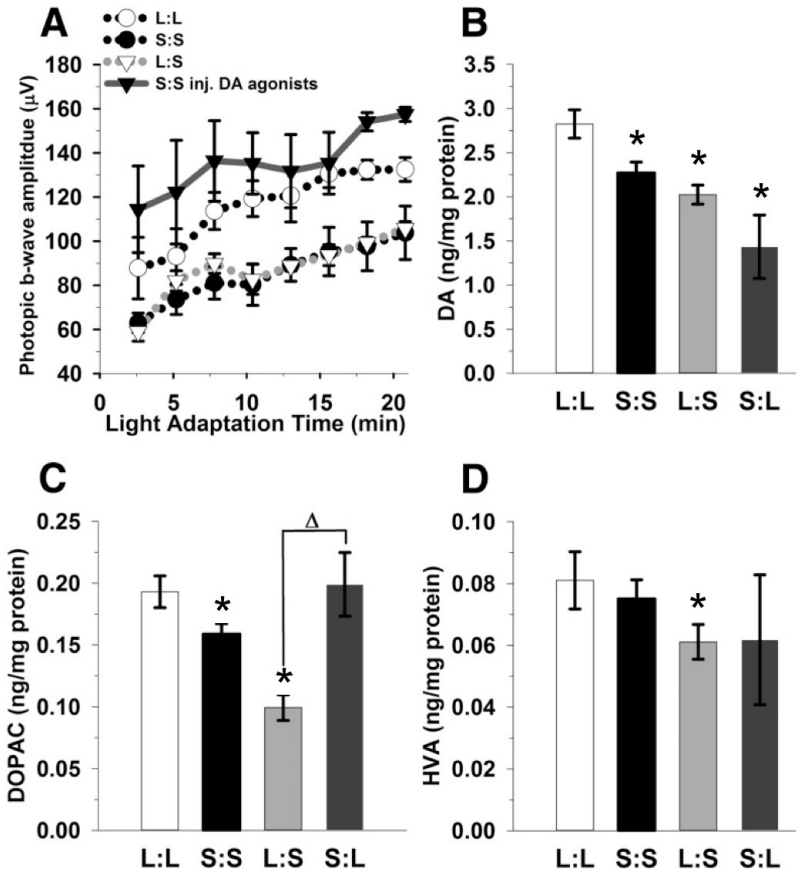

Fig. 3.5 Stimulating dopaminergic signaling rescues the photopic ERG.

(**A**) Injection of SKF38393 and PD168077 (1 mg/kg, dopamine D1 and D4 receptor-selective agonists, respectively) significantly increases photopic ERG b-wave amplitudes in the S:S group (solid gray line with black triangles) compared with the untreated group (black dotted line; *$P = 0.018$). (**B**) Retinal dopamine is reduced in S:S, L:S, and S:L groups compared with L:L mice (*$P < 0.05$). (**C**) Retinal DOPAC concentrations are lower in S:S and L:S mice in relation to L:L mice (*$P < 0.05$); however, S:L does not significantly differ. (**D**) In contrast, only the L:S mice display a significant reduction in HVA compared with L:L mice (*$P < 0.05$). All data represent means ± SEM; n = 6–8 mice.

The observed decrease in dopamine content in short photoperiod retinas could be due to a decrease in dopamine synthesis or a decrease in the number of retinal dopaminergic amacrine/interplexiform cells. To address these possibilities, we determined retinal dopaminergic cell density in the L:L and S:S groups, using immunohistochemistry for tyrosine hydroxylase, the rate-limiting enzyme in dopamine synthesis. These groups did not differ in cell density (Fig. 3.6, L:L: 36.4 ± 4.1 cells/mm^2; S:S: 38.02 ± 3.0 cells/mm^2)

for cells that positively reacted to tyrosine hydroxylase antibody detection. These cell densities are similar to mice that were reared in Equinox conditions (34 cells/mm^2; [43]).

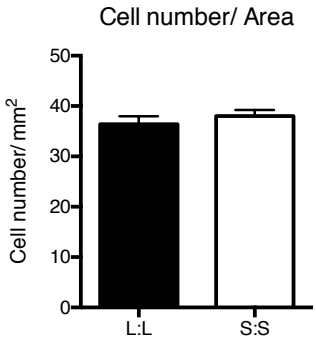

Fig. 3.6 The dopaminergic cell density in the L:L and S:S groups does not differ.

DA cells were immunostained with anti-TH (tyrosine hydroxylase) and counted within whole mount retinas. The cell density was calculated as the total cell number over the area of the retina in mm^2. L:L mice have 36.41 cells/ mm^2, while S:S have 38.03 cells/ mm^2 on average. There is no significant different in cell density (t = -0.798, P = 0.442, t-test). All data represent means ± SEM; n = 6-7 mice.

3.4.3 Restoration of dopamine signaling rescues retinal function

To test if restoring dopaminergic signaling rescues the photopic ERG deficit in the Short photoperiod group, we injected S:S mice with dopamine D1 and D4 receptor agonists (1 mg/kg per drug) 1 h before testing their photopic ERG. Dopamine agonist treatment indeed reversed the short photoperiod-induced deficit, increasing the light-adapted b-wave amplitudes by an average of 37% compared with the untreated S:S group (Fig. 3.5A; *P = 0.018). Previous studies show that the scotopic a-wave and b-wave ERG light response is not affected by retinal dopamine depletion; therefore, this test was not performed [2].

3.4.4 Photoperiod influences dopamine synthetic gene expression

Given the reduction in dopamine content in S:S retinae, but lack of change in dopamine cell number, we assayed for changes in the expression of tyrosine hydroxylase (*Th*), the rate-limiting enzyme for dopamine synthesis. *Th* mRNA levels were assayed at 4 h intervals over a 24 h period to determine both the overall and temporal expression patterns. *Th* mRNA levels were, on average, ~60% lower in retinas from S:S photoperiod mice, compared with L:L or Equinox mice (Fig. 3.7; ***P < 0.001, both comparisons). In addition, the temporal expression pattern between all groups appeared to differ; even so, each showed a similar peak in *Th* expression following the light/dark transition (Fig. 3.7).

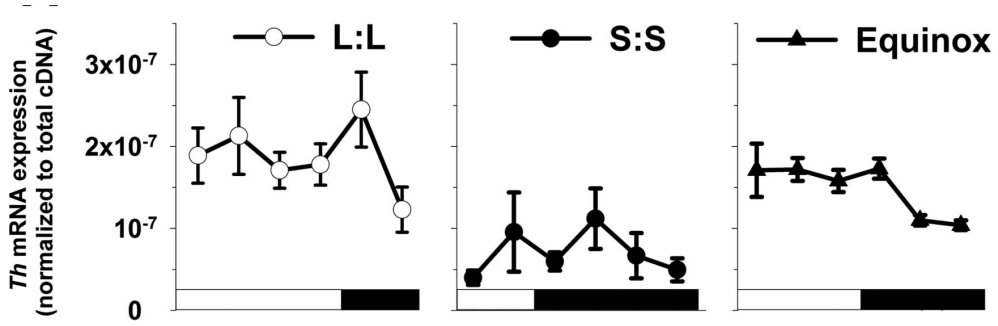

Fig. 3.7 Tyrosine hydroxylase mRNA expression levels are influenced by perinatal photoperiod.

Th retinal mRNA levels, assayed over 24 h, differ among all photoperiods ($p < 0.01$); even so, mice exposed to the S:S photoperiod display the lowest *Th* mRNA levels compared with L:L and Equinox reared mice (***$P < 0.001$).

3.5 Discussion

Overall, we observed that circadian light cycles experienced during retinal development/maturation have an enduring influence on retinal physiology and a marked impact on vision in adulthood. Altered retinal dopamine signaling is likely a key contributor to the functional deficits observed in this study.

3.5.1 Photoperiod has enduring and transient effects on retinal function

The retina adjusts its functional capacity to handle exponential changes in daily illumination, for example, the shift from nighttime to daytime vision. Retinal dopamine is a primary factor coordinating this functional transition from a rod- to cone-dominated state, which is observed in the light-adapted ERG response and closure of photoreceptor gap junction connectivity [2, 164]. Light drives retinal tyrosine hydroxylase activity and subsequently dopamine production [165]; acute light exposure of 15 min or 96 h results in increased activity of tyrosine hydroxylase and more active enzymes, respectively [46]. However, this activity amplification is readily reversed with 24 h of dark exposure. In contrast, the short photoperiod model limited light exposure to 8 h per day during development, which results in enduring changes in the retinal dopamine phenotype that are not reversed by weeks of 16 h daylight exposure. Therefore, the enduring deficits observed in light-adaptive vision in mice exposed to short light cycles are likely due to the insufficient photoperiodic programming of the retinal dopaminergic system due to less daily light stimulation during development. It is plausible that the retinal dopamine decreases observed in adult mice switched from the long to short photoperiod are due to less proximal daily light drive, which could result in a similar functional phenotype. Also, untested retinal processes, such as a reduction in the light-adaptation kinetics, could play a role in the photopic response deficits.

Reduced levels of retinal dopamine and a possible dopamine D4 receptor expression alteration, as a result of photoperiod exposure, could explain why there are incremental differences among the spatial frequencies in the contrast sensitivity test. Dopamine controls contrast sensitivity through activation of the dopamine D4 receptor [166]. This receptor's expression in the retina is rhythmic and driven by light [161, 163]; thus, it is possible that, in conjunction with lower retinal dopamine, the dopamine D4 receptor levels are altered by exposure to short daily light cycles. Mice are most sensitive in detecting difference in contrast at 0.064 cycles/degree. The other frequencies (i.e., 0.103 cycles/degree) do not refine contrast at a similar level [98]; therefore, slight photoperiodic retinal dopaminergic modifications may not be resolved at the other spatial frequencies.

The observed reduction in scotopic a-wave and b-wave properties in short photoperiod mice is unlikely due to a change in dopamine signaling since (1) substantially reducing retinal dopamine does not impact the scotopic ERG light response and (2) rod photoreceptors, which mediate this response, do not express dopamine receptors [2]. Previous reported evidence does suggest that lighting conditions can affect photoreceptor synaptic ribbon numbers and morphology [167]. Photoperiod input could alter ribbon synapse structure leading to the transient changes we observe in the scotopic b-wave of the Short to Long photoperiod group. Also, it is plausible that 3 weeks is insufficient to transition this system to a new light cycle, which could explain why we did not detect complete a-wave or b-wave amplitude photoperiod reversal.

Our developmental photoperiod exposures cover the entire time course of development and maturation of the retina. Within that interval, there are a variety of time points that could serve as a critical period. Light, as early as E16, influences the development of the retina [160]. In the mouse fetus, light stimulation of the melanopsin system is critical for normal retinal vascular development, which if perturbed, leads to increased vascular growth [160]. This system is known to affect the retinal dopaminergic system. Rearing mice in complete darkness alters inner nuclear layer retinal synaptic organization and dopamine storage, demonstrated by changes in light-evoked retinal ganglion cell responses, ERG measured oscillatory potentials, and retinal ON-/OFF-pathways [157, 168]. Short-term light deprivation has no detectable effects on retinal function; however, light exposure influences retinal physiology during a critical period, between P22 and P40 in mice [157]. Dopamine and melanopsin phototransduction influences the generation of retinal waves (P4–P7), which are required for visual development [169, 170]. Altering the duration of light input during retinal development could significantly impact how the retina refines inner retinal circuits for contrast detection and vision, thereby, shaping retinal function along several dimensions.

The developmental light cycles in our experiments varied in three ways: the timing of daily light/dark transitions for circadian entrainment, the duration of light each day, and the total number of daily photons.

These parameters mimic the seasonal changes in light cycles as experienced in the natural environment, which was our goal, but a limitation of our study is that we cannot strictly ascribe the effects observed to any one parameter of the three that were varied

3.5.2 Photoperiod impacts monoamine content

Light causes a surge in dopamine release that acts via volume transmission to reconfigure the retina signaling capacity for daytime vision [44]. Here, mice exposed to the short photoperiod, either developmentally, or as adults, display significantly lower dopamine content than those reared and maintained on long photoperiods. However, uniquely among the groups, mice moved from a short to long photoperiod also show an increase in DOPAC and HVA, which indicates higher levels of dopamine metabolism. It is plausible that increased dopamine use and metabolism could contribute to the low retinal dopamine levels observed in this group. Previous studies show that the development of the retinal dopaminergic system requires stimulation from light-sensitive retinal cells [165] and rearing mice in constant darkness results in both lower retinal dopamine and tyrosine hydroxylase expression [158, 171]. Here, we show that reduced light input from short photoperiods also reduces retinal dopamine and tyrosine hydroxylase mRNA (~60%), suggesting that retinal light stimulation duration into dopaminergic amacrine cells plays an integral role in regulating this system during development and in the adult retina. Further studies need to be conducted to determine whether this molecular change has a developmental critical period, or can be evoked acutely.

In addition to decreased *Th* expression, the mice maintained on short photoperiods also display decreased retinal transcript levels of *Egr-1*(data not shown). *Egr-1*, present in multiple retinal cell types, is known to drive *Th* expression in PC12 cells and is an active transcription factor that mediates diverse cellular systems [172]. Its semi-ubiquitous presence could explain why its expression differs among the photoperiod groups compared with *Th*. Further investigation is required to determine *Egr-1*'s specific role within the retinal dopaminergic system in response to seasonal light cycles.

Light input has long-term effects on dopaminergic neurons in other brain areas as well. Six weeks of constant darkness increases apoptotic markers in the nuclei of ventral tegmental dopamine neurons. Furthermore, exposing rats to short and long circadian light cycles results in loss of dopamine expression and increase in somatostatin hypothalamic neurons [173, 174]. Our results, in conjunction with these previous findings, show that circadian light input can regulate the activity and neurotransmitter expression in monoamine neurons in a number of neural centers, beginning with the retina.

Mice proficient in melatonin exhibit rhythmic dopamine levels; however, in our study, C57 mice were used and do not produce biologically relevant levels of melatonin, eliminating this rhythmic pattern

[49]. Therefore, the observed decrease in retinal dopamine expression is not influenced by any potential changes in melatonin driven by seasonal light cycles.

3.5.3 Photoperiodic programming of retinal physiology and seasonal affective disorder

Disruption of retinal signaling is implicated in the pathophysiology of certain subtypes of clinical depression [175, 176]. For example, Seasonal Affective Disorder (SAD) affects a portion of the human population during winter months when photoperiods are shorter. These patients display irregularities in photopic and scotopic luminance responses, plus deficits in contrast sensitivity [151, 177-179], essentially similar to those we observed in mice exposed to short light cycles. Recent studies show that SAD patients have lower retinal sensitivity as measured by ERG, which correlates with day length and can be readily treated with light therapy[179, 180].

This study presents mechanistic evidence that retinal light responses, visual contrast sensitivity, and retinal dopamine are persistently decreased in mice by perinatal exposure to short light cycles. Interestingly, some seasonal human birth cohorts have increased the risk of SAD [181], suggesting the possibility that mechanisms similar to those we have described in mice may operate in humans.

CHAPTER IV

D1 and D4 Dopaminergic Receptors Have Differential Effects on Retinal Ganglion Cell Classes

4.1 Summary

Dopamine is a principle neuromodulator that acts to functionally reconfigure the retinal neural network for light-adapted, high spatiotemporal resolution vision. Previous work in our lab found that DA mediates multiple dimensions of the retinal and visual responses in intact animals. By employing separately D1 and D4 receptor signaling in the retina, DA supports four aspects of vision, namely high amplitude light responses, high acuity, high contrast sensitivity and circadian regulation of light-adapted response amplitude. However, it is unknown whether these psychophysical changes manifest at the retinal ganglion cell level, the output neurons of the retinal processing. To assay the neural correlates, here we used two DA receptor knockout mouse models and multi-electrode array recordings to assess the influence of D1 and D4 receptor signaling on ganglion cells, specifically, ON-center sustained (ON-S) and OFF-center (OFF) ganglion cells. Our preliminary results showed that the absence of D4 receptors (D4RKO) significantly increased the background firing rate, as well as the integrated activity duration and receptive field center size of ON-S ganglion cells during the dark-adapted condition. D4RKO ON-S cells also exhibited reduced size of light-adapted receptive field surround during the contrast sensitivity and spatial tuning test. Due to the shrinkage of the receptive field, D4RKO ON-S ganglion cells increased contrast gain. D1 receptors, on the other hand, only affected the dark-adapted receptive field center and activity duration of ON-S cells. However, neither the D1 nor D4 receptor knockout mice showed deficits in the spike rate adaptation to flickering light stimulation. These preliminary findings suggest that D1 and D4 receptors mediate distinct aspects of cell response properties specifically in ON-S ganglion cells. The findings here need to be verified with proper littermate controls of D4RKO mice and also with single cell recordings of a subpopulation of ON-S functional type of ganglion cells.

* This chapter is unpublished. Dai H., Sprinzen D., Risner M.L., and McMahon D.G. designed research; Dai H. collected multi-electrode array recordings; Dai H. and Sprinzen D. analyzed data.

4.2 Introduction

Dopamine (DA) is the principal modulatory neurotransmitter in the retina, which is believed to transition retinal circuits to cone-dominated, high-spatiotemporal resolution photopic vision. In the mouse retina, DA is synthesized and released by ~500 dopaminergic amacrine neurons located in the inner nuclear layer (INL). DA exerts influence throughout the retina by volume transmission, acting on all levels of retinal circuitry and all major classes of retinal neurons [44]. Activation of DA receptors, particularly the dopaminergic D1 and D4 receptors, occurs at distinct locations in the retina, responding to differing DA levels in the retina [44]. D1 receptors are largely present in the INL and ganglion cell layer (GCL), while D4 receptors are concentrated in cone photoreceptors and some ganglion cells. In particular, D1 receptors have been found to act on gap junctions at the level of horizontal cells [69], AII amacrine cells [70], and ganglion cells [72]. In addition, D1 receptors also have been reported to modulate acetylcholine release from amacrine cells [182, 183], GABA release from horizontal cells [184], and ion currents in bipolar [79], horizontal [78] and ganglion cells [80, 82]. D4, on the other hand, acts on the gap junctions between rods and cones, and thus restrict the flow of visual signals from saturated rods to retinal ganglion cells during photopic conditions [85].

Previously we have defined the overall contribution of retinal DA to vision in intact behaving mice using a novel mouse model (rTHKO) in which tyrosine hydroxylase (TH) is genetically excised in the retina [2], and retinal DA levels thus are reduced by ~90-95%. Using additional D1 and D4 knockout animals, we found that D1 and D4 receptors support differential aspects of light-adapted vision. D1 receptors are accounted for behavioral visual acuity, whereas D4 receptors regulate contrast sensitivity [2]. However, it is unknown how this clear separation of DA receptor signaling on visual performance at the behavioral level is preserved in the population of retinal ganglion cells, which carry all output of the retina. More than 30 different functional types of ganglion cells have been characterized in the mouse retina [16]. To extract specific features of the visual scene in parallel for transmission to the brain, each type of ganglion cell possesses distinct light response profile and anatomical architecture, featured with distinguishable response polarity, receptive field, preference for temporal frequencies and contrasts, direction and orientation selectivity, and chromatic preference [16].

Direct DA modulations of ganglion cell properties has been studied in small-scale samples. Through D1 and D4 receptors in ganglion cells, DA alters the electrical coupling between neighboring α-ganglion cells, thereby increasing the concerted activity during daytime vision [72]. The coupling of OFF-sustained ganglion cells, in contrast, is reduced by D1 receptor activation, causing a shrinkage of the receptive field [185]. In addition, D1 receptor signaling has also been reported to be involved in changing many of the response properties of ganglion cells, such as spike count, response latency [186], cAMP levels [83], and sensitivity to light [79], through either direct actions on the receptors on the ganglion cells or modulations

of the upstream circuitry. While the cellular actions of retinal DA are well documented, it is not well understood how these multiple effects interact to shape overall retinal information processing especially at the level of ganglion cells, the output of the retinal processing.

In this study, we seek to understand which properties of ganglion cell function are driven by D1 or D4 receptor signaling, and how these changes in ganglion cells underlie the effects of the absence of D1 and D4 receptors on acuity and contrast sensitivity, respectively. Here, we used the D1 and D4 receptor knockout mouse models combined with multi-electrode array (MEA) recordings to sample in depth the actions of DA on retinal ganglion cell classes, specifically evaluating baseline dark-adapted responses, spike rate adaptation to light, and sensitivity to contrast and acuity. We, therefore, assessed the relative contribution of D1 and D4 receptors to ganglion cell function. To categorize each functional type of ganglion cell, we broadly parsed the ganglion cell population based on ON, OFF, or ON-OFF response polarity, activity duration (either transient or sustained), and direction selectivity. Overall, we found evidence that D1 and D4 receptors are mainly involved in regulating ON-sustained retinal pathways, but have divergent controls of DA's action on visual processing.

4.3 Materials and Methods

4.3.1 Animal usage and care. Mouse C57BL/6N/A/a embryonic stem cells harboring the $Drd1^{tma1a(KOMP)Wtsi}$ or $Drd4^{tm1a(EUCOMM)Wtsi}$ reporter-tagged insertion with conditional potential were obtained from the KOMP International Knockout Mouse Consortium (Fig. 4.1). This is a versatile 'knockout-first allele' (tm1a) [187] in C57BL/6N embryonic stem cells [188]. This strategy relies on the identification of a "critical" exon, common to all transcript variants that, when deleted, creates a frame-shift mutation. In Drd1 and Drd4, the 2^{nd} and 2^{nd}-4^{th} exons are interrupted, respectively, and thus no protein product is predicted to be produced. The KO-first allele is flexible and can produce reporter knockouts, conditional knockouts, and null alleles following exposure to site-specific recombinases Cre and Flp (Fig. 4.1A). Founder mouse lines on C57BL/6J background were produced from this construct by the Vanderbilt Transgenic Mouse Core. Following verification of the intact insertional construct and loss of D1 or D4 receptor expression in the Ventral tegmental area (VTA) of founder mice. In our study, these mice with the homozygous "knockout-first" alleles of D1 or D4 receptors (D1RKO or D4RKO) were compared to a control population of wild-type (D1RWT) littermates of D1RKO. Both male and female mice aged 60-120 days old were used in these experiments. Animals were maintained on a 12:12 light-dark cycle and electrophysiological recordings were performed between the hours of 12 to 5 pm CST. All animal protocols were in accordance with the guidelines established by Vanderbilt Animal Care Division and the National Institutes of Health Guide for the Care and Use of Laboratory Animals.

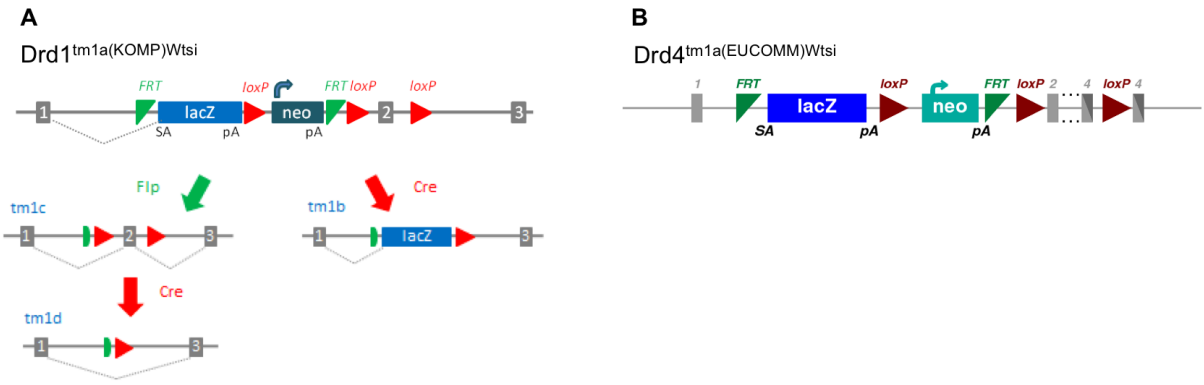

Fig. 4.1 Allele map of "knockout-first allele" in D1RKO and D4RKO mice.

(**A**) Drd1$^{tm1a(KOMP)Wtsi}$ reporter-insertion construct interrupts the second exon of *Drd1* gene that encodes D1 receptors, while (**B**) Drd4$^{tm1a(EUCOMM)Wtsi}$ construct affects second to fourth exons of *Drd4* gene that encodes D4 receptors. Therefore, no protein product is predicted to be produced. Using Drd1$^{tm1a(KOMP)Wtsi}$ as an example, we showed all available alleles that can be generated from this construct with conditional potential (modified from the KOMP International Knockout Mouse Consortium, https://www.komp.org/alleles.php#conditional-promoter-csd, http://www.mousephenotype.org/data/alleles/MGI:94926/tm1a(EUCOMM)Wtsi)

4.3.2 Mouse retina preparation. Prior to experiments, animals were dark-adapted for 1-2 hours. Eyes were enucleated under dim red light (660nm) and then placed in carboxygenated Ames' medium (A1420, Sigma Aldrich, St. Louis, MO). Retinas were isolated under a dissecting microscope illuminated using a 660±30 nm light-emitting diode (LED; Roithner-Lasertechnik, Vienna, Austria), which minimizes light-adaptation given mouse spectral sensitivity [189]. To remove excess vitreous, retinas were incubated in an enzyme solution of Ames' medium, with 240.9 units/mL collagenase (LS005273, Worthington, Lakewood, NJ), and 2mg/mL hyaluronidase (LS002592, Worthington, Lakewood NJ) for 10 minutes (detailed protocol see [190]). The retina was cut in half and trimmed at the periphery to flatten the retina. The retina was then mounted ganglion-side down onto a 6×10 perforated multi-electrode array (MEA) and held in place with a slice anchor (HSG-5BD, Multichannel Systems, Reutlingen, Germany). Tissue was perfused at a rate of 2 mL/min with carboxygenated Ames' medium heated to 36.5 °C using a temperature regulator (Warner Instruments, Hamden, CT). Prior to recordings, tissue was allowed to settle on the MEA for approximately 30 minutes.

4.3.3 Electrophysiology and data acquisition. Spiking activity of each ganglion cell was recorded from an electrode connected to an individual differential amplifier. The electrodes were 30μm in diameter and the inter-electrode distance was 100μm. The electrode impedance ranged from 30 - 400 kΩ. The MEA

was placed in an MEA amplifier (1060 Up, Multichannel Systems, Reutlingen, Germany) with a gain of 1200 and a band-pass filter of 10 – 3000 Hz.

Analog signals were digitized using the MC-Rack software suite (Multichannel Systems, Reutlingen, Germany) at a sampling rate of 10 kHz. We did not use an online threshold to detect spikes. Instead, spikes were sorted offline. Data capture was synced to stimulus display using an external trigger (NIUSB-6009, National Instruments, Austin, TX) that sent a TTL pulse to MC-Rack software to start or end recordings. This external trigger was executed within the visual stimulus programs. Raw data was saved to the computer's hard disk for offline analysis. In the experiments using the multielectrode technique, we recorded on average 11 cells during each recording session from a patch of the mouse retina.

4.3.4 Visual stimuli. Light stimuli were presented using a monochrome (λ_{max} = 545 nm) LCD monitor (Lucivid XMR, MBF Biosciences, Williston, VT). Under photopic conditions, this wavelength will primarily stimulate cone photoreceptors containing the middle-wavelength sensitive opsin [189]. The active region of the LCD display measured 12.78×9 mm, corresponding to 1.92×1.44 mm on the surface of the retina. The LCD monitor was attached to an auxiliary port on an upright microscope (Examiner A1, Zeiss, Germany) using a standard C-mount. Visual stimuli were focused onto the retinal surface using a 10× water-immersion objective (Zeiss, Germany). The luminance of the monitor was calibrated using a photometer (LS-110, Minolta, Ramsey, NJ) and linearly ranged from 1.4-2.45 log cd/m^2 corresponding to 50-250 grayscale value.

Visual stimuli were programmed in MATLAB using the Psychophysics toolbox extension package [191, 192]. To assess retinal function, we presented four stimulation protocols in sequence: Pseudorandomly-positioned flashed squares of light (random square), flickering checkerboard to assess spike rate adaptation to light (checkerboard), drifting sinusoidal gratings that vary in spatial frequency and contrast to measure contrast sensitivity (contrast sensitivity test), and lastly bars of light drifting in different directions (DS test, direction selectivity).

The random square stimulus was used to measure ganglion cell response polarity (ON-, OFF-, or ON-OFF-center) and response integration time (transient or sustained). In this protocol, a 120×120μm square of 2.2 log cd/m^2 on a dark background was randomly indexed through a 12×16 grid projected onto the retina surface. For each position, the square was flashed on for 1 sec followed by 6 sec of stimulus off time so ganglion cells could rebound from stimulus effects. This stimulus protocol lasted for approximately 22 minutes.

The flickering checkerboard stimulation was used to light adapt the retina and measure spike rate adaptation. In this protocol, a 12×16 grid of independently modulated square stimulus elements was updated at 75 Hz and presented for 12 minutes. At each update, there was a 20% probability of a given

square being active at 2.34 log cd/m^2 as defined by the MATLAB rand function. The integrated intensity of the flickering checkerboard stimulus was 1.64 log cd/m^2.

To assess contrast sensitivity, drifting sinusoidal gratings were presented to the retinal surface. Sinusoidal gratings were varied in both spatial frequency, ranging from -3.0 to -0.2 log cycles/degree (c/d) and contrast, ranging from 5 to 30 percent Michelson contrast. The mean luminance was 2.2 log cd/m^2, which should saturate rod responses [193, 194]. Each spatial frequency-contrast combination was presented for 30-45 cycles (20-30 sec) in four directions (0-270°). The temporal frequency was 1.5 c/sec, which is the peak behavioral temporal sensitivity for mice [10]. This stimulus protocol lasted between 80-90 minutes.

Finally, ganglion cell direction selectivity (DS) was measured by presenting moving bars in eight different directions in 45º increments from 0-315°. There were 4 trials for each direction. The cumulative number of spikes produced by each cell for each direction was plotted on a polar plot. Bars measured 100 μm in width and ≥9000 μm in length with a luminance of 2 log cd/m^2. Bars were separated by 912 μm and were translated across the extent of the monitor at a temporal frequency of 1.6 c/sec. This visual stimulus protocol lasted for approximately 10 minutes.

4.3.5 Spike sorting and data inclusion criteria. After data was acquired, spike sorting was done using Plexon Offline Sorter [195, 196] (Plexon, Dallas, TX). Raw data were filtered using 250 Hz low-cut 4-pole Bessel filter and then spikes detected at -4σ threshold. Sorting was performed by cluster analysis using the first three principal components of the spike waveform, and manually verified based on the spike train to ensure spikes were sorted to correct clusters. The majority of our ganglion cell sample stemmed from MEA channels containing spikes from a single cell or from the cell producing the greatest spike amplitude on a particular MEA channel. However, on some MEA channels, the spikes were sorted into multiple cells when spike waveforms and principal components revealed two distinct ganglion cells. Waveforms and principal component clusters were compared across stimulus protocols to verify data was from the same ganglion cell. Cells were excluded in data analysis if responses significantly changed over the recording time (i.e., cell death) or if responses were not easily detectable above the noise.

4.3.6 Retinal ganglion cell classification. Ganglion cells were grouped into distinct classes by their basic light-evoked responses, including the center response polarity, response duration, and direction selective (DS) index. Response polarity (i.e. ON, OFF, ON-OFF) and duration (i.e. sustained, transient) were measured using the ganglion cell responses to the random square stimulus. Polarity was defined as the dominant response to either onset or offset of the light square when stimulated over the receptive field center. When both onset and offset had similar response magnitude, cells were labeled as ON-OFF.

Response duration was quantified as the normalized integrated spike rate during either 1 second of light pulse for ON cells or 1 second following light offset for OFF cells. OFF-center ganglion cells were not separated by duration because no clear distinction between sustained and transient responses could be determined visually or by cluster analysis. This may be because in this set of experiments we only examined responses to offset of a light square on a dark background rather than looking at the onset of a dark square on a light background which may be optimal for OFF type cells [38]. However, OFF cells were grouped into OFF and OFF-low, based on induced firing rate during the random square stimulus. DS index was obtained using the data from the moving bars light stimulus protocol and calculated as the vector average of the mean spike rate in each direction [197]. The index was 0 when the cell responded equally in all directions and 1 when the cell only responded to stimuli in a single direction. We defined ganglion cells that scored higher than 0.3 of the DS index as the direction selective cells. A total of 6 clusters of cells were consistently presented across all genotypes: ON-center sustained (ON-S), ON-center transient (ON-T), ON-center DS (ON-DS), OFF-center (OFF), OFF-center-low (OFF-low), and ON-OFF-center DS (ON-OFF-DS).

4.3.7 Visual psychophysical testing. The visual-behavioral performance was assessed using the optokinetic head-tracking reflex, testing for contrast detection (sensitivity) using the OptoMotry system (Cerebral Mechanics). Video analysis enabled an observer to track the reflexive head movements of mice in response to rotating sinusoidal-wave gradients projected by four interfacing Dell LCD monitors. Tracking was defined as smooth head movements tracked in the same direction and speed as the rotation of the sinusoidal-wave gradient. Contrast sensitivity detection was measured by presenting the sinusoidal contrast gradients sequentially reduced from 100% contrast, at each spatial frequency, until no reflexive head movements were observed. The last contrast level where the observer noticed tracking was deemed the animals contrast sensitivity threshold. As described by Prusky et al. (2004) [98], we measured contrast sensitivity threshold at six spatial frequencies (0.031, 0.064, 0.092, 0.103, 0.192, and 0.272 cycles/degree). The contrast sensitivity was calculated using a Michelson contrast from the screen's luminance (maximum-minimum)/(maximum+minimum) as previously described [98, 162].

4.3.8 Statistical analysis. One-way ANOVA and two-way with repeated measures ANOVAs were used where applicable and reported. *Post hoc* analyses followed ANOVAs to confirm the difference among groups. Significance levels were set at $P < 0.05$ and represented as means ± SEM as indicated in each graph (GraphPad, La Jolla, CA and Sigmaplot, San Jose, CA).

4.3.9 Data analysis.

Spontaneous activity and light-driven response parameters. To inspect the possible effects of knocking out retinal dopamine on typical spiking parameters we measured pre-stimulus spontaneous spike rate, peak spike rate, response duration, the size of dark-adapted receptive field center, and inhibition strength by light offset for ON cells or onset for OFF cells. All parameters were measured during the random square stimulation. Retinal ganglion cell spiking activity was spatially averaged over the receptive field center as defined by the spatial positions where the ganglion cell produced a response greater than 20% of the maximum light-evoked response at light onset for ON cells and at light offset for OFF cells. The peak spike rate was defined as the maximum firing rate during 250 msec bins for each ganglion cell minus the spontaneous activity. Response duration, which we also refer to as integrated response time, was defined as the integrated firing rate during 1 sec on for ON cells and 1 sec off for OFF cells. Responses were normalized such that baseline activity was set to zero and peak firing rate was set to one. It is known that the response duration decreases away from the center of the receptive field, thus, the integrated response time, as calculated here, may underestimate the optimal center response duration because it is spatially averaged over a larger area [198]. Inhibition strength was defined as the difference between the baseline and lowest point during 1 sec of light off for ON cells and 1 sec of light on for OFF cells.

Spike rate adaptation. Ganglion cell spike rate adaptation was measured by assessing the spike rate output produced by the flickering checkerboard visual stimulus protocol, which was used to light adapt the retina. Spike rate adaptation profiles show the average spike rate within 60 sec bins, over the course of 720 sec of stimulation. To evaluate statistical significance a one between-subjects (genotype) and one within-subjects (time) two -way repeated measures ANOVA was performed using ranked data followed by *post-hoc* pairwise comparisons as indicated in the text.

Response to different levels of stimulus contrast and spatial frequency. To measure the contrast sensitivity function of ganglion cells we calculated the first harmonic response of spike trains produced by each contrast and spatial frequency pair using similar methods as Dedek et al. (2008)[199]. The first harmonic response was defined as

$$R(\mathbf{k}) = \left| \frac{2\pi}{\omega} \frac{1}{N_C} \sum_j exp\left[- i\omega t_j(\mathbf{k}) \right] \right|$$

where R(k) was the first harmonic, ω was the temporal frequency (set to 1.5 c/sec), Nc was the number of cycles (30-45), and $t_j(k)$ was the time of the j^{th} spike produced by grating with the spatial frequency (k). The first harmonic response at each spatial frequency was then fit to a spatial tuning model to estimate cell's receptive field properties

$$\hat{H}(k) = \sqrt{(\alpha_c e^{-(\pi r_c k)^2})^2 + (\alpha_s e^{-(\pi r_s k)^2})^2 - 2\alpha_c \alpha_s e^{-(r_c^2 + r_s^2)(\pi k)^2} \cos(\phi)}$$

where k was spatial frequency, α_c was the center strength, r_c was the center radius of the receptive field, α_s was the surround strength, r_s was the surround radius, and Φ was the phase offset [200].

4.4 Results

4.4.1 D1RKO and D4RKO ON-S ganglion cells exhibit changed spontaneous activity and light-driven spiking parameters

We obtained extracellular recordings from 96 ganglion cells from 3 D1RKO animals, 74 ganglion cells from 4 D1RWT animals and 72 ganglion cells from 4 D4RKO animals. Ganglion cells of each genotype can be classified into five major groups: ON-center sustained (ON-S), ON-center transient (ON-T), OFF-center (OFF), OFF-center with low baseline spike rate (OFF low), and ON-center direction selective (ONDS). ON-S and OFF ganglion cells are the most abundant cell types, together making up of 50% of the total ganglion cells. Our previous study (unpublished data by Risner, M.L., Sprinzen, D and McMahon D.G.) shows that ON-S and OFF ganglion cells are the most affected cell population in retinal DA depletion mouse line (rTHKO), exhibiting deficits in spike rate adaptation to light and reduced response to contrast. Therefore, our study mainly is focused on the comparisons of ON-S and OFF cells across all genotypes.

Under the dark-adapted condition, D4RKO ON-S ganglion cells exhibited a significantly higher base firing rate prior to the one second of light flash, compared to D1RWT and D1RKO (Fig. 4.2A, B, $^{**}P$= 0.006, Kruskal-Wallis one-way ANOVA on ranks, *post hoc* Dunn's method). In both D1RKO and D4RKO retinas, ON-S ganglion cells showed expanded receptive field center (Fig. 4.2C, $^{***}P < 0.001$, Kruskal-Wallis one-way ANOVA on ranks, *post hoc* Dunn's method) as well as increased integrated response time (Fig. 4.2D, $^{***}P < 0.001$, one-way ANOVA, *post hoc* Student-Newman-Keuls method). The knockout of D1 and D4 receptors did not change the peak firing rate (Fig. 4.2E, $P = 0.625$, one-way ANOVA), however, the absence of D1 receptors attenuated light offset inhibition of ON-S ganglion cells (Fig. 4.2F, $^{***}P < 0.001$, one-way ANOVA, *post hoc* Dunn's method). No differences were detected for OFF ganglion cells in spontaneous activity, size of the receptive field center, peak response, response duration, and response inhibition during light onset (Fig. 4.3A-F).

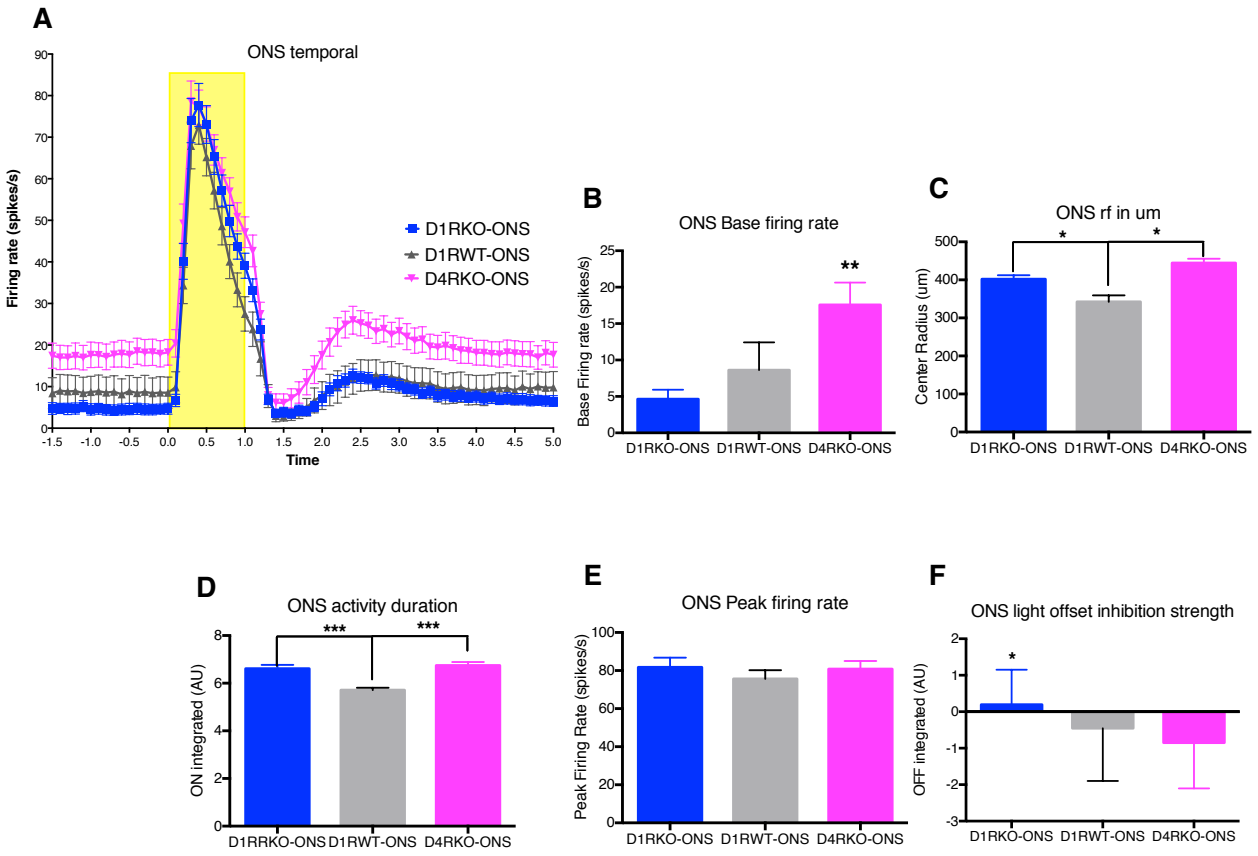

Fig. 4.2 Knocking out retinal D1 or D4 receptors alters spontaneous spiking activity and light-driven responses in ON-S ganglion cells.

(**A**) The firing rate of ON-S ganglion cells is plotted as a function of time during the random square test. The yellow block indicates one second of light's on. (**B**) Base spike rate is significantly increased in D4RKO ON-S ganglion cells ($H = 10.21$, $^{**}P = 0.006$, Kruskal-Wallis one-way ANOVA on ranks, *post hoc* Dunn's method). The dark-adapted receptive field (**C**) and response duration (**D**) increase in both D1RKO and D4RKO ON-S cells (receptive field, $H = 22.372$, $^{***}P < 0.001$, Kruskal-Wallis one-way ANOVA on ranks, *post hoc* Dunn's method; response duration, $F_{(2,63)} = 16.435$, $^{***}P < 0.001$, one-way ANOVA, *post hoc* Student-Newman-Keuls method). Peak spike rate remains at the similar level across genotypes (**E**, ($F_{(2,63)} = 0.474$, $P = 0.625$, one-way ANOVA). However, the inhibition caused by light offset is attenuated in D1RKO (**F**, $H = 15.369$, $^{***}P < 0.001$, Kruskal-Wallis one-way ANOVA on ranks, *post hoc* Dunn's method). D1RKO is presented in blue, D1RWT in dark grey and D4RKO in magenta. The color scheme is consistent throughout the chapter unless noted. All data represent means ± SEM; n = 3-4 mice.

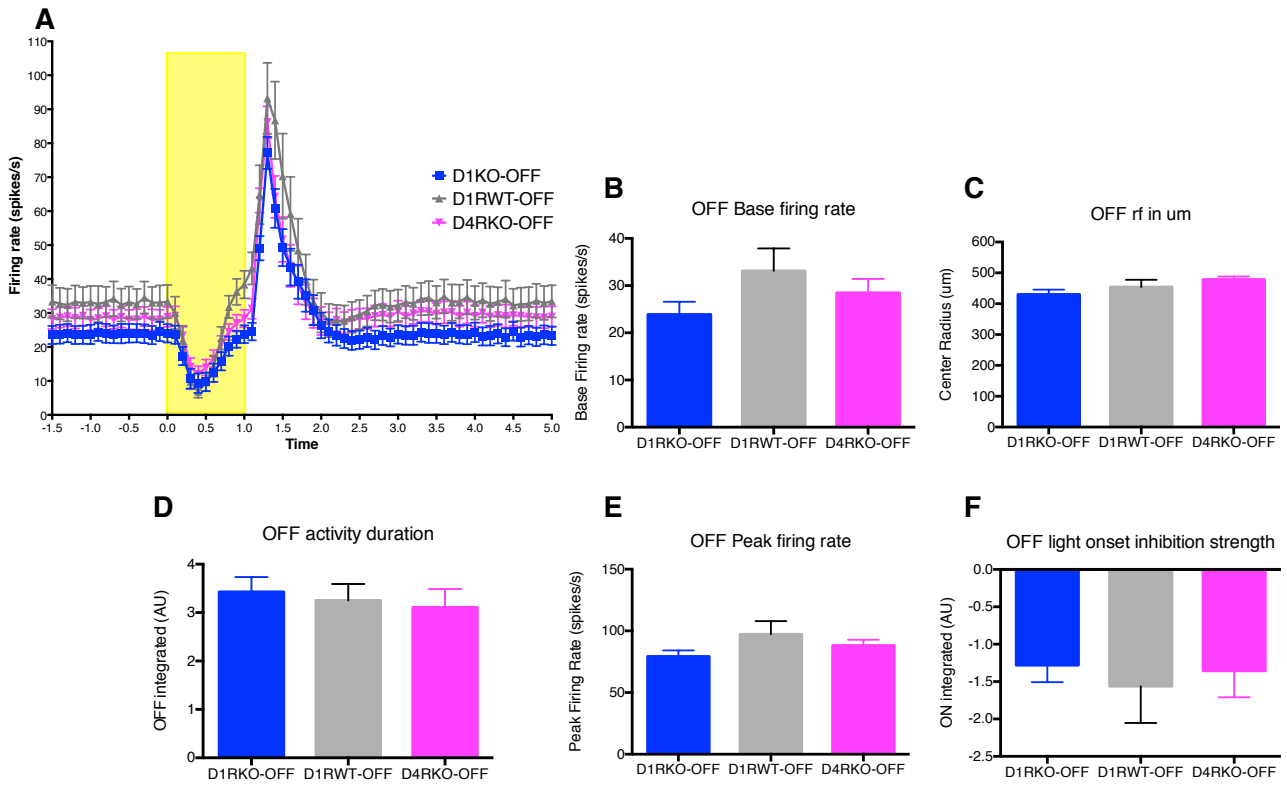

Fig. 4.3 Knocking out retinal D1 or D4 receptors does not change spontaneous spiking activity and light-driven responses in OFF ganglion cells.

(**A**) The firing rate of OFF ganglion cells is plotted as a function of time during the random square test. The yellow block indicates one second of light's on. None of the parameters is changed in the OFF cells of D1 or D4 receptor knockout mice (**B**, base spike rate, H = 3.986, $P = 0.136$; **C**, dark-adapted receptive field, $F_{(2,58)} = 3.132$, $P = 0.051$; **D**, response duration, H = 0.690, $P = 0.708$; **E,** peak firing rate, $F_{(2,58)} = 1.940$, $P = 0.153$; **F**, light onset inhibition, H = 0.323, $P = 0.851$, Kruskal-Wallis one-way ANOVA on ranks or one-way ANOVA). All data represent means ± SEM; n = 3-4 mice.

4.4.2 Light adaption of ON-S and OFF ganglion cells to flickering light is not affected in D1RKO and D4RKO animals

DA is thought to be a key neurotransmitter involved in light-dependent spike rate adaptation [201]. Extracellular dopamine levels increase during both steady full-field illumination and to flickering light stimulation [47, 202-205]. Flickering light, in particular, has been shown to produce physiological effects such as altering gap junction coupling of horizontal and ganglion cells through increases in extracellular DA content [201, 206-208].

Here we sought to examine the effects of genetically knocking out retinal D1 and D4 receptors on spike rate adaptation of ganglion cells by assessing the response produced during flickering checkerboard stimulation. The deficiency of D1 and D4 receptors did not affect the spike rate adaptation, with ON-S

cells showing gradually decreased spike rate while OFF cells exhibiting increased spike rate across all genotypes during the beginning of light adaptation. Although D4RKO showed a trend of increased overall spike rate during the light adaptation, statistically the light adaptation of ON-S and OFF cells in D4RKO animals was not different than those of D1RKO and D1RWT (Fig. 4.4A, ON-S cells, $P = 0.639$; B, OFF cells, $P = 0.612$, two-way repeated measures ANOVA). We normalized the absolute spike rate to average spike rate over the period of light adaptation to examine the shape of adaptation curves, and found that the normalized spike rate adaptation of D4RKO and D1RKO ganglion cells overlapped with those of D1RWT with no significant differences (Fig. 4.4 C-D). Our previous work showed that the lack of D1 or D4 receptors led to a reduction of ERG b-wave amplitudes under the light-adapted condition [2]. Given that ERG b-wave amplitudes correspond primarily to the activities of ON-bipolar cells, the result obtained from ON-S ganglion cells is inconsistent with what we observed previously. The deficits in the light adaption might not be revealed due to much dimmer light stimulus projected by LCD monitor. In the previous ERG experiments, we presented animals with a steady background intensity of 1.6 log cd/m^2, and flash intensity of 0.9 log cd*s/m^2, whereas the LED monitor we used here could only project integrated light intensity of 1.64 log cd/m^2 with a maximum of 2.34 log cd/m^2. Therefore, using a brighter LED bulb for the background could overcome the limitation of LCD monitor, and thus helps us to examine if the firing rate of ON-S cells would recapitulate the decreased b-wave amplitudes observed in ERG.

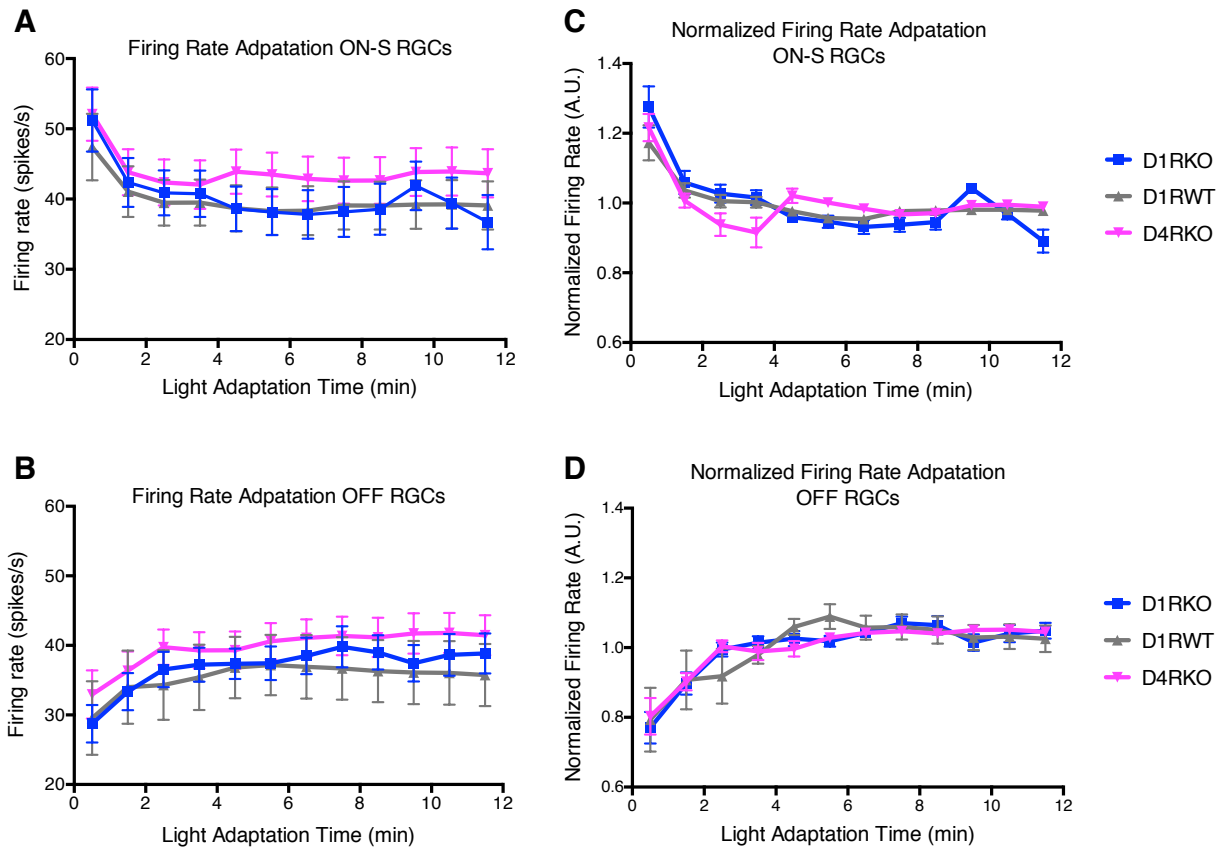

Fig. 4.4 The firing rate adaptation of ON-S and OFF ganglion cells to flickering checkerboard does not significantly differ in D1RKO and D4RKO mice.

The firing rate of ON-S and OFF cells of each genotype (**A**-**B**) was normalized to the average firing rate during the light adaptation to show the shape of the adaptation curves (**C**-**D**). ON-S cells do not exhibit any significant difference in the firing rate adaption to flickering light in D1 or D4 knockout retinas ($F_{(2, 693)} = 0.451$, $P = 0.639$), nor OFF cells ($F_{(2, 616)} = 0.495$, $P = 0.612$, two-way repeated measures ANOVA). All data represent means ± SEM; n = 3-4 mice.

4.4.3 Disruption of D4 receptor signaling shrinks the size of the receptive field surround and increases contrast gain of ON-S ganglion cells

Using the spatial tuning modeling, we first characterized the property of the receptive field. D4RKO ON-S cells experienced a shrinkage of their receptive field surround (Fig. 4.5B, ON-S cells, $^{***}P \leq 0.001$, Kruskal-Wallis one-way ANOVA on ranks, *post hoc* Dunn's method) whereas the receptive field surround of OFF cells was not affected (Fig. 4.5D, OFF cells, $P = 0.341$, Kruskal-Wallis one-way ANOVA on ranks). As expected, the center size of the receptive field of both ON-S and OFF cell types were reduced after prolonged light adaptation compared to dark-adapted condition, however, the depletion of D1 and D4 receptors did not change the size of the light-adapted receptive field center

relative to WT (Fig. 4.5A, ON-S cells, $P = 0.739$; C, OFF cells, $P = 0.447$, Kruskal-Wallis one-way ANOVA on ranks).

To determine if knocking out D1 and D4 receptors affects the response to different levels of contrast we presented sinusoidal gratings varying in both contrast and spatial frequency at a fixed temporal frequency. To assess the strength of periodicity of spiking activity to each stimulus, we measured first harmonic response of spike trains, defined as response power, and found that responses to different levels of contrast at the peak spatial frequency were not altered in ON-S and OFF cells in D1RKO and D4RKO animals (Fig. 4.5E, ON-S cells, $P = 0.690$; F, OFF cells, $P = 0.233$, two-way repeated measures ANOVA).

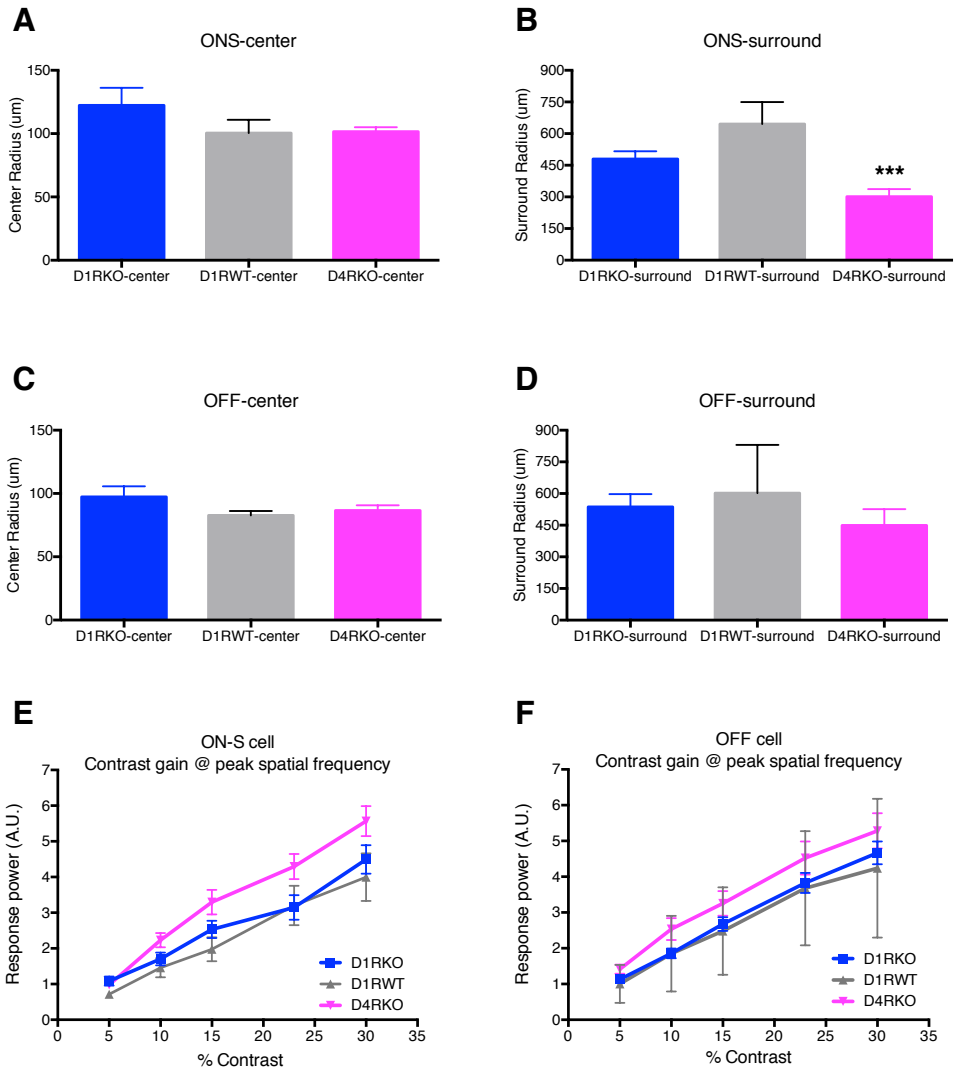

Fig. 4.5 D4RKO ON-S ganglion cells exhibit reduced receptive field surround size.

Although the size of the receptive field center of both ON-S and OFF ganglion cells does not show genotype dependent changes (**A,** ON-S cells, H = 0.604, $P = 0.739$; **C**, OFF cells, H = 1.612, $P = 0.447$, Kruskal-Wallis one-way ANOVA on ranks), the surround of D4RKO ON-S cells is significantly smaller (**B**, H = 16.650, ***$P < 0.001$,

Kruskal-Wallis one-way ANOVA on ranks). However, this change of receptive field does not alter the contrast gain of ON-S and OFF ganglion cells at the peak spatial frequency that evokes the highest response within the spatial frequency range we tested (**E**, ON-S cells, $F_{(2,200)} = 2.822$, $P = 0.069$; **F**, OFF cells, $F_{(2,216)} = 1.496$, $P = 0.233$, two-way repeated measures ANOVA). All data represent means ± SEM; n = 3-4 mice.

Interestingly, at peak contrast 30%, we found that D4RKO ON-S cells exhibited higher response power at lower and middle-to-high spatial frequencies (Fig. 4.6A, $^{**}P = 0.010$, two-way repeated measures ANOVA, *post hoc* Tukey Test), suggesting that at the given spatial frequencies D4RKO ON-S cells had higher contrast gain. Indeed, when we plotted the responses of D4RKO ON-S cells at 23% of contrast (Fig. 4.6B, $P = 0.685$, two-way repeated measures ANOVA), it completely overlapped with those of D1RKO and D1RWT ON-S cells at 30%. We further followed upon this lead and tested the contrast sensitivity (i.e. threshold for contrast detection) using OKT. Compared to Dr. Michael Iuvone group's D4 receptor knockout mouse model, our D4RKO only showed deficits in detecting contrast at lower spatial frequencies, but performed as well as the WT at high spatial frequencies (Fig. 4.6D). The range of spatial frequencies tested in ganglion cell was narrower than that of OKT, only covering up to ~ -0.8 log c/d, suggesting an inconsistency of ON-S ganglion cell with behavioral capability in contrast gain. OFF cells showed a similar trend where the response power of D4RKO OFF cells was higher than that of D1RKO and D1RWT within the spatial frequency range we test. However, the difference in contrast detection was not statistically significant (Fig. 4.6C, $P = 0.113$, two-way repeated measures ANOVA).

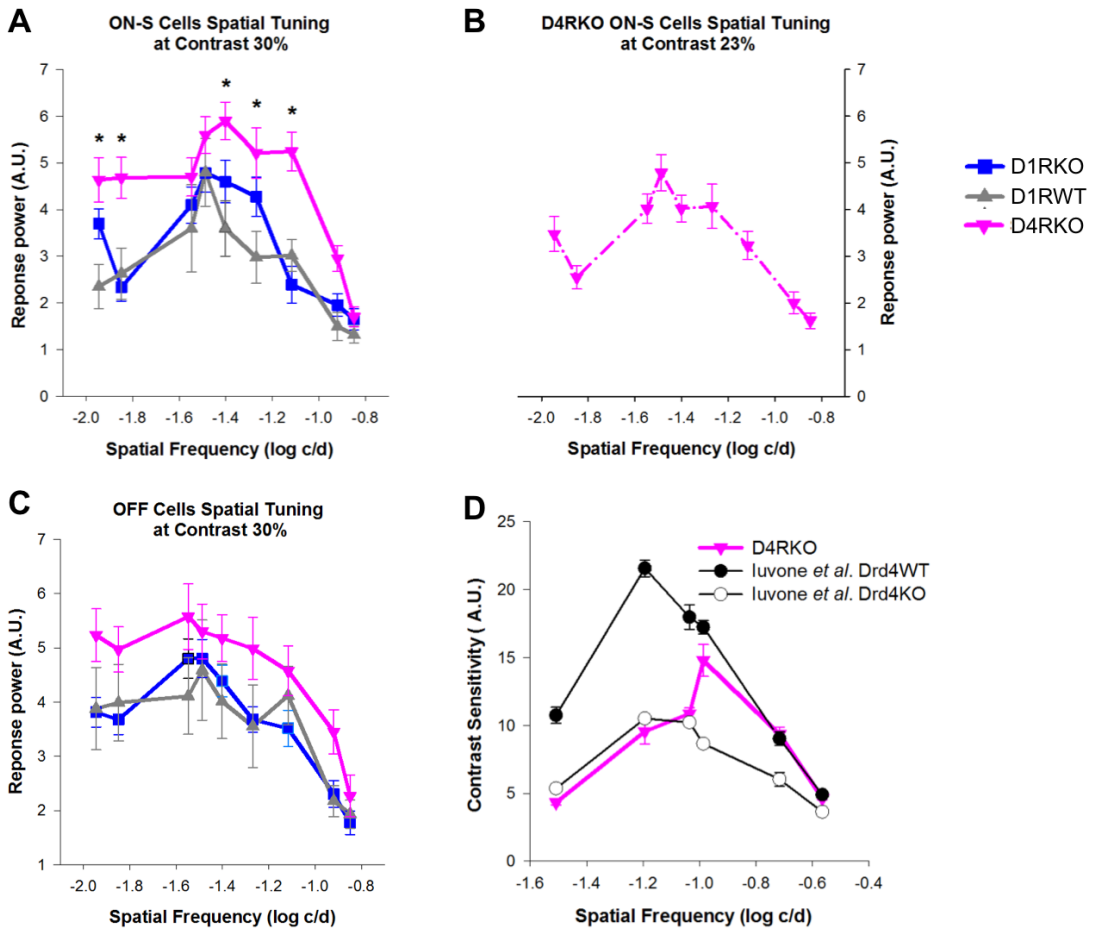

Fig. 4.6 D4RKO ON-S ganglion cells have increased contrast gain.

(**A**) The response power of D4RKO ON-S ganglion cells is significantly higher than the other two groups at spatial frequencies at -1.95, -1.85, -1.40, -1.27, and -1.12 log c/d ($F_{(2, 400)} = 5.053$, $^{**}P = 0.010$, two-way repeated measures ANOVA, *post hoc* Tukey Test). The responses of D4RKO ON-S ganglion cells at 23% are equivalent to those of D1RKO and D1RWT at contrast 30%, with a similar shape of responses and spatial frequency (-1.48 log c/d) at peak response (**B**, $F_{(2, 400)} = 0.382$, $P = 0.685$). D4RKO mice also exhibit normal contrast sensitivity at high spatial frequencies when comparing our data to Drd4WT generated by Dr. Michael Iuvone's group (**D**). OFF cells do not demonstrate statistical differences across genotypes in detecting contrast at various spatial frequencies (**C**, $F_{(2, 432)} = 2.275$, $P = 0.113$). Two-way repeated measures ANOVA was used for statistical analysis. All data represent means ± SEM; n = 3-6 mice

4.5 Discussion

In our current study, we examined the effects of knocking out D1 or D4 receptors on ON-S and OFF-ganglion cell physiology from 3 aspects: (1) spontaneous activity and light-driven response dynamics in

dark-adapted condition; (2) spike rate adaptation to light; and (3) contrast sensitivity and spatial frequency tuning profiles. We found the receptive field of ON-S ganglion cells was altered due to the lack of D4 receptors under both dark- and light-adapted conditions, whereas D1 receptors appeared only to be involved in the regulation of dark-adapted receptive field center of ON-S. The absence of D4 receptors led to abnormal dark-adapted spontaneous activity and an increased receptive field center, as well as decreased surround size and better contrast gain under light conditions. Across all light paradigms, OFF ganglion cells exhibited no deficits in their response dynamics to light, spike rate adaptation, nor responses to varying contrasts and spatial frequencies.

4.5.1 D1 receptors mediate dark-adapted receptive field of ON-S ganglion cells

In our previous study of retina-specific depletion of DA (rTHKO) (unpublished data by Risner, M.L., Sprinzen, D and McMahon D.G.), we observed a trend that dark-adapted receptive fields of ON-S cells increased in size. As we expected, D1RKO ON-S cells recapitulated this increase in dark-adapted receptive fields, which could be attributed to the involvement of D1 receptors in modulating horizontal cell gap junctions [44]. Although D1 receptors have been shown to suppress spontaneous activity in rat ganglion cells [81], the ON-S ganglion spontaneous baseline activity was not affected in our present study.

4.5.2 D4 receptors contribute to the regulation of the receptive field of ON-S ganglion cells in both dark- and light-adapted condition

The increased dark-adapted receptive field and base firing rate could originate from a failure of uncoupling between rods and cones, which is regulated by D4 receptors on cones [85]. *Drd4* mRNA levels are upregulated during darkness and confined to the photoreceptors [209]. The maintained coupling of rods and cones would increase the baseline "noise" from rods to the ganglion cells and also increase the number and range of photoreceptors that input to ganglion cells. D4 receptors might mediate extended activity duration of ON-S cells through their role in cone photoreceptors. The absence of D4 receptors affects light adaptation, altering the transmission of light responses from photoreceptors to inner retinal neurons by interfering the modulation of cAMP cascade [86].

We surprisingly found that D4 receptors also participate in modulating the size of receptive field surround of ON-S cells during the contrast sensitivity and spatial frequency tuning. Conventionally, horizontal cells are considered as the major contributor to the formation of the surround, whose coupling is mediated by D1 receptors. Although D4 receptors have been reported to express in the inner retina with less abundance [209], they can be only detected in amacrine cells and ganglion cells [210, 211]. Therefore, instead of directly acting on horizontal cells, D4 receptors are more likely to influence horizontal cell light responses by modifying signals from cones onto horizontal cells. Alternatively, D4 receptors could

potentially modulate GABAergic amacrine cells that contribute to the generation of antagonistic surrounds of ganglion cells. The surround suppression of excitatory inputs is mediated by a combination of $GABA_C$ receptors in ON ganglion cells and in ON bipolar cells [76, 212, 213]. Consistent with the reduced size of the receptive field, D4RKO ON-S cells thus gained higher contrast sensitivity. This result seems to contradict our previous findings that *Drd4* knockout leads to compromised contrast sensitivity as measured by optokinetic tracking (OKT) [2] as well as reported by Dr. Michael Iuvone's group. However, the reduced contrast sensitivity observed in OKT is likely to be biased towards the NPAS-2 expressing ganglion cells, as the contrast sensitivity is similarly reduced in *Drd4* knockout and *Npas2* knockout animals [166]. ON-S cells are not the same cell population as the NPAS-2 containing ganglion cells. Our study thus reported a differential effect of DA on a different subpopulation of ganglion cells. Further verifications are needed given that we compared D4RKO with the wild-type littermate controls of D1RKO. The potential variances in the mouse background and breeding strategy could lead to differences in wild-type control of different mouse lines, which could mislead our interpretation of the present data. If the increase in contrast gain in D4RKO animals persists compared to the proper control, we would then follow up on dissecting the subtypes of ON-S ganglion cells that are primarily responsible of the observed phenotype. We will start with ON α-ganglion cells, which have been recently found to express melanopsin and are intrinsically photosensitive [214]. ON α-ganglion cells themselves demonstrate high contrast sensitivity and are necessary for contrast detection in mice at the behavioral level. Colocalization of D4 receptor expression on this type of ganglion cells could be revealed by in situ hybridization of *Drd4* mRNA with ON-S α-ganglion cell markers Opn and calbindin [215].

CHAPTER V

Conclusions and Future Directions

5.1 Summary

The initial steps of vision - the transduction and encoding of physical light stimuli into neural signals - occur in the retina, a multi-layered sheet of neurons that lines the back of the eye. Retinal dopamine (DA) acts as the principal modulatory neurotransmitter, whose signaling is driven by both light-sensitive and intrinsic circadian mechanisms. DA critically shapes retinal circuits and alters the processing of visual signals by initiating slow and sustained changes in the physiology of retinal neurons and synapses. Here, to achieve a mechanistic understanding of how DA reconfigures retinal circuits according to background illumination, we employed various mouse models, electrophysiological, psychophysical, and pharmacological techniques to answer three fundamental questions: (1) how does dopamine transporter (DAT)-mediated volume transmission contribute to retinal physiology? (2) how are the retinal dopaminergic system and overall visual function shaped by circadian perinatal photoperiod? and lastly, (3) how do DA receptors direct differential signaling pathways and influence ganglion cell function?

We found that physiological signatures of DAT-dependent anomalous dopamine efflux (ADE) can be revealed by elevated retinal light-adapted responses in male mice, but not in female mice. Given that the specific DAT variant in our study is associated with Attention-Deficit/Hyperactivity Disorder (ADHD), our work not only delivers a highly novel contribution to the fuller understanding of the retinal phenotype of a specific DAT variant, but also provides an excellent foundation upon which future work may be built, establishing for the first time protocols for the effective use of non-invasive, in vivo evaluation of retinal responses for segregation of neurobehavioral disorders based on the DAT-dependent control of synaptic DA availability.

In addition, we showed that developmental photoperiod imprints retinal function. Short, winter-like light cycles during retinal development and maturation have enduring detrimental effects on photopic retinal light responses and visual contrast sensitivity in mice, which is likely through developmental programming of retinal DA. The levels of DA and the molecular machinery known to be active in its production are both negatively impacted by perinatal exposure to short light cycles. This study shed light on mechanisms underlying seasonal human birth cohorts having increased risks of Seasonal Affective Disorder (SAD).

Lastly, we uncovered differential effects mediated by D1 and D4 receptors on a specific functional type of retinal ganglion cells, ON-center sustained ganglion cells. The absence of D4 receptors led to an increase in dark-adapted, spontaneous activity and the size of the receptive field center. Under light

conditions, the surround of ON-S cells shrunk and had elevated contrast gain in D4RKO mice. D1 receptors appeared to be only involved in regulating the size of the receptive field in the dark-adapted condition. However, the results here are preliminary and need further assessment. These results have therefore provided a mechanistic framework for DA's role in modulating the multiple dimensions of light-adapted vision.

5.2 Developing electrophysiological, diagnostic tools for human health

Retinal DA exerts extensive influence on every major retinal cell type and multiple retinal synapses [44, 70]. Thus, understanding the effects of DA at the level of retinal circuits and physiology is fundamental to understanding normal retinal and visual function, in addition to its involvement in retinal health and eye development [216-218]. Our previous results surprisingly found that retinal DA transmission manifests in retinal physiology and visual function of intact animals, in addition to specific neurons and circuits. In humans, deficits in visual function caused by DA have been implicated in Parkinson's disease [219, 220] and diabetic retinopathy[221, 222]. The electrophysiological analysis is especially useful in characterizing changes in human patients, because of its non-invasive nature and mature usage in clinical settings.

Our work in ADHD-associated DAT is of high interest to a broad readership as it presents new findings addressing that noninvasive tests of DA action that could be employed in ADHD subjects demonstrating ADE and thus may allow for improved ADHD diagnosis and/or treatment. ADHD is one of the most prevailing neuropsychiatric disorders affecting 4-12% of school-age children and 4-5% of adults. Current diagnostic methods rely solely on behavior observation and questionnaires without any reliance on biomarkers. Though our results are particularly critical to the neuropsychiatry field in general, the data and experimental strategy we present will distinguish alternative disorders or subtypes and could even assist in quantifying treatment response. Thus, a follow-up study should first be conducted in a different DAT deficient mouse model created by Dr. Aurelio Galli's lab, in which constitutive ADE conveyed by missense DAT mutations is more prominent [223], to examine whether the DAT-dependent ADE phenotype is consistently presented by signature electroretinogram (ERG) responses. We would also be interested in establishing a collaboration with ophthalmologists in the clinic to initiate the measurements in patient and non-patient groups to further validate this methodology. A challenge is that patients carry DAT variants that are both heterozygous and homozygous [224], whereas we only observed changes in DAT homogenous mutant mice, thus it is possible that we could only identify the most severe manifestation of the disorder. We expect to see photopic ERG response amplitudes that are higher in the patients with ADHD than the non-patient groups. With the treatment of prescriptions containing

amphetamine, we expect to see a trend of decreasing ERG responses, as a result of the normal DA recycling/release system restoring to normal conditions.

5.3 Linking dopamine and melanopsin in the retinal development during short daily light cycles

In our study of the impact of circadian perinatal photoperiod on retinal function, we found that the retinal DA system is altered significantly due to insufficient perinatal light exposure during retinal development and maturation. Given that melanopsin-containing intrinsically photosensitive retinal ganglion cells (ipRGCs) are the link between the circadian and dopaminergic system, it is, therefore, logical to follow up on this lead to examine the involvement of ipRGCs in shaping DA signaling during development. In mice with the gene encoding melanopsin knocked out ($Opn4^{-/-}$), photopic ERG amplitudes are significantly lower than the wild-type controls when measured at midday [225]. Similarly, we observed this phenotype in mice experiencing a short photoperiod. In the future, we will focus on ON-sustained DA cells, characterizing any changes in their response profile by loose patch extracellular recording. We expect that ON-sustained DA cells might show changed firing patterns or reduced firing rate in short-photoperiod animals, whereas the ON-transient cells should be affected to a lesser extent. Another direction of this project will include an investigation of the critical period that once applied, will rescue the deficits we observed in short-photoperiod animals. In our present study, we did not reverse the photoperiod in which the animals were reared until P40, however, melanopsin expression in the fetus is detected at embryonic 15 (E15) [226] and functionally mediates the light-response pathway at E16, responsible for regulating the number of retinal neurons and the pattern of ocular blood vessels. Although cone photoreceptors develop (become post-mitotic) early, commencing at embryonic day E10 [227, 228], cone opsin protein expression cannot be detected until postnatal day 0 (P 0, S-cone opsin) [229]. Rod photoreceptor birthing happens even later, with a peak of histogenesis in the early postnatal period (P1) [228, 230]. Therefore, prolonged light treatment should occur within a time frame in which only melanopsin is functional to test if melanopsin is sufficient to rescue the deficits we saw in short-photoperiod mice. An initial study could start with the light cycle reversal at E16. We expect short-photoperiod animals with an early reversal of light cycles during embryonic development would exhibit increased light-adapted ERG responses, elevated DA contents, and contrast sensitivity to the level of those of long photoperiod animals. This study has clinical implications, as it provides a potential treatment for women whose early stage of pregnancy spans mostly during late autumn and winter time when the duration of light is short. Blue light treatment usually provided to SAD patients could be used for these pregnant population to avoid any possible adverse consequences of short perinatal light cycles on babies.

5.4 Cell-specific roles of upstream circuit elements and actions of DA on ganglion cells

Our preliminary results suggest that global knockout of D1 or D4 receptors change the response profile of ON-center-sustained ganglion cells, leading us toward identifying dopaminergic mechanisms and circuit elements influenced by D1 and D4 receptors. Due to the widespread expression of D1 and D4 receptors in the retina, it poses a problem for understanding the role of any one cell type or synapse in retinal processing read-out at the ganglion cell or behavioral levels. For example, blocking D1 receptors in the retina blocks DA effects on the electrical coupling of horizontal cells, but also prevents the known D1 receptor effects on bipolar cells, AII cells, and ganglion cells. Therefore, follow-up studies would attempt to dissect out each key site where DA acts to fundamentally alter retinal circuit action. By taking advantage of the versatile 'knockout-first allele', we plan to create two mouse models that carry cell-specific conditional depletion of D1 and/or D4 receptors: (1) HCD1RKO- horizontal cell-specific knockout of D1 receptor by crossing the post-flip conditional allele with the cx57-iCre (obtained from Dr. Nich Brecha); (2) MCD4RKO-cone cell-specific knockout of D4 receptor in M-cones using RGP-cre mice (will be obtained from Dr. Anand Swaroop).

D1 receptor modulation of horizontal cell coupling and responses has been long hypothesized to play a key role in the reorganizing of ganglion cell receptive fields in light and dark adaptation [73, 74], which is in line with our findings that the global knock-out of D1 receptors increases the dark-adapted receptive field. However, increasing evidence shows that ganglion cell receptive fields are modulated by other inner retinal mechanisms [75, 76, 231-233]. Our study will facilitate the understanding of whether horizontal cells contribute at all to ganglion cell receptive fields. Our initial results showed that deletion of D1 receptors specifically in horizontal cells resulted in striking changes in the receptive field of ON-center-sustained ganglion cells. In particular, it prevented shrinkage of receptive field in response to light adaptation, and in fact, increased and broadened the center response relative to the surround in light adaptation, which could be attributed to the loss of dopaminergic modulation of horizontal cell electrical coupling. To test this, we will inject horizontal cells *in situ* and measure dye coupling and quantify horizontal cell receptive fields by the length constant of horizontal cell light responses. We expect that HCD1RKO retinas will not exhibit decreased dye coupling nor length constant as in the WT retina when introducing DA or a D1 agonist. In addition, light-evoked spike rates are reduced in both dark and light-adapted states in HCD1RKO retinas compared to wild-type.

Hence, we will extend experiments to follow this lead to test ON channel function in HCD1RKO to the bipolar cell level using the ERG and the role of horizontal cells in visual function beyond the ganglion cell level using optokinetic tracking (OKT). We expect that HCD1RKO will not show time-dependent increases in b-wave adaptation and lower spatial frequency thresholds.

D4 receptors are highly expressed in cones, where they mediate the rod-cone coupling and also cAMP metabolism which influence light adaptation. Through D4 receptors, DA uncouples rod-cone gap junctions and increased latency and duration of horizontal cell light responses. It is compelling to define the roles of D4 receptors specifically in cones in dopaminergic modulation of ganglion cell function and vision. We will test for changes in rod-cone and cone-cone coupling in MCD4KO using cut loading of neurobiotin and test functionally using ganglion cell MEA recording and OKT. We expect that cut loading will indicate increased rod-cone and cone-cone coupling in light-adapted MCD4KO retinas, increased spontaneous activity and decreased contrast sensitivity, possibly accounted by abnormal rod input to cones in the absence of D4 receptor signaling in cones.

5.5 Conclusions

Overall our study supports the indispensable role of DA in high-resolution, light-adapted vision. We have elucidated key underlying cellular and network mechanisms by which DA signals shape retinal function and vision. Dynamic DA signaling is regulated by neurotransmitter reuptake, synthesis shaped by developmental light cycles, and segregated actions of receptors on the output of the retina. These pathways might not be isolated but have potential interactions between two or all of them, although we did not investigate them in depth in our study. A comprehensive understanding of the retinal dopaminergic system has important human health relevance, providing preventive and diagnostic tools for certain neuropsychiatry disorder conditions.

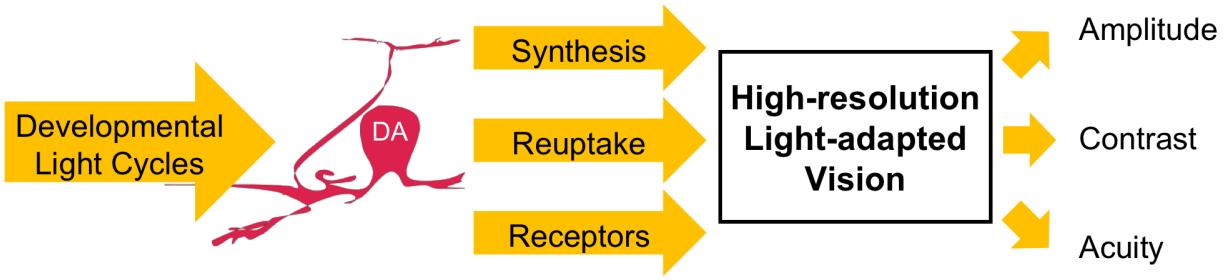

Fig. 5 Proposed model of how dopamine supports light-adapted high spatiotemporal resolution vision.

In our study, we have intensively studied three DA signaling pathways covering DA reuptake, synthesis, and receptor signaling. These modulations of retinal dopaminergic system control different aspects of the light-adapted vision, contributing to the amplitude of the light responses and the capability to resolve complex contrast and spatial frequency information.

REFERENCES

1. McMahon DG, Zhang D: *Retina: Morphology of interneurons: Interpexiform cells*. Elsevier; 2010.
2. Jackson CR, Ruan G-X, Aseem F, Abey J, Gamble K, Stanwood G, Palmiter RD, Iuvone PM, McMahon DG: **Retinal Dopamine Mediates Multiple Dimensions of Light-Adapted Vision.** *J Neurosci* 2012, **32:**9359-9368.
3. Purves D, Augustine GJ, Fitzpatrick D, Hall WC, Lamantia A-S, McNamara JO, Williams SM: **NEUROSCIENCE.** 2004.
4. Kolb H: **Gross Anatomy of the Eye** *Webvision: The Organization of the Retina and Visual System*.
5. Morgan J, Wong R: **Development of Cell Types and Synaptic Connections in the Retina.** In *Webvision: The Organization of the Retina and Visual System*. Edited by Kolb H, Fernandez E, Nelson R. Salt Lake City (UT); 2007
6. Ebrey T, Koutalos Y: **Vertebrate photoreceptors.** *Prog Retin Eye Res* 2001, **20:**49-94.
7. Jeon CJ, Strettoi E, Masland RH: **The major cell populations of the mouse retina.** *J Neurosci* 1998, **18:**8936-8946.
8. Eric R. Kandel JHS, Jessell TM: **Principles of Neural Science. Chapter 26:**507-522.
9. Kalloniatis M, Luu C: **Psychophysics of Vision.** *Webvision: The Organization of the Retina and Visual System*.
10. Umino Y, Solessio E, Barlow RB: **Speed, spatial, and temporal tuning of rod and cone vision in mouse.** *J Neurosci* 2008, **28:**189-198.
11. Tsukamoto Y, Morigiwa K, Ueda M, Sterling P: **Microcircuits for night vision in mouse retina.** *J Neurosci* 2001, **21:**8616-8623.
12. Tsukamoto Y, Omi N: **Some OFF bipolar cell types make contact with both rods and cones in macaque and mouse retinas.** *Front Neuroanat* 2014, **8:**105.
13. Masland RH: **The fundamental plan of the retina.** *Nat Neurosci* 2001, **4:**877-886.
14. Tsukamoto Y, Omi N: **Classification of Mouse Retinal Bipolar Cells: Type-Specific Connectivity with Special Reference to Rod-Driven AII Amacrine Pathways.** *Front Neuroanat* 2017, **11:**92.
15. Dowling JE: **Retina.** *Encyclopedia of the Human Brain* 2002, **4**.
16. Baden T, Berens P, Franke K, Roman Roson M, Bethge M, Euler T: **The functional diversity of retinal ganglion cells in the mouse.** *Nature* 2016, **529:**345-350.
17. Dunn FA, Wong RO: **Wiring patterns in the mouse retina: collecting evidence across the connectome, physiology and light microscopy.** *J Physiol* 2014, **592:**4809-4823.
18. Kolb H: **Morphology and Circuitry of Ganglion Cells.** *Webvision: The Organization of the Retina and Visual System*.
19. Sanes JR, Masland RH: **The types of retinal ganglion cells: current status and implications for neuronal classification.** *Annu Rev Neurosci* 2015, **38:**221-246.

20. Lazzerini Ospri L, Prusky G, Hattar S: **Mood, the Circadian System, and Melanopsin Retinal Ganglion Cells.** *Annu Rev Neurosci* 2017, **40:**539-556.

21. Dustin M. Graham KYW: **Melanopsin-expressing, Intrinsically Photosensitive Retinal Ganglion Cells (ipRGCs)** *Webvision: The Organization of the Retina and Visual System*.

22. Schmidt TM, Do MT, Dacey D, Lucas R, Hattar S, Matynia A: **Melanopsin-positive intrinsically photosensitive retinal ganglion cells: from form to function.** *J Neurosci* 2011, **31:**16094-16101.

23. Perlman I, Weiner E, Kolb H: **Retinal Horizontal Cells.** *Encyclopedia of Neuroscience* 2009.

24. Raven MA, Oh EC, Swaroop A, Reese BE: **Afferent control of horizontal cell morphology revealed by genetic respecification of rods and cones.** *J Neurosci* 2007, **27:**3540-3547.

25. Samuel MA, Voinescu PE, Lilley BN, de Cabo R, Foretz M, Viollet B, Pawlyk B, Sandberg MA, Vavvas DG, Sanes JR: **LKB1 and AMPK regulate synaptic remodeling in old age.** *Nat Neurosci* 2014, **17:**1190-1197.

26. Park SJ, Kim IB, Choi KR, Moon JI, Oh SJ, Chung JW, Chun MH: **Reorganization of horizontal cell processes in the developing FVB/N mouse retina.** *Cell Tissue Res* 2001, **306:**341-346.

27. Trumpler J, Dedek K, Schubert T, de Sevilla Muller LP, Seeliger M, Humphries P, Biel M, Weiler R: **Rod and cone contributions to horizontal cell light responses in the mouse retina.** *J Neurosci* 2008, **28:**6818-6825.

28. Kamermans M, Fahrenfort I: **Ephaptic interactions within a chemical synapse: hemichannel-mediated ephaptic inhibition in the retina.** *Curr Opin Neurobiol* 2004, **14:**531-541.

29. Kamermans M, Kraaij D, Spekreijse H: **The dynamic characteristics of the feedback signal from horizontal cells to cones in the goldfish retina.** *J Physiol* 2001, **534:**489-500.

30. Thoreson WB, Mangel SC: **Lateral interactions in the outer retina.** *Prog Retin Eye Res* 2012, **31:**407-441.

31. Hombach S, Janssen-Bienhold U, Sohl G, Schubert T, Bussow H, Ott T, Weiler R, Willecke K: **Functional expression of connexin57 in horizontal cells of the mouse retina.** *Eur J Neurosci* 2004, **19:**2633-2640.

32. Dorgau B, Herrling R, Schultz K, Greb H, Segelken J, Stroh S, Bolte P, Weiler R, Dedek K, Janssen-Bienhold U: **Connexin50 couples axon terminals of mouse horizontal cells by homotypic gap junctions.** *J Comp Neurol* 2015, **523:**2062-2081.

33. Kolb H: **Roles of Amacrine Cells.** *Webvision: The Organization of the Retina and Visual System*.

34. Perez de Sevilla Muller L, Azar SS, de Los Santos J, Brecha NC: **Prox1 Is a Marker for AII Amacrine Cells in the Mouse Retina.** *Front Neuroanat* 2017, **11:**39.

35. Masland RH: **The neuronal organization of the retina.** *Neuron* 2012, **76:**266-280.

36. Demb JB, Singer JH: **Intrinsic properties and functional circuitry of the AII amacrine cell.** *Vis Neurosci* 2012, **29:**51-60.

37. Majumdar S, Weiss J, Wassle H: **Glycinergic input of widefield, displaced amacrine cells of the mouse retina.** *J Physiol* 2009, **587:**3831-3849.

38. van Wyk M, Wassle H, Taylor WR: **Receptive field properties of ON- and OFF-ganglion cells in the mouse retina.** *Vis Neurosci* 2009, **26:**297-308.

39. Mills SL, O'Brien JJ, Li W, O'Brien J, Massey SC: **Rod pathways in the mammalian retina use connexin 36.** *J Comp Neurol* 2001, **436:**336-350.

40. Zhang DQ, Zhou TR, McMahon DG: **Functional heterogeneity of retinal dopaminergic neurons underlying their multiple roles in vision.** *J Neurosci* 2007, **27:**692-699.

41. Contini M, Lin B, Kobayashi K, Okano H, Masland RH, Raviola E: **Synaptic input of ON-bipolar cells onto the dopaminergic neurons of the mouse retina.** *J Comp Neurol* 2010, **518:**2035-2050.

42. Contini M, Raviola E: **GABAergic synapses made by a retinal dopaminergic neuron.** *Proc Natl Acad Sci U S A* 2003, **100:**1358-1363.

43. Zhang D-Q, Stone JF, Zhou T, Ohta H, McMahon DG: **Characterization of genetically labeled catecholamine neurons in the mouse retina.** *Neuroreport* 2004, **15:**1761-1765.

44. Witkovsky P: **Dopamine and retinal function.** *Doc Ophthalmol* 2004, **108:**17-40.

45. Puopolo M, Hochstetler SE, Gustincich S, Wightman RM, Raviola E: **Extrasynaptic release of dopamine in a retinal neuron: activity dependence and transmitter modulation.** *Neuron* 2001, **30:**211-225.

46. Iuvone PM, Galli CL, Neff NH: **Retinal tyrosine hydroxylase: comparison of short-term and long-term stimulation by light.** *Mol Pharmacol* 1978, **14:**1212-1219.

47. Mills SL, Xia XB, Hoshi H, Firth SI, Rice ME, Frishman LJ, Marshak DW: **Dopaminergic modulation of tracer coupling in a ganglion-amacrine cell network.** *Vis Neurosci* 2007, **24:**593-608.

48. Nir I, Haque R, Iuvone PM: **Diurnal metabolism of dopamine in dystrophic retinas of homozygous and heterozygous retinal degeneration slow (rds) mice.** *Brain Res* 2000, **884:**13-22.

49. Doyle SE, Grace MS, McIvor W, Menaker M: **Circadian rhythms of dopamine in mouse retina: the role of melatonin.** *Vis Neurosci* 2002, **19:**593-601.

50. Meiser J, Weindl D, Hiller K: **Complexity of dopamine metabolism.** *Cell Commun Signal* 2013, **11:**34.

51. Zhang DQ, Wong KY, Sollars PJ, Berson DM, Pickard GE, McMahon DG: **Intraretinal signaling by ganglion cell photoreceptors to dopaminergic amacrine neurons.** *Proc Natl Acad Sci U S A* 2008, **105:**14181-14186.

52. Dumitrescu ON, Pucci FG, Wong KY, Berson DM: **Ectopic retinal ON bipolar cell synapses in the OFF inner plexiform layer: contacts with dopaminergic amacrine cells and melanopsin ganglion cells.** *J Comp Neurol* 2009, **517:**226-244.

53. Hoshi H, Liu W-L, Massey SC, Mills SL: **ON inputs to the OFF layer: bipolar cells that break the stratification rules of the retina.** *J Neurosci* 2009, **29:**8875-8883.

54. Schmidt TM, Chen S-K, Hattar S: **Intrinsically photosensitive retinal ganglion cells: many subtypes, diverse functions.** *Trends in Neurosciences* 2011, **34:**572-580.

55. Zhang D-Q, Belenky MA, Sollars PJ, Pickard GE, McMahon DG: **Melanopsin mediates retrograde visual signaling in the retina.** *PLoS ONE* 2012, **7:**e42647.

56. Viney TJ, Balint K, Hillier D, Siegert S, Boldogkoi Z, Enquist LW, Meister M, Cepko CL, Roska B: **Local retinal circuits of melanopsin-containing ganglion cells identified by transsynaptic viral tracing.** *Curr Biol* 2007, **17:**981-988.

57. Vugler AA, Redgrave P, Semo M, Lawrence J, Greenwood J, Coffey PJ: **Dopamine neurones form a discrete plexus with melanopsin cells in normal and degenerating retina.** *Exp Neurol* 2007, **205:**26-35.

58. Zhang D-Q, Wong KY, Sollars PJ, Berson DM, Pickard GE, McMahon DG: **Intraretinal signaling by ganglion cell photoreceptors to dopaminergic amacrine neurons.** *Proc Natl Acad Sci USA* 2008, **105:**14181-14186.

59. Bjelke B, Goldstein M, Tinner B, Andersson C, Sesack SR, Steinbusch HW, Lew JY, He X, Watson S, Tengroth B, Fuxe K: **Dopaminergic transmission in the rat retina: evidence for volume transmission.** *J Chem Neuroanat* 1996, **12:**37-50.

60. Witkovsky P, Nicholson C, Rice ME, Bohmaker K, Meller E: **Extracellular dopamine concentration in the retina of the clawed frog, Xenopus laevis.** *Proc Natl Acad Sci U S A* 1993, **90:**5667-5671.

61. Hirasawa H, Contini M, Raviola E: **Extrasynaptic release of GABA and dopamine by retinal dopaminergic neurons.** *Philos Trans R Soc Lond B Biol Sci* 2015, **370**.

62. Versaux-Botteri C, Gibert JM, Nguyen-Legros J, Vernier P: **Molecular identification of a dopamine D1b receptor in bovine retinal pigment epithelium.** *Neurosci Lett* 1997, **237:**9-12.

63. Ogata G, Stradleigh TW, Partida GJ, Ishida AT: **Dopamine and full-field illumination activate D1 and D2-D5-type receptors in adult rat retinal ganglion cells.** *J Comp Neurol* 2012, **520:**4032-4049.

64. Cohen AI, Todd RD, Harmon S, O'Malley KL: **Photoreceptors of mouse retinas possess D4 receptors coupled to adenylate cyclase.** *Proc Natl Acad Sci U S A* 1992, **89:**12093-12097.

65. Veruki ML, Wässle H: **Immunohistochemical localization of dopamine D1 receptors in rat retina.** *Eur J Neurosci* 1996, **8:**2286-2297.

66. Nguyen-Legros J, Simon A, Caille I, Bloch B: **Immunocytochemical localization of dopamine D1 receptors in the retina of mammals.** *Vis Neurosci* 1997, **14:**545-551.

67. Veruki ML: **Dopaminergic neurons in the rat retina express dopamine D2/3 receptors.** *Eur J Neurosci* 1997, **9:**1096-1100.

68. Ribelayga C, Mangel SC: **Absence of circadian clock regulation of horizontal cell gap junctional coupling reveals two dopamine systems in the goldfish retina.** *J Comp Neurol* 2003, **467:**243-253.

69. He S, Weiler R, Vaney DI: **Endogenous dopaminergic regulation of horizontal cell coupling in the mammalian retina.** *J Comp Neurol* 2000, **418:**33-40.

70. Mills SL, Massey SC: **Differential properties of two gap junctional pathways made by AII amacrine cells.** *Nature* 1995, **377:**734-737.

71. Hampson EC, Vaney DI, Weiler R: **Dopaminergic modulation of gap junction permeability between amacrine cells in mammalian retina.** *J Neurosci* 1992, **12:**4911-4922.

72. Hu EH, Pan F, Völgyi B, Bloomfield SA: **Light increases the gap junctional coupling of retinal ganglion cells.** *The Journal of Physiology* 2010, **588:**4145-4163.

73. Mangel SC, Dowling JE: **Responsiveness and receptive field size of carp horizontal cells are reduced by prolonged darkness and dopamine.** *Science* 1985, **229:**1107-1109.

74. Zhang A-J, Jacoby R, Wu SM: **Light- and dopamine-regulated receptive field plasticity in primate horizontal cells.** In *J Comp Neurol*, vol. 519. pp. 2125-2134; 2011:2125-2134.

75. Sinclair JR, Jacobs AL, Nirenberg S: **Selective ablation of a class of amacrine cells alters spatial processing in the retina.** *J Neurosci* 2004, **24:**1459-1467.

76. Flores-Herr N, Protti DA, Wassle H: **Synaptic currents generating the inhibitory surround of ganglion cells in the mammalian retina.** *J Neurosci* 2001, **21:**4852-4863.

77. Roska B, Nemeth E, Orzo L, Werblin FS: **Three levels of lateral inhibition: A space-time study of the retina of the tiger salamander.** *J Neurosci* 2000, **20:**1941-1951.

78. Liu X, Grove JC, Hirano AA, Brecha NC, Barnes S: **Dopamine D1 receptor modulation of calcium channel currents in horizontal cells of mouse retina.** *J Neurophysiol* 2016**;**jn.00990.02015.

79. Ichinose T, Lukasiewicz PD: **Ambient light regulates sodium channel activity to dynamically control retinal signaling.** *J Neurosci* 2007, **27:**4756-4764.

80. Hayashida Y, Ishida AT: **Dopamine receptor activation can reduce voltage-gated Na+ current by modulating both entry into and recovery from inactivation.** *J Neurophysiol* 2004, **92:**3134-3141.

81. Hayashida Y, Rodríguez CV, Ogata G, Partida GJ, Oi H, Stradleigh TW, Lee SC, Colado AF, Ishida AT: **Inhibition of adult rat retinal ganglion cells by D1-type dopamine receptor activation.** *The Journal of neuroscience : the official journal of the Society for Neuroscience* 2009, **29:**15001-15016.

82. Chen L, Yang XL: **Hyperpolarization-activated cation current is involved in modulation of the excitability of rat retinal ganglion cells by dopamine.** *Neuroscience* 2007, **150:**299-308.

83. Vaquero CF, Pignatelli A, Partida GJ, Ishida AT: **A dopamine- and protein kinase A-dependent mechanism for network adaptation in retinal ganglion cells.** *J Neurosci* 2001, **21:**8624-8635.

84. Van Hook MJ, Wong KY, Berson DM: **Dopaminergic modulation of ganglion-cell photoreceptors in rat.** *Eur J Neurosci* 2012, **35:**507-518.

85. Ribelayga C, Cao Y, Mangel SC: **The circadian clock in the retina controls rod-cone coupling.** *Neuron* 2008, **59:**790-801.

86. Nir I, Harrison JM, Haque R, Low MJ, Grandy DK, Rubinstein M, Iuvone PM: **Dysfunctional light-evoked regulation of cAMP in photoreceptors and abnormal retinal adaptation in mice lacking dopamine D4 receptors.** *J Neurosci* 2002, **22:**2063-2073.

87. Mills SL, Xia X-B, Hoshi H, Firth SI, Rice ME, Frishman LJ, Marshak DW: **Dopaminergic modulation of tracer coupling in a ganglion-amacrine cell network.** *Vis Neurosci* 2007, **24:**593-608.

88. Perlman I: **The Electroretinogram.** *Webvision: The Organization of the Retina and Visual System*.

89. Clark ME, Kraft TW: **Measuring rodent electroretinograms to assess retinal function.** *Methods Mol Biol* 2012, **884:**265-276.

90. Cameron MA, Barnard AR, Lucas RJ: **The electroretinogram as a method for studying circadian rhythms in the mammalian retina.** *J Genet* 2008, **87:**459-466.

91. McCulloch DL, Marmor MF, Brigell MG, Hamilton R, Holder GE, Tzekov R, Bach M: **ISCEV Standard for full-field clinical electroretinography (2015 update).** *Doc Ophthalmol* 2015, **130:**1-12.

92. Bach M, Brigell MG, Hawlina M, Holder GE, Johnson MA, McCulloch DL, Meigen T, Viswanathan S: **ISCEV standard for clinical pattern electroretinography (PERG): 2012 update.** *Doc Ophthalmol* 2013, **126:**1-7.

93. Hood DC, Bach M, Brigell M, Keating D, Kondo M, Lyons JS, Marmor MF, McCulloch DL, Palmowski-Wolfe AM, International Society For Clinical Electrophysiology of V: **ISCEV standard for clinical multifocal electroretinography (mfERG) (2011 edition).** *Doc Ophthalmol* 2012, **124:**1-13.

94. Creel DJ: **The Electroretinogram and Electro-oculogram: Clinical Applications by** *Webvision: The Organization of the Retina and Visual System*.

95. Wood C, Williams C, Waldron GJ: **Patch clamping by numbers.** *Drug Discov Today* 2004, **9:**434-441.

96. Obien ME, Deligkaris K, Bullmann T, Bakkum DJ, Frey U: **Revealing neuronal function through microelectrode array recordings.** *Front Neurosci* 2014, **8:**423.

97. Reinhard K, Tikidji-Hamburyan A, Seitter H, Idrees S, Mutter M, Benkner B, Munch TA: **Step-by-step instructions for retina recordings with perforated multi electrode arrays.** *PLoS One* 2014, **9:**e106148.

98. Prusky GT, Alam NM, Beekman S, Douglas RM: **Rapid quantification of adult and developing mouse spatial vision using a virtual optomotor system.** *Invest Ophthalmol Vis Sci* 2004, **45:**4611-4616.

99. Kretschmer F, Sajgo S, Kretschmer V, Badea TC: **A system to measure the Optokinetic and Optomotor response in mice.** *J Neurosci Methods* 2015, **256:**91-105.

100. Dai H, Jackson CR, Davis GL, Blakely RD, McMahon DG: **Is dopamine transporter-mediated dopaminergic signaling in the retina a noninvasive biomarker for attention-deficit/ hyperactivity disorder? A study in a novel dopamine transporter variant Val559 transgenic mouse model.** *J Neurodev Disord* 2017, **9:**38.

101. Bannon MJ: **The dopamine transporter: role in neurotoxicity and human disease.** *Toxicol Appl Pharmacol* 2005, **204:**355-360.

102. Giros B, Caron MG: **Molecular characterization of the dopamine transporter.** *Trends Pharmacol Sci* 1993, **14:**43-49.

103. Palmiter RD: **Dopamine signaling in the dorsal striatum is essential for motivated behaviors: lessons from dopamine-deficient mice.** *Ann N Y Acad Sci* 2008, **1129:**35-46.

104. Faraone SV, Biederman J: **Neurobiology of attention-deficit hyperactivity disorder.** *Biol Psychiatry* 1998, **44:**951-958.

105. Mazei-Robison MS, Couch RS, Shelton RC, Stein MA, Blakely RD: **Sequence variation in the human dopamine transporter gene in children with attention deficit hyperactivity disorder.** *Neuropharmacology* 2005, **49:**724-736.

106. Hayden EP, Nurnberger JI, Jr.: **Molecular genetics of bipolar disorder.** *Genes Brain Behav* 2006, **5:**85-95.

107. Snyder SH: **The dopamine hypothesis of schizophrenia: focus on the dopamine receptor.** *The American Journal of Psychiatry* 1976, **133:**197-202.

108. Horga G, Cassidy CM, Xu X, Moore H, Slifstein M, Van Snellenberg JX, Abi-Dargham A: **Dopamine-Related Disruption of Functional Topography of Striatal Connections in Unmedicated Patients With Schizophrenia.** *JAMA Psychiatry* 2016, **73:**862-870.

109. Temlett JA: **Parkinson's disease: biology and aetiology.** *Curr Opin Neurol* 1996, **9:**303-307.

110. Kulisevsky J: **Role of dopamine in learning and memory: implications for the treatment of cognitive dysfunction in patients with Parkinson's disease.** *Drugs Aging* 2000, **16:**365-379.

111. Li Y: **To understand the brain - the 2016 annual meeting of society for neurosciences: a conference report.** *Neural Regen Res* 2016, **11:**1912-1913.

112. Iuvone PM, Morasco J, Delanoy RL, Dunn AJ: **Peptides and the conversion of [3H]tyrosine to catecholamines: effects of ACTH-analogs, melanocyte-stimulating hormones and lysine-vasopressin.** *Brain Res* 1978, **139:**131-139.

113. Kothmann WW, Massey SC, O'Brien J: **Dopamine-stimulated dephosphorylation of connexin 36 mediates AII amacrine cell uncoupling.** *J Neurosci* 2009, **29:**14903-14911.

114. Giros B, Jaber M, Jones SR, Wightman RM, Caron MG: **Hyperlocomotion and indifference to cocaine and amphetamine in mice lacking the dopamine transporter.** *Nature* 1996, **379:**606-612.

115. Gainetdinov RR, Jones SR, Caron MG: **Functional hyperdopaminergia in dopamine transporter knock-out mice.** *Biol Psychiatry* 1999, **46:**303-311.

116. Jones SR, Gainetdinov RR, Jaber M, Giros B, Wightman RM, Caron MG: **Profound neuronal plasticity in response to inactivation of the dopamine transporter.** *Proc Natl Acad Sci U S A* 1998, **95:**4029-4034.

117. Biederman J, Faraone SV: **Attention-deficit hyperactivity disorder.** *The Lancet* 2005, **366:**237-248.

118. Biederman J, Lopez FA, Boellner SW, Chandler MC: **A randomized, double-blind, placebo-controlled, parallel-group study of SLI381 (Adderall XR) in children with attention-deficit/hyperactivity disorder.** *Pediatrics* 2002, **110:**258-266.

119. Chen NH, Reith ME, Quick MW: **Synaptic uptake and beyond: the sodium- and chloride-dependent neurotransmitter transporter family SLC6.** *Pflugers Arch* 2004, **447:**519-531.

120. Cheng Z, Zhong YM, Yang XL: **Expression of the dopamine transporter in rat and bullfrog retinas.** *Neuroreport* 2006, **17:**773-777.

121. Witkovsky P, Gabriel R, Krizaj D: **Anatomical and neurochemical characterization of dopaminergic interplexiform processes in mouse and rat retinas.** *J Comp Neurol* 2008, **510:**158-174.

122. Lavoie J, Illiano P, Sotnikova TD, Gainetdinov RR, Beaulieu JM, Hebert M: **The electroretinogram as a biomarker of central dopamine and serotonin: potential relevance to psychiatric disorders.** *Biol Psychiatry* 2014, **75:**479-486.

123. Zhao J, Qu X, Qi Y, Zhou W, Liu X: **Study on retinal dopamine transporter in form deprivation myopia using the radiopharmaceutical tracer 99mTc-TRODAT-1.** *Nucl Med Commun* 2010, **31:**910-915.

124. Grunhage F, Schulze TG, Muller DJ, Lanczik M, Franzek E, Albus M, Borrmann-Hassenbach M, Knapp M, Cichon S, Maier W, et al: **Systematic screening for DNA sequence variation in the coding region of the human dopamine transporter gene (DAT1).** *Mol Psychiatry* 2000, **5:**275-282.

125. Bowton E, Saunders C, Reddy IA, Campbell NG, Hamilton PJ, Henry LK, Coon H, Sakrikar D, Veenstra-VanderWeele JM, Blakely RD, et al: **SLC6A3 coding variant Ala559Val found in two autism probands alters dopamine transporter function and trafficking.** *Translational Psychiatry* 2014, **4**.

126. Mazei-Robison MS, Bowton E, Holy M, Schmudermaier M, Freissmuth M, Sitte HH, Galli A, Blakely RD: **Anomalous dopamine release associated with a human dopamine transporter coding variant.** *J Neurosci* 2008, **28:**7040-7046.

127. Mergy MA, Gowrishankar R, Gresch PJ, Gantz SC, Williams J, Davis GL, Wheeler CA, Stanwood GD, Hahn MK, Blakely RD: **The rare DAT coding variant Val559 perturbs DA neuron function, changes behavior, and alters in vivo responses to psychostimulants.** *Proc Natl Acad Sci U S A* 2014, **111:**E4779-4788.

128. Williamson D, Johnston C: **Gender differences in adults with attention-deficit/hyperactivity disorder: A narrative review.** *Clin Psychol Rev* 2015, **40:**15-27.

129. Jackson CR, Capozzi M, Dai H, McMahon DG: **Circadian perinatal photoperiod has enduring effects on retinal dopamine and visual function.** *The Journal of neuroscience : the official journal of the Society for Neuroscience* 2014, **34:**4627-4633.

130. Cransac H, Cottet-Emard JM, Pequignot JM, Peyrin L: **Monoamines (norepinephrine, dopamine, serotonin) in the rat medial vestibular nucleus: endogenous levels and turnover.** *J Neural Transm (Vienna)* 1996, **103:**391-401.

131. Lindsey JW, Jung AE, Narayanan TK, Ritchie GD: **Acute effects of a bicyclophosphate neuroconvulsant on monoamine neurotransmitter and metabolite levels in the rat brain.** *J Toxicol Environ Health A* 1998, **54:**421-429.

132. Ruan GX, Allen GC, Yamazaki S, McMahon DG: **An autonomous circadian clock in the inner mouse retina regulated by dopamine and GABA.** *PLoS Biol* 2008, **6:**2248-2265.

133. Cameron MA, Barnard AR, Hut RA, Bonnefont X, van der Horst GT, Hankins MW, Lucas RJ: **Electroretinography of wild-type and Cry mutant mice reveals circadian tuning of photopic and mesopic retinal responses.** *J Biol Rhythms* 2008, **23:**489-501.

134. Zeidler I: **The clinical electroretinogram. IX. The normal electroretinogram. Value of the b-potential in different age groups and its differenes in men and women.** *Acta Ophthalmol (Copenh)* 1959, **37:**294-301.

135. Brule J, Lavoie MP, Casanova C, Lachapelle P, Hebert M: **Evidence of a possible impact of the menstrual cycle on the reproducibility of scotopic ERGs in women.** *Doc Ophthalmol* 2007, **114:**125-134.

136. Ozawa GY, Bearse MA, Jr., Harrison WW, Bronson-Castain KW, Schneck ME, Barez S, Adams AJ: **Differences in neuroretinal function between adult males and females.** *Optom Vis Sci* 2014, **91:**602-607.

137. Nightingale S, Mitchell KW, Howe JW: **Visual evoked cortical potentials and pattern electroretinograms in Parkinson's disease and control subjects.** *J Neurol Neurosurg Psychiatry* 1986, **49:**1280-1287.

138. Di Paolo T, Rouillard C, Bedard P: **17 beta-Estradiol at a physiological dose acutely increases dopamine turnover in rat brain.** *Eur J Pharmacol* 1985, **117:**197-203.

139. Xie T, Ho S-L, Ramsden D: **Characterization and Implications of Estrogenic Down-Regulation of Human Catechol-O-Methyltransferase Gene Transcription.** *Molecular Pharmacology* 1999, **56:**31-38.

140. Hruska R, Silbergeld E: **Increased dopamine receptor sensitivity after estrogen treatment using the rat rotation model.** *Science* 1980, **208:**1466-1468.

141. Roy EJ, Buyer DR, Licari VA: **Estradiol in the striatum: Effects on behavior and dopamine receptors but no evidence for membrane steroid receptors.** *Brain Research Bulletin* 1990, **25:**221-227.

142. Smith KM, Dahodwala N: **Sex differences in Parkinson's disease and other movement disorders.** *Experimental Neurology* 2014, **259:**44-56.

143. Disshon KA, Dluzen DE: **Estrogen as a neuromodulator of MPTP-induced neurotoxicity: effects upon striatal dopamine release.** *Brain Research* 1997, **764:**9-16.

144. Bitter I, Simon V, Balint S, Meszaros A, Czobor P: **How do different diagnostic criteria, age and gender affect the prevalence of attention deficit hyperactivity disorder in adults? An epidemiological study in a Hungarian community sample.** *Eur Arch Psychiatry Clin Neurosci* 2010, **260:**287-296.

145. Kessler RC, Adler L, Barkley R, Biederman J, Conners CK, Demler O, Faraone SV, Greenhill LL, Howes MJ, Secnik K, et al: **The prevalence and correlates of adult ADHD in the United States: results from the National Comorbidity Survey Replication.** *Am J Psychiatry* 2006, **163:**716-723.

146. Polanczyk G, Silva de Lima M, Lessa Horta B, Biederman J, Augusto Rohde L: **The Worldwide Prevalence of ADHD: A Systematic Review and Metaregression Analysis.** *Am J Psychiatry* 2007, **1646**.

147. Willcutt EG: **The Prevalence of DSM-IV Attention-Deficit/Hyperactivity Disorder: A Meta-Analytic Review.** *Neurotherapeutics* 2012, **9:**490-499.

148. Fayyad J, De Graaf R, Kessler R, Alonso J, Angermeyer M, Demyttenaere K, De Girolamo G, Haro JM, Karam EG, Lara C, et al: **Cross-national prevalence and correlates of adult attention-deficit hyperactivity disorder.** *The British journal of psychiatry : the journal of mental science* 2007, **190:**402-409.

149. de Graaf R, Kessler RC, Fayyad J, ten Have M, Alonso J, Angermeyer M, Borges G, Demyttenaere K, Gasquet I, de Girolamo G, et al: **The prevalence and effects of adult attention-deficit/hyperactivity disorder (ADHD) on the performance of workers: results from the WHO World Mental Health Survey Initiative.** *Occupational and Environmental Medicine* 2008, **65:**835-842.

150. Hebert M, Beattie CW, Tam EM, Yatham LN, Lam RW: **Electroretinography in patients with winter seasonal affective disorder.** *Psychiatry Res* 2004, **127:**27-34.

151. Lavoie MP, Lam RW, Bouchard G, Sasseville A, Charron MC, Gagne AM, Tremblay P, Filteau MJ, Hebert M: **Evidence of a biological effect of light therapy on the retina of patients with seasonal affective disorder.** *Biol Psychiatry* 2009, **66:**253-258.

152. Fan XF, Miles JH, Takahashi N, Yao G: **Abnormal Transient Pupillary Light Reflex in Individuals with Autism Spectrum Disorders.** *Journal of Autism and Developmental Disorders* 2009, **39:**1499-1508.

153. Ritvo ER, Creel D, Realmuto G, Crandall AS, Freeman BJ, Bateman JB, Barr R, Pingree C, Coleman M, Purple R: **Electroretinograms in autism: a pilot study of b-wave amplitudes.** *Am J Psychiatry* 1988, **145:**229-232.

154. Constable PA, Gaigg SB, Bowler DM, Jagle H, Thompson DA: **Full-field electroretinogram in autism spectrum disorder.** *Doc Ophthalmol* 2016, **132:**83-99.

155. Hubel DH, Wiesel TN: **Receptive fields, binocular interaction and functional architecture in the cat's visual cortex.** *J Physiol* 1962, **160:**106-154.

156. Ciarleglio CM, Axley JC, Strauss BR, Gamble KL, McMahon DG: **Perinatal photoperiod imprints the circadian clock.** *Nat Neurosci* 2011, **14:**25-27.

157. Tian N, Copenhagen DR: **Visual deprivation alters development of synaptic function in inner retina after eye opening.** *Neuron* 2001, **32:**439-449.

158. Melamed E, Frucht Y, Vidauri J, Uzzan A, Rosenthal J: **Effect of postnatal light deprivation on the ontogenesis of dopamine neurons in rat retina.** *Brain Res* 1986, **391:**280-284.

159. Goldman BD: **Pattern of melatonin secretion mediates transfer of photoperiod information from mother to fetus in mammals.** *Science's STKE* 2003, **2003:**PE29.

160. Rao S, Chun C, Fan J, Kofron JM, Yang MB, Hegde RS, Ferrara N, Copenhagen DR, Lang RA: **A direct and melanopsin-dependent fetal light response regulates mouse eye development.** *Nature* 2013, **494:**243-246.

161. Jackson CR, Chaurasia SS, Hwang CK, Iuvone PM: **Dopamine D_4 receptor activation controls circadian timing of the adenylyl cyclase 1/cyclic AMP signaling system in mouse retina.** *Eur J Neurosci* 2011, **34:**57-64.

162. Prusky GT, Alam NM, Douglas RM: **Enhancement of vision by monocular deprivation in adult mice.** *J Neurosci* 2006, **26:**11554-11561.

163. Storch K-F, Paz C, Signorovitch J, Raviola E, Pawlyk B, Li T, Weitz CJ: **Intrinsic circadian clock of the mammalian retina: importance for retinal processing of visual information.** *Cell* 2007, **130:**730-741.

164. Li H, Zhang Z, Blackburn MR, Wang SW, Ribelayga CP, O'Brien J: **Adenosine and dopamine receptors coregulate photoreceptor coupling via gap junction phosphorylation in mouse retina.** *J Neurosci* 2013, **33:**3135-3150.

165. Iuvone PM, Galli CL, Garrison-Gund CK, Neff NH: **Light stimulates tyrosine hydroxylase activity and dopamine synthesis in retinal amacrine neurons.** *Science* 1978, **202:**901-902.

166. Hwang CK, Chaurasia SS, Jackson CR, Chan GC-K, Storm DR, Iuvone PM: **Circadian Rhythm of Contrast Sensitivity Is Regulated by a Dopamine-Neuronal PAS-Domain Protein 2-Adenylyl Cyclase 1 Signaling Pathway in Retinal Ganglion Cells.** *J Neurosci* 2013, **33:**14989-14997.

167. Fuchs M, Sendelbeck A, Atorf J, Kremers J, Brandstatter JH: **Strain differences in illumination-dependent structural changes at mouse photoreceptor ribbon synapses.** *J Comp Neurol* 2013, **521:**69-78.

168. Vistamehr S, Tian N: **Light deprivation suppresses the light response of inner retina in both young and adult mouse.** *Vis Neurosci* 2004, **21:**23-37.

169. Renna JM, Weng S, Berson DM: **Light acts through melanopsin to alter retinal waves and segregation of retinogeniculate afferents.** *Nat Neurosci* 2011, **14:**827-829.

170. Kirkby LA, Feller MB: **Intrinsically photosensitive ganglion cells contribute to plasticity in retinal wave circuits.** *Proceedings of the National Academy of Sciences* 2013, **110:**12090-12095.

171. Shelke RR, Lakshmana MK, Ramamohan Y, Raju TR: **Levels of dopamine and noradrenaline in the developing of retina--effect of light deprivation.** *Int J Dev Neurosci* 1997, **15:**139-143.

172. Papanikolaou NA, Sabban EL: **Ability of Egr1 to activate tyrosine hydroxylase transcription in PC12 cells. Cross-talk with AP-1 factors.** *J Biol Chem* 2000, **275:**26683-26689.

173. Gonzalez MMC, Aston-Jones G: **Light deprivation damages monoamine neurons and produces a depressive behavioral phenotype in rats.** *Proc Natl Acad Sci USA* 2008, **105:**4898-4903.

174. Dulcis D, Jamshidi P, Leutgeb S, Spitzer NC: **Neurotransmitter switching in the adult brain regulates behavior.** *Science* 2013, **340:**449-453.

175. Lam RW, Beattie CW, Buchanan A, Mador JA: **Electroretinography in seasonal affective disorder.** *Psychiatry Res* 1992, **43:**55-63.

176. Oren DA: **Retinal melatonin and dopamine in seasonal affective disorder.** *J Neural Transm Gen Sect* 1991, **83:**85-95.

177. Terman JS, Terman M: **Photopic and scotopic light detection in patients with seasonal affective disorder and control subjects.** *Biol Psychiatry* 1999, **46:**1642-1648.

178. Wesner MF, Tan J: **Contrast sensitivity in seasonal and nonseasonal depression.** *J Affect Disord* 2006, **95:**19-28.

179. Szabo Z, Antal A, Tokaji Z, Kalman J, Keri S, Benedek G, Janka Z: **Light therapy increases visual contrast sensitivity in seasonal affective disorder.** *Psychiatry Res* 2004, **126:**15-21.

180. Gagne AM, Gagne P, Hebert M: **Impact of light therapy on rod and cone functions in healthy subjects.** *Psychiatry Res* 2007, **151:**259-263.

181. Foster RG, Roenneberg T: **Human responses to the geophysical daily, annual and lunar cycles.** *Curr Biol* 2008, **18:**R784-R794.

182. Hensler JG, Dubocovich ML: **D1-dopamine receptor activation mediates [3H]acetylcholine release from rabbit retina.** *Brain Res* 1986, **398:**407-412.

183. Hensler JG, Cotterell DJ, Dubocovich ML: **Pharmacological and biochemical characterization of the D-1 dopamine receptor mediating acetylcholine release in rabbit retina.** *J Pharmacol Exp Ther* 1987, **243:**857-867.

184. Herrmann R, Heflin SJ, Hammond T, Lee B, Wang J, Gainetdinov RR, Caron MG, Eggers ED, Frishman LJ, McCall MA, Arshavsky VY: **Rod vision is controlled by dopamine-dependent sensitization of rod bipolar cells by GABA.** *NEURON* 2011, **72:**101-110.

185. Li H, Liu WZ, Liang PJ: **Adaptation-dependent synchronous activity contributes to receptive field size change of bullfrog retinal ganglion cell.** *PLoS One* 2012, **7:**e34336.

186. Xiao L, Zhang PM, Gong HQ, Liang PJ: **Effects of dopamine on response properties of ON-OFF RGCs in encoding stimulus durations.** *Front Neural Circuits* 2014, **8:**72.

187. Skarnes WC, Rosen B, West AP, Koutsourakis M, Bushell W, Iyer V, Mujica AO, Thomas M, Harrow J, Cox T, et al: **A conditional knockout resource for the genome-wide study of mouse gene function.** *Nature* 2011, **474:**337-342.

188. Pettitt SJ, Liang Q, Rairdan XY, Moran JL, Prosser HM, Beier DR, Lloyd KC, Bradley A, Skarnes WC: **Agouti C57BL/6N embryonic stem cells for mouse genetic resources.** *Nat Methods* 2009, **6:**493-495.

189. Jacobs GH, Williams GA, Fenwick JA: **Influence of cone pigment coexpression on spectral sensitivity and color vision in the mouse.** *Vision Res* 2004, **44:**1615-1622.

190. Schmidt TM, Kofuji P: **An isolated retinal preparation to record light response from genetically labeled retinal ganglion cells.** *J Vis Exp* 2011.

191. Brainard DH: **The Psychophysics Toolbox.** *Spat Vis* 1997, **10:**433-436.

192. Pelli DG: **The VideoToolbox software for visual psychophysics: transforming numbers into movies.** *Spat Vis* 1997, **10:**437-442.

193. Hood DC, Finkelstein MA: *Sensitivity to light*. 1986.

194. Stockman A, Sharpe LT: **Into the twilight zone: the complexities of mesopic vision and luminous efficiency.** *Ophthalmic Physiol Opt* 2006, **26:**225-239.

195. Segev R, Goodhouse J, Puchalla J, Berry MJ, 2nd: **Recording spikes from a large fraction of the ganglion cells in a retinal patch.** *Nat Neurosci* 2004, **7:**1154-1161.

196. Farrow K, Masland RH: **Physiological clustering of visual channels in the mouse retina.** *Journal of Neurophysiology* 2011, **105:**1516-1530.

197. Farrow K, Masland RH: **Physiological clustering of visual channels in the mouse retina.** *J Neurophysiol* 2011, **105:**1516-1530.

198. Kuffler SW: **Discharge patterns and functional organization of mammalian retina.** *J Neurophysiol* 1953, **16:**37-68.

199. Dedek K, Pandarinath C, Alam NM, Wellershaus K, Schubert T, Willecke K, Prusky GT, Weiler R, Nirenberg S: **Ganglion cell adaptability: does the coupling of horizontal cells play a role?** *PLoS ONE* 2008, **3:**e1714.

200. Enroth-Cugell C, Robson JG, Schweitzer-Tong DE, Watson AB: **Spatio-temporal interactions in cat retinal ganglion cells showing linear spatial summation.** *J Physiol* 1983, **341:**279-307.

201. Bu JY, Li H, Gong HQ, Liang PJ, Zhang PM: **Gap junction permeability modulated by dopamine exerts effects on spatial and temporal correlation of retinal ganglion cells' firing activities.** *J Comput Neurosci* 2014, **36:**67-79.

202. Bauer B, Ehinger B, Åberg L: **[3H]-Dopamine release from the rabbit retina.** *Albrecht von Graefes Archiv für klinische und experimentelle Ophthalmologie* 1980, **215:**71-78.

203. Godley BF, Wurtman RJ: **Release of endogenous dopamine from the superfused rabbit retina in vitro: effect of light stimulation.** *Brain Res* 1988, **452:**393-395.

204. Dearry A, Burnside B: **Light-induced dopamine release from teleost retinas acts as a light-adaptive signal to the retinal pigment epithelium.** *J Neurochem* 1989, **53:**870-878.

205. Kirsch M, Wagner HJ: **Release pattern of endogenous dopamine in teleost retinae during light adaptation and pharmacological stimulation.** *Vision Res* 1989, **29:**147-154.

206. Umino O, Lee Y, Dowling JE: **Effects of light stimuli on the release of dopamine from interplexiform cells in the white perch retina.** *Vis Neurosci* 1991, **7:**451-458.

207. Kramer SG: **Dopamine: A retinal neurotransmitter. I. Retinal uptake, storage, and light-stimulated release of H3-dopamine in vivo.** *Invest Ophthalmol* 1971, **10:**438-452.

208. Hu EH, Pan F, Volgyi B, Bloomfield SA: **Light increases the gap junctional coupling of retinal ganglion cells.** *J Physiol* 2010, **588:**4145-4163.

209. Klitten LL, Rath MF, Coon SL, Kim J-S, Klein DC, Møller M: **Localization and regulation of dopamine receptor D4 expression in the adult and developing rat retina.** *Experimental Eye Research* 2008, **87:**471-477.

210. Derouiche A, Asan E: **The dopamine D2 receptor subfamily in rat retina: ultrastructural immunogold and in situ hybridization studies.** *Eur J Neurosci* 1999, **11:**1391-1402.

211. Wagner HJ, Luo BG, Ariano MA, Sibley DR, Stell WK: **Localization of D2 dopamine receptors in vertebrate retinae with anti-peptide antibodies.** *J Comp Neurol* 1993, **331:**469-481.

212. Lukasiewicz PD: **Synaptic mechanisms that shape visual signaling at the inner retina.** *Prog Brain Res* 2005, **147:**205-218.

213. Buldyrev I, Taylor WR: **Inhibitory mechanisms that generate centre and surround properties in ON and OFF brisk-sustained ganglion cells in the rabbit retina.** *J Physiol* 2013, **591:**303-325.

214. Schmidt TM, Alam NM, Chen S, Kofuji P, Li W, Prusky GT, Hattar S: **A role for melanopsin in alpha retinal ganglion cells and contrast detection.** *Neuron* 2014, **82:**781-788.

215. Krieger B, Qiao M, Rousso DL, Sanes JR, Meister M: **Four alpha ganglion cell types in mouse retina: Function, structure, and molecular signatures.** *PLoS One* 2017, **12:**e0180091.

216. Ogilvie JM: **Photoreceptor rescue in an organotypic model of retinal degeneration.** *Prog Brain Res* 2001, **131:**641-648.

217. Ogilvie JM, Speck JD: **Dopamine has a critical role in photoreceptor degeneration in the rd mouse.** *Neurobiol Dis* 2002, **10:**33-40.

218. Stone RA, Lin T, Laties AM, Iuvone PM: **Retinal dopamine and form-deprivation myopia.** *Proc Natl Acad Sci U S A* 1989, **86:**704-706.

219. Bodis-Wollner I, Jo MY: **Getting around and communicating with the environment: visual cognition and language in Parkinson's disease.** *J Neural Transm Suppl* 2006**:**333-338.

220. Bodis-Wollner I, Tagliati M: **The visual system in Parkinson's disease.** *Adv Neurol* 1993, **60:**390-394.

221. Gastinger MJ, Singh RS, Barber AJ: **Loss of cholinergic and dopaminergic amacrine cells in streptozotocin-diabetic rat and Ins2Akita-diabetic mouse retinas.** *Invest Ophthalmol Vis Sci* 2006, **47:**3143-3150.

222. Seki M, Tanaka T, Nawa H, Usui T, Fukuchi T, Ikeda K, Abe H, Takei N: **Involvement of brain-derived neurotrophic factor in early retinal neuropathy of streptozotocin-induced diabetes in rats: therapeutic potential of brain-derived neurotrophic factor for dopaminergic amacrine cells.** *Diabetes* 2004, **53:**2412-2419.

223. Hansen FH, Skjorringe T, Yasmeen S, Arends NV, Sahai MA, Erreger K, Andreassen TF, Holy M, Hamilton PJ, Neergheen V, et al: **Missense dopamine transporter mutations associate with adult parkinsonism and ADHD.** *J Clin Invest* 2014, **124:**3107-3120.

224. Mergy MA, Gowrishankar R, Davis GL, Jessen TN, Wright J, Stanwood GD, Hahn MK, Blakely RD: **Genetic targeting of the amphetamine and methylphenidate-sensitive dopamine transporter: on the path to an animal model of attention-deficit hyperactivity disorder.** *Neurochem Int* 2014, **73:**56-70.

225. Barnard AR, Hattar S, Hankins MW, Lucas RJ: **Melanopsin regulates visual processing in the mouse retina.** *Curr Biol* 2006, **16:**389-395.

226. Gonzalez-Menendez I, Contreras F, Garcia-Fernandez JM, Cernuda-Cernuda R: **Perinatal development of melanopsin expression in the mouse retina.** *Brain Res* 2011, **1419:**12-18.

227. Carter-Dawson LD, LaVail MM: **Rods and cones in the mouse retina. II. Autoradiographic analysis of cell generation using tritiated thymidine.** *J Comp Neurol* 1979, **188:**263-272.

228. Lakowski J, Baron M, Bainbridge J, Barber AC, Pearson RA, Ali RR, Sowden JC: **Cone and rod photoreceptor transplantation in models of the childhood retinopathy Leber congenital amaurosis using flow-sorted Crx-positive donor cells.** *Hum Mol Genet* 2010, **19:**4545-4559.

229. Applebury ML, Farhangfar F, Glosmann M, Hashimoto K, Kage K, Robbins JT, Shibusawa N, Wondisford FE, Zhang H: **Transient expression of thyroid hormone nuclear receptor TRbeta2 sets S opsin patterning during cone photoreceptor genesis.** *Dev Dyn* 2007, **236:**1203-1212.

230. Morrow EM, Belliveau MJ, Cepko CL: **Two phases of rod photoreceptor differentiation during rat retinal development.** *J Neurosci* 1998, **18:**3738-3748.

231. Taylor WR: **TTX attenuates surround inhibition in rabbit retinal ganglion cells.** *Vis Neurosci* 1999, **16:**285-290.

232. Cook PB, McReynolds JS: **Lateral inhibition in the inner retina is important for spatial tuning of ganglion cells.** *Nat Neurosci* 1998, **1:**714-719.

233. Bieda MC, Copenhagen DR: **Sodium action potentials are not required for light-evoked release of GABA or glycine from retinal amacrine cells.** *J Neurophysiol* 1999, **81:**3092-3095.